UNCLASSIFIED

AD 423377

DEFENSE DOCUMENTATION CENTER
FOR
SCIENTIFIC AND TECHNICAL INFORMATION
CAMERON STATION ALEXANDRIA, VIRGINIA

DEPARTMENT OF DEFENSE

UNCLASSIFIED

NOTICE: When government or other drawings, specifications or other data are used for any purpose other than in connection with a definitely related government procurement operation, the U. S. Government thereby incurs no responsibility, nor any obligation whatsoever; and the fact that the Government may have formulated, furnished, or in any way supplied the said drawings, specifications, or other data is not to be regarded by implication or otherwise as in any manner licensing the holder or any other person or corporation, or conveying any rights or permission to manufacture, use or sell any patented invention that may in any way be related thereto.

TURAL DYNAMICS • ELECTRONIC SYSTEMS AND INSTRUMENTS • COMPUTER MODULES

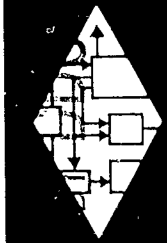

RESEARCH
ENGINEERING
PRODUCTION

423377

GENERAL APPLIED SCIENCE LABORATORIES, INC.

MERRICK and STEWART AVENUES WESTBURY [illegible] N. Y. [illegible]

Total No. Pages:
Copy No. (37) of (100)

PROPELLER BLADE VIBRATION AND STRESS ANALYSIS

FINAL REPORT

TECHNICAL REPORT NO. 283

By Edward Lieberman

Prepared Under Contract No. Nonr-3072(00)X

Prepared for

Department of the Navy
David Taylor Model Basin
Washington 7, D. C.

Prepared by

General Applied Science Laboratories, Inc.
Merrick and Stewart Avenues
Westbury, L.I., New York

Approved by Lee Arnold
Lee Arnold
Vice President

June 1963

I. SCOPE OF PROGRAMS

As indicated in References 2 and 3, the analyses by Dr. Frank Lane proved to be acceptable, using 45 degrees of freedom, only for flat plates, twisted bars , and, in general, for any geometrical configuration which was not characterized by severe twist, and large overhang of thin leading and trailing edges. Since many propeller blades do exhibit the geometrical configuration described above, it was suggested that the number of degrees of freedom be increased, to accommodate all propeller blade configurations.

Since the computer machine time increases roughly as the square of the number of degrees of freedom, it was decided to re-code the programs described in References 2 and 3, for the IBM 7090 computer, instead of for the IBM 704. Due to the size of the system, it was necessary to subdivide the program into 4 CHAIN LINKS, to accommodate the storage requirements. During the course of field testing, it was found that single-precision arithmetic was inadequate in one section, and therefore it was necessary to utilize triple-precision arithmetic.

To illustrate the sharp contrast in scope, between the subject programs and their IBM 704 predecessors, up to 108 degrees of freedom may now be utilized, as compared with 45; 10 tapes versus 3, up to 146 mesh points versus 56 (integrating quadrature), and about 1 hour of IBM7090 computer time versus 40 minutes of IBM 704 time. As before, provision is made to restart the program with a minimum loss of machine time, in the event it must be removed from the computer prematurely due to lack of available time. In addition, the program may be easily restored in the event of a machine error.

No attempt will be made in this report to repeat Dr. Lane's analyses, which are described in Reference 1, and summarized in References 2 and 3. Only that information which pertains to these IBM 7090 programs will be included. The expanded sets of Rayleigh functions are listed in Appendix I.

PROPELLER BLADE VIBRATION ANALYSIS

The purpose of this IBM computer program is to generate the natural frequencies, mode shapes, and modal stress distributions for the ten lowest modes of vibration of propeller blades. This information, coupled with the fact that the eigenvectors are normalized with respect to the strain energy matrix, $(q^T V q = I)$, is sufficient to conduct any response analyses of propeller blades.

After accepting the input data which describe the blade geometry, the program generates a polynomial which fits, in the least squares sense, the camber distribution over the planform of the blade. The program then constructs a quadrature mesh which is later used to integrate the strain energy and kinetic energy, matrices over the blade planform. The two-matrix eigenvalue problem is reduced to a one matrix eigenvalue problem by factoring the strain energy matrix in triple-precision. This problem is then solved, and the resulting eigenvalues and eigenvectors are written as output. The relative stresses and displacements are calculated at mesh points over the blade planform, and are written as output.

This program will process sets of input data automatically. Core memory is salvaged on tape three times during the execution of the program which permits the program to be restarted with a minimum loss of time in the event of a machine failure.

This program has been written for a 32K (32,768 words) capacity IBM 7090 computer, and utilizes ten tape units .

CHAIN LINK 1

The first two input cards, identification card and the first data card, are read and immediately written on tape A3. The program then reads and writes the remainder of the input data and calculates the thickness and the local distance from the y^1, y^2 plane of each input point. The distribution of camber, of the propeller blade, is then approximated with a least-squares surface fit. The LeGendre-Gauss Quadrature weighting constants are stored and the coordinates of the quadrature mesh points are calculated. The program then dumps core memory on tape A5 and calls for CHAIN LINK 2.

CHAIN LINK 2

This section generates the potential (strain) energy, and the kinetic energy matrices. At each quadrature mesh point, the program generates the fundamental forms, the Rayleigh functions, and the elements of the $T_{(i)}$ and $N_{(i)}$ matrices, as well as the local thickness. Utilizing these values, the local contribution to the strain energy and kinetic energy matrices is formed and multiplied by the local quadrature weight. All underflows are set to zero. The program scans the quadrature mesh points, adding the weighted contributions. The integrals are then modified to account for the root curvature. After the integrals are formed, core memory is again salvaged on tape A5, and CHAIN LINK 3 is called.

CHAIN LINK 3

The two-matrix eigenvalue problem is expressed as $Tq = \frac{1}{\lambda} Vq$. Using triple-precision arithmetic the strain energy matrix is factored, $V=M^T M$, where M is an upper triangular matrix. Then the system, $M^{-T}TM^{-1}Mq=\frac{1}{\lambda} Mq$, or $Fy = \frac{1}{\lambda} y$, where $F=M^{-T}TM^{-1}$ and $y = Mq$, is formed. This eigenvalue problem is solved using the SHARE routine, NYEVV, and the true eigenvectors calculated, $q = M^{-1}y$. These eigenvectors are normalized with respect to the strain energy matrix ($q^T Vq = I$). After saving core memory on tape A5, the program calls for CHAIN LINK 4.

CHAIN LINK 4

The ten lowest eigenvalues and their corresponding eigenvectors are stored in ascending order, and the mesh points at which the displacements and stresses will be evaluated, are calculated.

After writing the eigenvalues and eigenvectors for the lowest ten modes, and the mesh point coordinates on output tape A3, the program calculates the fundamental forms, Rayleigh functions, elements of the $T_{(i)}$ and $N_{(i)}$ matrices, the thickness at each mesh point, and then calculates displacements and stresses. Since the mesh is very dense, stresses are calculated at alternate mesh points while displacements are calculated at all mesh points, for all the ten modes of vibration. There are a total of 111 mesh points including the tip of the blade and 11 points along the blade root. The stresses and/or displacements at each mesh point are written on output tape A3. Control is returned to CHAIN LINK 1 to process the next run, if any. If no more data is available, the program exits.

The approximate computer production time for each set of input cards for an 8 x 9 quadrature mesh and 90 degrees of freedome is approximately 1 hour.

PROPELLER BLADE STATIC STRESS ANALYSIS

A. Program for Distributed Loads

The purpose of this IBM computer program is to generate the displacement and stress distribution of propeller blades for prescribed pressure-jump loadings. Provision is made for a "peaked" distributed loading with the singularity at the leading edge. The stresses are given directly; the displacements given must be divided by Young's Modulus.

After accepting the input data which describes the blade geometry, the program processes this data, and generates functions which accurately represent the blade configuration. A quadrature mesh is constructed which is then used to integrate the strain energy matrix over the blade planform. The program reads the pressure jump load data, and integrates this information over the blade planform to generate the forcing vector. To solve the resulting system of linear equations, the strain energy matrix is factored in triple-precision, and its inverse is computed. This approximate inverse is improved (if possible), and the solution vector is calculated and improved by use of iteration techniques. See Appendix II. The stresses and displacements at mesh points over the blade planform, are then calculated.

This program will process any sequence of inputs consisting of geometrical input data describing a particular blade, followed by any number of loading conditions for that blade, followed by another blade, etc. All inputs are written on the output tape, so that any error may be detected, and all output listings uniquely identified. Core memory is salvaged on tape four times during the execution of the program which permits the program to be restarted with a minimum loss of time in the event of a machine failure.

This program has been written for a 32K (32, 768 words) capacity IBM 7090 computer, and utilizes ten tape units.

The program is divided into four CHAIN LINKS, See pages 32 to 38 for detailed flow diagrams.

CHAIN LINK 1

The first two input cards, identification card and the first data card, are read and immediately written on tape A3. The program then reads and writes the remainder of the input data and calculates the thickness and the local distance from the y^1, y^2 plane of each input point. The distribution of camber of the propeller blade, is then approximated with a least-squares surface fit. The LeGendre-Gauss Quadrature weighting constants are stored and the coordinates of the quadrature mesh points are calculated. The program then dumps core memory on tape A5 and calls for CHAIN LINK 2.

CHAIN LINK 2

This section generates the potential (strain) energy matrix. At each quadrature mesh point, the program generates the fundamental forms, the Rayleigh functions, and the elements of the $T_{(i)}$ and $N_{(i)}$ matrices, as well as the local thickness. Utilizing these values, the local contribution to the strain energy matrix is formed and multiplied by the local quadrature weight.

All underflows are set to zero. The program scans the quadrature mesh points, adding the weighted contributions. The integral is then modified to account for the root curvature. After the integral is formed, core memory is again saved on tape A5, and CHAIN LINK 3 is called.

CHAIN LINK 3

A code word is read and written which describes the type of blade in the event the loading is "peaked" at the leading edge. The pressure-jump distributed loading is then read and written. A forcing vector is formed and integrated over the blade planform.

Core memory is saved on tape A5. The strain energy matrix is then factored into triangular matrices in the form, $V = M^T M$, using triple-precision arithmetic, and the matrix M^{-1} is generated. The inverse is then simply, $V^{-1} = M^{-1} M^{-T}$, and is written on binary tape, B2, for subsequent loading conditions, if desired. The solution vector is then calculated and improved by iteration. All subsequent loading conditions use this inverse; only the new forcing vector is computed. After saving core memory again on tape A5, the program calls CHAIN LINK 4.

CHAIN LINK 4

The mesh points at which the displacements and stresses will be evaluated, are calculated. After writing the solution vector and the mesh points on the output tape, the program calculates the fundamental forms, Rayleigh functions, elements of the $T_{(i)}$ and $N_{(i)}$ matrices, the thickness, and then calculates displacements and stresses at each mesh point. These values are written on the output tape. There are a total of 111 mesh points including the tip of the blade and 11 points along the blade root. If a new loading condition is to be read, CHAIN LINK 3 is called. If a new blade is to be analyzed, control is transferred to CHAIN LINK 1. Otherwise, the program exits.

The approximate computer production time for each complete set of input data cards for an 8 x 9 quadrature mesh and 90 degrees of freedom is approximately 1 hour. For each subsequent set of pressure-jump inputs alone, the computer production time is approximately 1/2 hour.

II GEOMETRY

Figure 1 illustrates the propeller blade geometry and the coordinate systems utilized. The (y^1, y^2) coordinates form a two-dimensional Cartesian system in the transverse projection at the blade and serve as a Gaussian coordinate system in the blade middle-surface. The coordinate y^3 is normal to the local blade middle-surface, directed so that (y^1, y^2, y^3) form a right-hand system. It is to be noted that the camber and twist of the blade result in non-orthogonality of the (y^1, y^2) coordinate system. The third coordinate y^3 is, however, locally normal to y^1 and y^2.

The blade middle-surface is defined completely by describing its projected planform in the (y^1, y^2) plane and its local distance $f(y^1, y^2)$ from this plane as shown in Figure 1. The description of the thickness distribution serves to complete the geometric description of the blade.

The thickness at any point is found by linear interpolation of the input data.

III INPUT FORMAT - VIBRATION

Card	Input Information
1	Identification
2	Poisson's Ratio, Blade Root Geometry, Size of System
3, 6, 9, ...	Section Properties
4, 7, 10,...	Offsets to Back Face Along Section
5, 8, 11,...	Offsets to Front Face Along Section
Final	Properties at Blade Tip

Refer to Figure 2.

Card No. 1:

Any identification statement of 72 characters or less will be accepted. The statement may be punched in columns 2 - 72 of a card; the digit, "1" should be punched in column 1 for output convenience.

Card No. 2:

Data	Columns	Format
ν	1-5	X.XXX
W_R	7-12	XX.XXX
W_L	14-19	XX.XXX
R_R	21-26	XX.XXX
R_L	28-33	XX.XXX
N	37-38	XX

The first word, ν, is Poisson's Ratio. The next 4 words, W_R, W_L, R_R, R_L are indicated in Figure 2. The number of degrees of freedom for each displacement component is N. Thus for 63 degrees of freedom, N is 21. If a full-scale problem is being run (108 degrees of freedom), N may be left blank.

Card No. 3:

Data	Columns	Format
% Radius	1-2	XX
Radius	4-9	XX.XXX or XXX.XX
Span	11-16	XX.XXX or XXX.XX
Pitch	18-24	±XX.XXX or ±XXX.XX
Rake	26-32	±X.XXXX
Skew	34-40	±X.XXXX

Card No. 4:

Data	Columns	Format
A	1-6	±X.XXX or ±XX.XX
E	7-12	↓
F	13-18	↓
G	19-24	↓
H	25-30	↓
J	31-36	↓
K	37-42	↓
L	43-48	↓
M	49-54	↓
N	55-60	↓
P	61-66	↓

Card No. 5:

Identical in format to Card No. 4.

Final Card

Data	Columns	Format
-	1-2	Must be blank
Radius	4-9	XX.XXX or XXX.XX
Thickness	11-16	XX.XXX
Pitch	18-24	XXX.XXX
Rake	26-32	±X.XXXX
Skew	34-40	±X.XXXX

The program can accept a maximum of 12 sections corresponding to a total of 40 input cards per set.

Cards 4 and 5 specify the thickness offsets along a section at equal chord increments, from leading-edge to trailing-edge. The offset of A is the offset near the leading edge, the offset of E is at one-tenth the chord distance from the leading edge, etc. The offset of P refers to the trailing-edge. See sketch below.

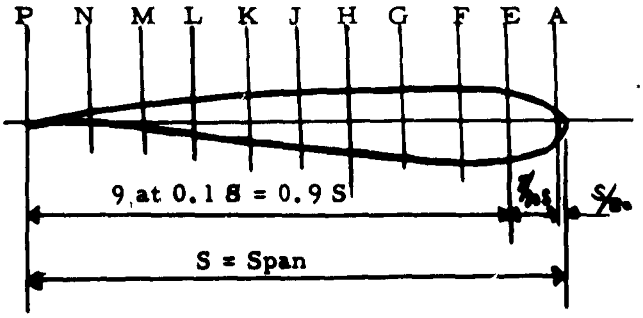

INPUT FORMAT - STRESS

Card	Input Information
1	Identification
2	Poisson's Ratio, Blade Root Geometry
3, 6, 9, . . .	Section Properties
4, 7, 10, . . .	Offsets to Back Face Along Section
5, 8, 11, . . .	Offsets to Front Face Along Section
T-1	Properties of Blade Tip
T	Code Card
T+1, T+3, T+5, . . .	Pressure-jumps at points on sections corresponding respectively to those sections of input cards 3, 6, 9, . . . These points are from leading edge to 25% of chord.
T+2, T+4, T+6, . . .	Pressure-jumps at points on sections corresponding respectively to those sections of input cards 3, 6, 9, . . . These points are from 30% of chord to trailing edge.
C	Control Card

Next set of inputs, if any.

Refer to Figure 2.

Card No. 1:

Any identification statement of 71 characters or less will be accepted. The statement must be punched in columns 2-72 of a card. The digit, "1" should be punched in column 1 for convenience of output.

Card No. 2;

Data	Columns	Format
ν	1-5	X.XXX
W_R	7-12	XX.XXX
W_L	14-19	XX.XXX
R_R	21-26	XX.XXX
R_L	28-33	XX.XXX
N	37-38	XX

The first word, ν, is Poisson's Ratio. The next 4 words, W_R, W_L, R_R, R_L, are indicated in Figure 2. The number of degrees of freedom for each displacement component is N. Thus for 63 degrees of freedom, N is 21. If a full-scale problem is being run (108 degrees of freedom), N may be left blank.

Card No. 3:

Data	Columns	Format
% Radius	1-2	XX
Radius	4-9	XX.XXX or XXX.XX
Span	11-16	XX.XXX or XXX.XX
Pitch	18-24	±XX.XXX or ±XXX.XX
Rake	26-32	±X.XXXX
Skew	34-40	±X.XXXX

Card No. 4:

Data	Columns	Format
A	1-6	±X.XXX or ± XX.XX
E	7-12	↓
F	13-18	
G	19-24	
H	25-30	
J	31-36	
K	37-42	
L	43-48	
M	49-54	
N	55-60	
P	61-66	

Card No. 5:

Identical in format to Card No. 4.

Card T-1:

Data	Columns	Format
-	1-2	Must be blank
Radius	4-9	XX.XXX or XXX.XX
Thickness	11-16	XX.XXX
Pitch	18-24	XXX.XXX
Rake	26-32	±X.XXXX
Skew	34-40	±X.XXXX

Card T:

Data	Column	Format
Code	1	X

Card T + 1:

Data	Columns	Format
P_o	1-7	XXX.XXX
$P_{1.25}$	9-15	↓
$P_{2.5}$	17-23	
$P_{5.0}$	25-31	
$P_{7.5}$	33-39	
P_{10}	41-47	
P_{15}	49-55	
P_{20}	57-63	
P_{25}	65-71	

Card T + 2:

Data	Columns	Format
P_{30}	1-7	XXX.XXX
P_{40}	9-15	↓
P_{50}	17-23	
P_{60}	25-31	
P_{70}	33-39	
P_{80}	41-47	
P_{90}	49-55	
P_{95}	57-63	
P_{100}	65-71	

Card C:

Data	Column	Format
Code	1	X

The program can accept a maximum of 12 sections corresponding to a total of 65 input cards per set.

Cards 4 and 5 specify the thickness offsets along a section at equal chord increments, from leading-edge to trailing-edge. The offset of A is the offset near the leading edge, the offset of E is at one-tenth the chord distance from the leading edge, etc. The offset of P refers to the trailing edge. See sketch below.

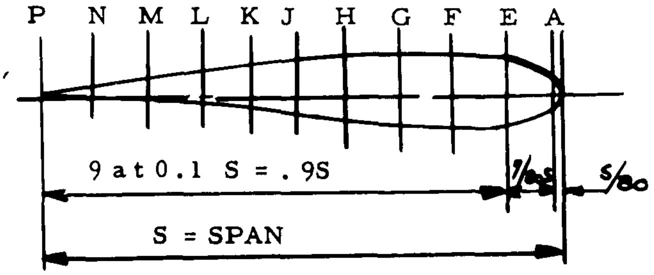

Card T specifies the type of peaked loading if any. The code is "1" for a "peaked" load and a super-cavitating blade, 0 for a "peaked" load and a fully wetted blade, and blank for any load which is not "peaked".

Cards T+1 and T+2 specify the complete pressure-jump loading acting on that section described on cards 3, 4 and 5. The subscripts of the p's are the percentages of chord, counting from leading edge to trailing edge. For example, p_0 is the pressure-jump loading acting at the leading edge of the section under consideration; p_{20} acts at 20% of chord, or one-fifth the distance from the leading edge (this corresponds to F on the above sketch). Of course, p_{100} is the pressure-jump loading at the trailing edge (invariably, zero). Cards T+3 and T + 4 specify the pressure-jump loading on that section described on cards 6, 7, and 8; cards T + 5 and T + 6 pertain to cards 9, 10, and 11, etc. For a peaked loading, $p_o, p_{1.25}$ and $p_{2.5}$ must be zero.

The control card dictates the action of the program after a "run" has been completed. If no more inputs follow, the control card may be blank. If it is desired to conduct an additional analysis on the same blade using a different loading, the control card must have a "2" punched in column 1, and be followed immediately by cards specifying the loading, as described above (cards T through C). Should it be desired to conduct an analysis on another blade (no matter what the loading may be), a "1" must be punched in Column 1, followed by cards describing the new geometry and corresponding pressure-jump loading (cards 1, 2, 3..., C).

The formats indicated are representative. The decimal points may be shifted in either direction, so long as the input "word" is confined within the columns specified.

The program assumes that the tip of the blade is a point (span equal to zero) as is the case of a propeller blade. If the section at the blade tip has some span, such as the flat plates (Ref. 2 and 3), it will be necessary to input two sections extremely close to the tip. In general, both sections should be within the outer 1% of the total blade span.

IV OPERATING INSTRUCTIONS

These programs consist of rather large binary decks which should be loaded on tape using off-line peripheral equipment such as the IBM 1401, and mounted as input tape A2 on the main computer. The data cards are placed in the hopper of the on-line card reader as detailed below. .

The IB Monitor system must be used to run this program on the IBM 7090. The tape assignment cards (IOU tables) are included as part of the program deck. Tapes A1 through A5 and B1 through B5 are required for these programs. All output data is written on tape A3 which is to be printed using program control. Tape A5 is used as a salvage tape to store the entire contents of core periodically, so as to minimize loss of machine time. The restart procedure is described below. Tape A1 contains the IB Monitor Systems tape, tape A4 is used to store the chain links of the program, and tapes B-1 through B-5 are used as intermediate tapes by the Monitor system and as binary scratch tapes by the program itself. All tapes should be in the high density mode to conserve machine time.

Restart Procedure

A. In the event the program must be interrupted, due to some scheduling conflict or similar reason, dismount tape A5, and save. Print tape A3 and save this abridged output.

1. To restart the vibration program, re-mount tape A5 (but do not "ready" the tape unit), the systems tape, A1, and reload the program deck and data in the usual procedure, described above, as for a new run. As soon as EXECUTION commences, (on-line printer will indicate this word), depress

MANUAL key to MANUAL position, then "ready" tape A5. Depress the console keys to read, 0 02000 0 00175, (transfer to location $(0175)_8$). Press ENTER INSTRUCTION key. Depress MANUAL key to AUTOMATIC position. Press START key.

Tape A5 will then be read, and the most recent condition of core, prior to the last salvage, will be restored. The program will then commence to execute, automatically.

2. To restart the stress program. , it is necessary that the pressure-jump data be in core memory at the time of salvage. Thus, the program must have initially executed either the 3rd or 4th dump on tape A5, both taking place in the third CHAIN LINK, prior to manual termination of run. If so, the procedure described above for the vibration program, will apply,otherwise, the program must be run from the beginning. Note that sequential runs are not possible when the program is restarted.

B. In the event of a machine failure, the restart procedure is somewhat simpler. Transfer via the console to location $(0175)_8$ as described above, and the program will be restored. In this case, the restrictions for the stress programs do not apply.

The only STOP anticipated, is when the accumulated round-off error causes a number, whose square-root is required, to become negative. This will only occur in LINK 3, and the program will exit automatically, with a statement describing the cause.

This situation can only be remedied by re-running the program using lower number of degrees of freedom. For a full discussion of this difficulty, refer to section of conclusions.

Another STOP which may occur, is at location $(210)_8$. This is the result of being unable to write on tape A5 due (probably) to a "bad" tape. Replace this tape with another reel, and press START key. If this STOP persists, transfer via console to location $(213)_8$ to by-pass the dump. The program will not be affected unless a subsequent machine error occurs, in which case it will be necessary to restart the program from the beginning.

With the programs stored permanently on magnetic tape, the data cards will be read via the on-line card reader as follows:

1. Load the FORTRAN START card.
2. After IB Monitor begins to function (a few seconds), FEED out this START card.
3. Place data cards in card reader hopper and depress reader START key until READY light goes on.
4. Program will automatically read these cards. for END-OF-FILE convenience, place two blank cards at the end of the deck of data cards.

V BLADE VIBRATION ANALYSIS FLOW DIAGRAM

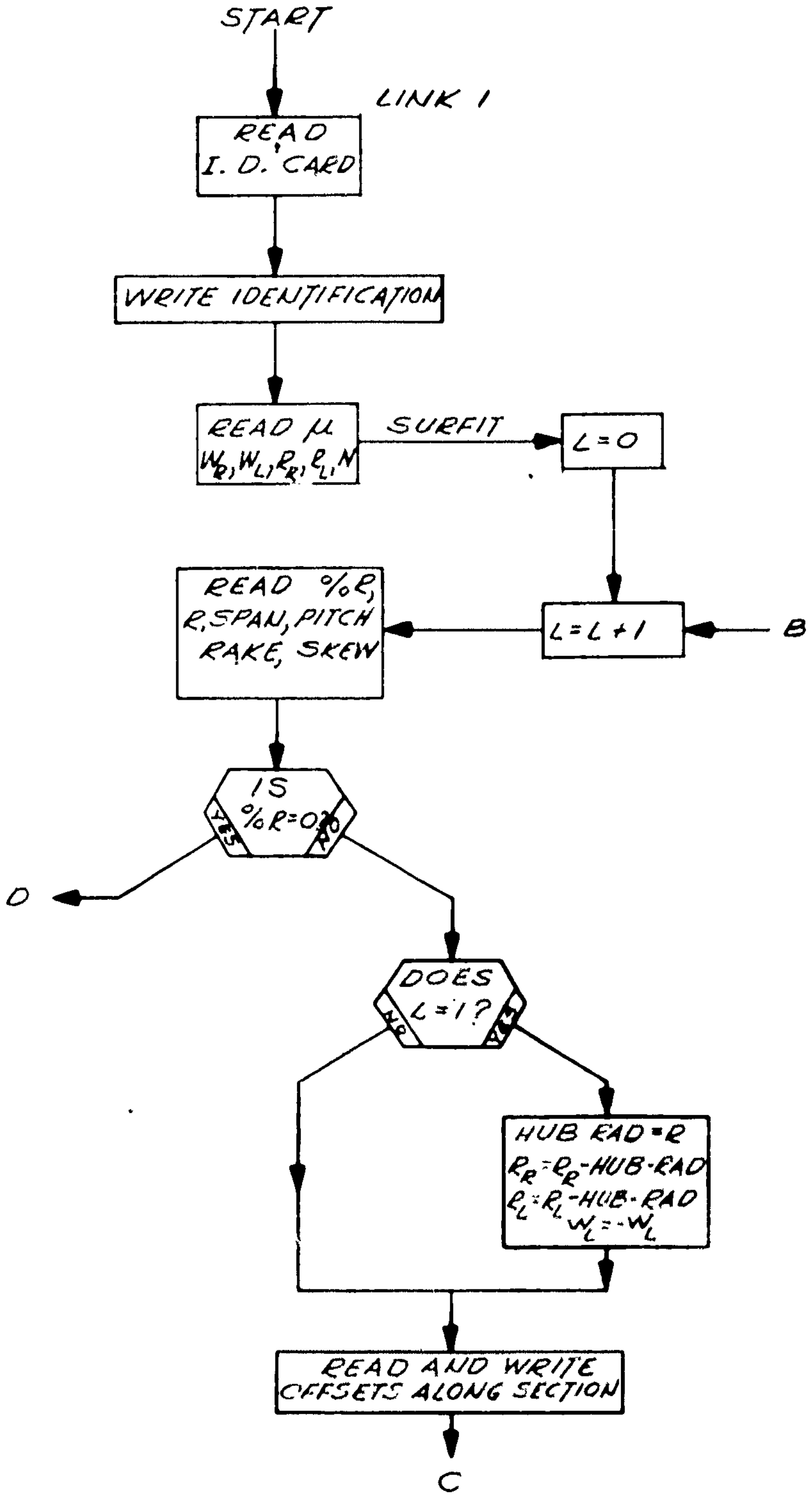
START
LINK 1
READ I.D. CARD
WRITE IDENTIFICATION
READ μ $W_R, W_L, \ell_R, \ell_L, N$
SURFIT
L=0
READ %R, R, SPAN, PITCH RAKE, SKEW
L=L+1
B
IS %R=0?
YES
NO
D
DOES L=1?
NO
YES
HUB RAD=R
$R_R=\ell_R$-HUB-RAD
$\ell_L=R_L$-HUB-RAD
$W_L=-W_L$
READ AND WRITE OFFSETS ALONG SECTION
C

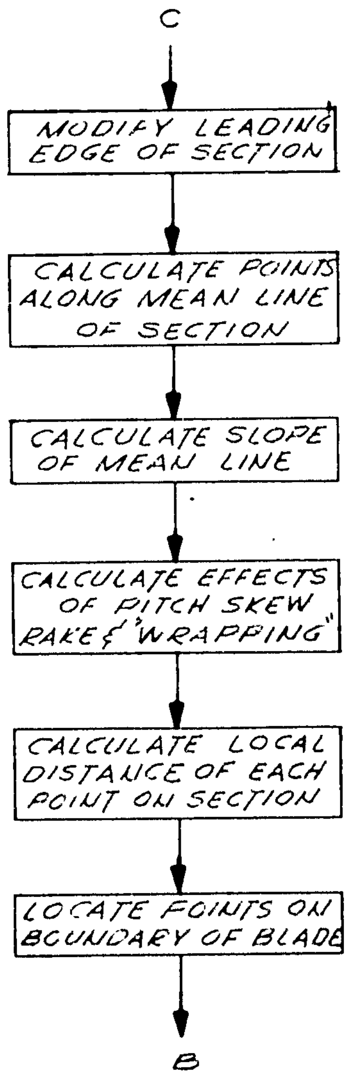
C
MODIFY LEADING EDGE OF SECTION
CALCULATE POINTS ALONG MEAN LINE OF SECTION
CALCULATE SLOPE OF MEAN LINE
CALCULATE EFFECTS OF PITCH SKEW RAKE & "WRAPPING"
CALCULATE LOCAL DISTANCE OF EACH POINT ON SECTION
LOCATE POINTS ON BOUNDARY OF BLADE
B

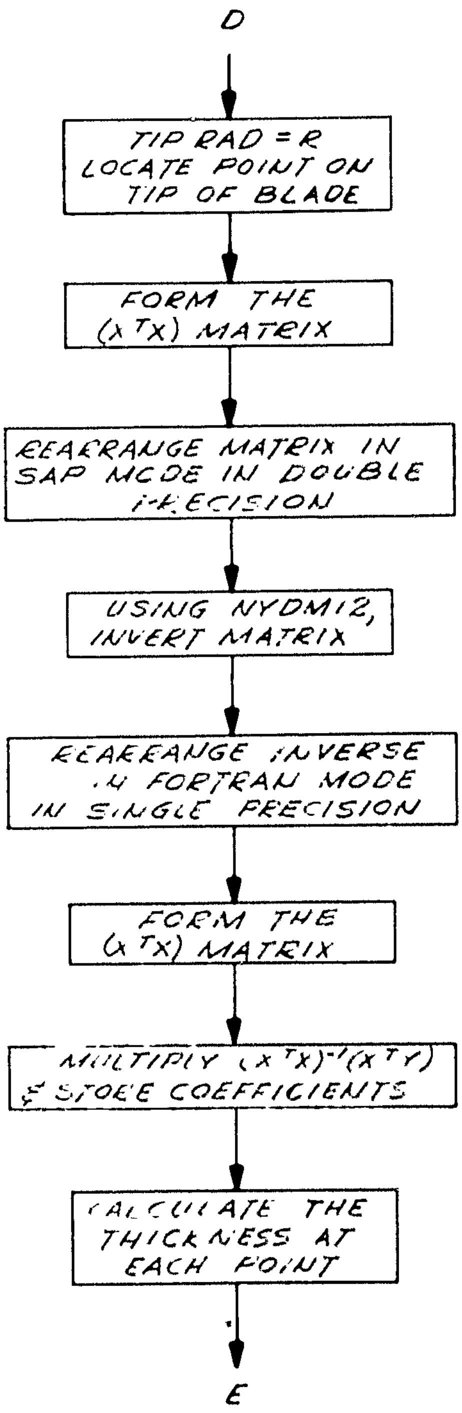
D
TIP RAD = R LOCATE POINT ON TIP OF BLADE
FORM THE $(X^T X)$ MATRIX
REARRANGE MATRIX IN SAP MODE IN DOUBLE PRECISION
USING NYDM12, INVERT MATRIX
REARRANGE INVERSE IN FORTRAN MODE IN SINGLE PRECISION
FORM THE $(X^T X)$ MATRIX
MULTIPLY $(X^T X)^{-1}(X^T Y)$ & STORE COEFFICIENTS
CALCULATE THE THICKNESS AT EACH POINT
E

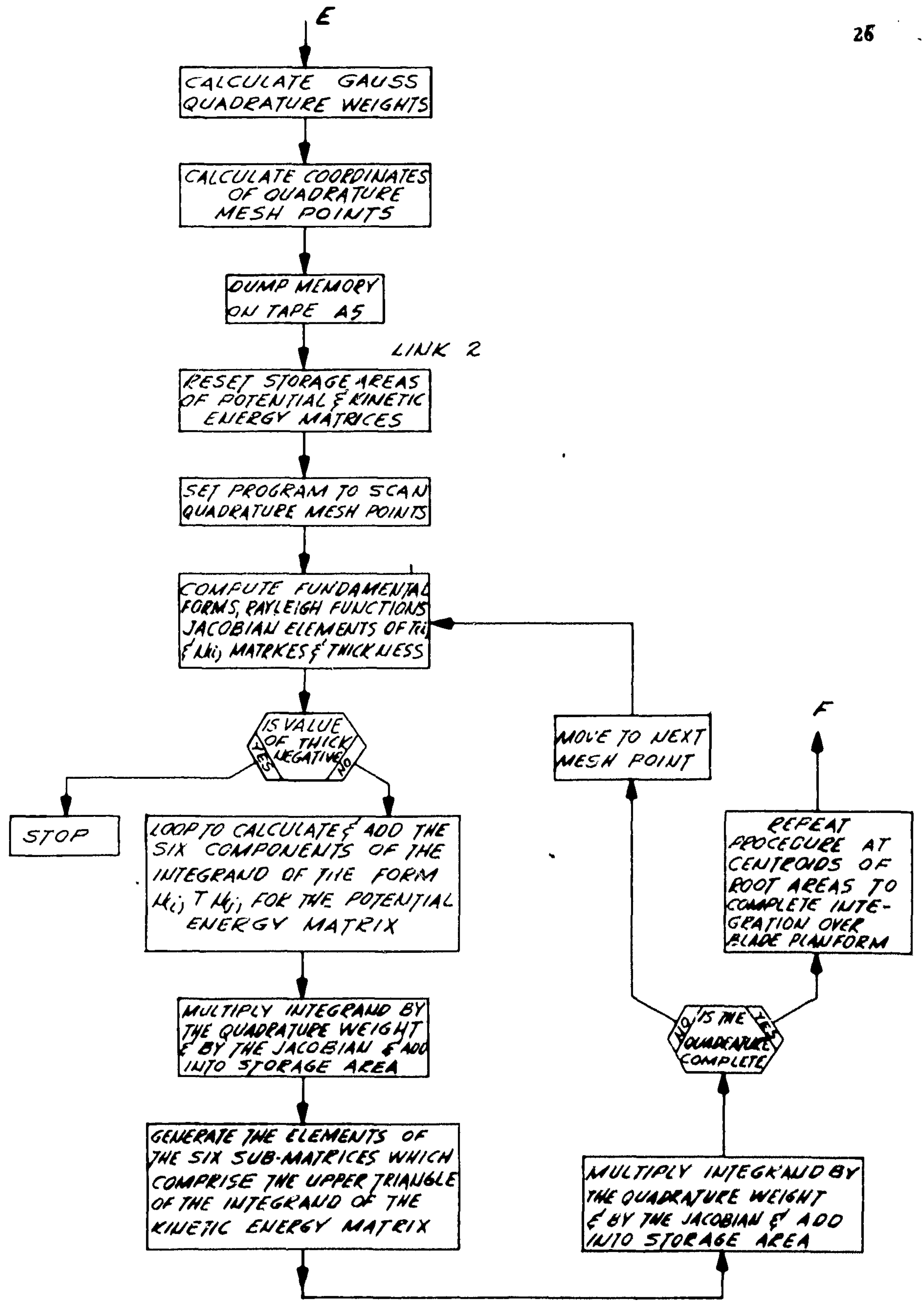
E
CALCULATE GAUSS QUADRATURE WEIGHTS
CALCULATE COORDINATES OF QUADRATURE MESH POINTS
DUMP MEMORY ON TAPE A5
LINK 2
RESET STORAGE AREAS OF POTENTIAL & KINETIC ENERGY MATRICES
SET PROGRAM TO SCAN QUADRATURE MESH POINTS
COMPUTE FUNDAMENTAL FORMS, RAYLEIGH FUNCTIONS JACOBIAN ELEMENTS OF T_{ij} & M_{ij} MATRICES & THICKNESS
IS VALUE OF THICK NEGATIVE
YES
NO
STOP
LOOP TO CALCULATE & ADD THE SIX COMPONENTS OF THE INTEGRAND OF THE FORM M_{ij} T M_{ij} FOR THE POTENTIAL ENERGY MATRIX
MULTIPLY INTEGRAND BY THE QUADRATURE WEIGHT & BY THE JACOBIAN & ADD INTO STORAGE AREA
GENERATE THE ELEMENTS OF THE SIX SUB-MATRICES WHICH COMPRISE THE UPPER TRIANGLE OF THE INTEGRAND OF THE KINETIC ENERGY MATRIX
MOVE TO NEXT MESH POINT
F
REPEAT PROCEDURE AT CENTROIDS OF ROOT AREAS TO COMPLETE INTEGRATION OVER BLADE PLANFORM
NO
IS THE QUADRATURE COMPLETE
YES
MULTIPLY INTEGRAND BY THE QUADRATURE WEIGHT & BY THE JACOBIAN & ADD INTO STORAGE AREA

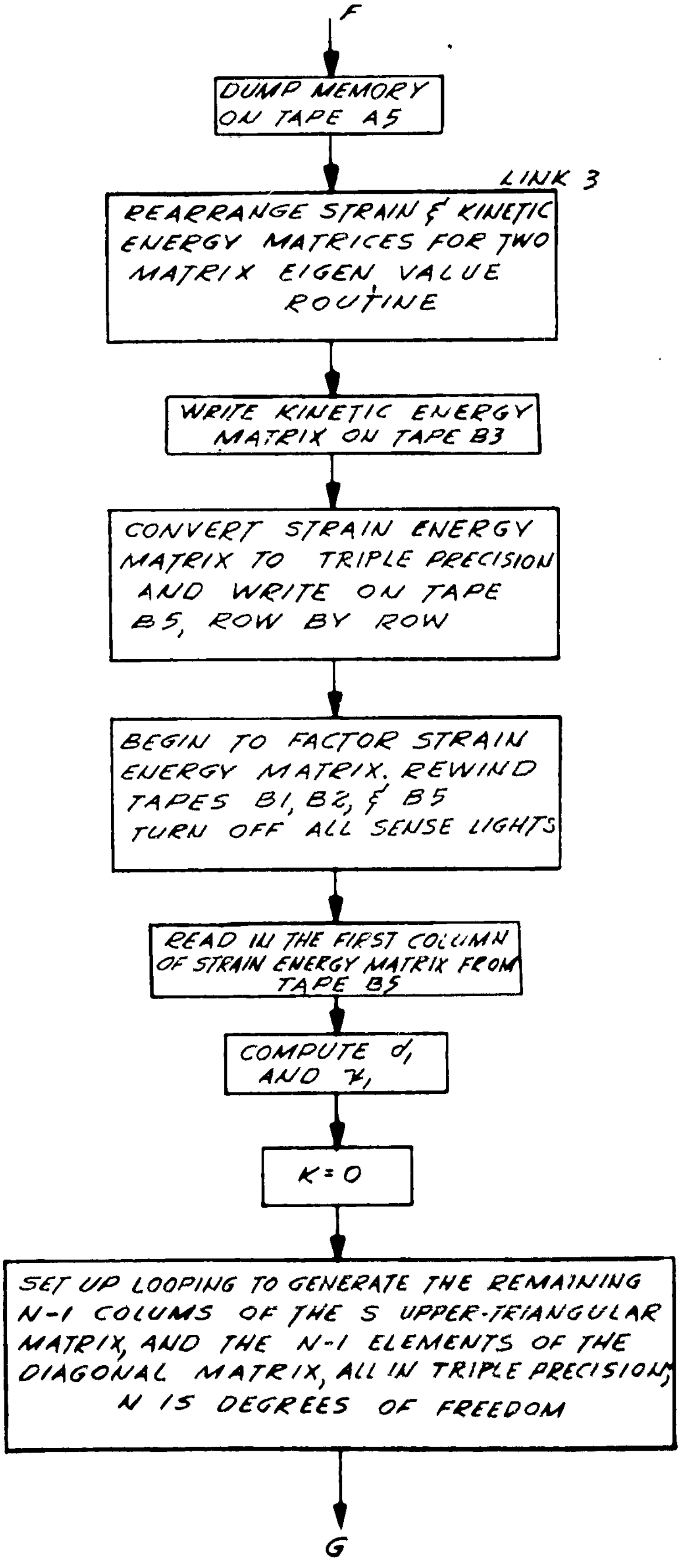
F
DUMP MEMORY ON TAPE A5
LINK 3
REARRANGE STRAIN & KINETIC ENERGY MATRICES FOR TWO MATRIX EIGEN VALUE ROUTINE
WRITE KINETIC ENERGY MATRIX ON TAPE B3
CONVERT STRAIN ENERGY MATRIX TO TRIPLE PRECISION AND WRITE ON TAPE B5, ROW BY ROW
BEGIN TO FACTOR STRAIN ENERGY MATRIX. REWIND TAPES B1, B2, & B5 TURN OFF ALL SENSE LIGHTS
READ IN THE FIRST COLUMN OF STRAIN ENERGY MATRIX FROM TAPE B5
COMPUTE δ1 AND γ1
K=0
SET UP LOOPING TO GENERATE THE REMAINING N-1 COLUMS OF THE S UPPER-TRIANGULAR MATRIX, AND THE N-1 ELEMENTS OF THE DIAGONAL MATRIX, ALL IN TRIPLE PRECISION; N IS DEGREES OF FREEDOM
G

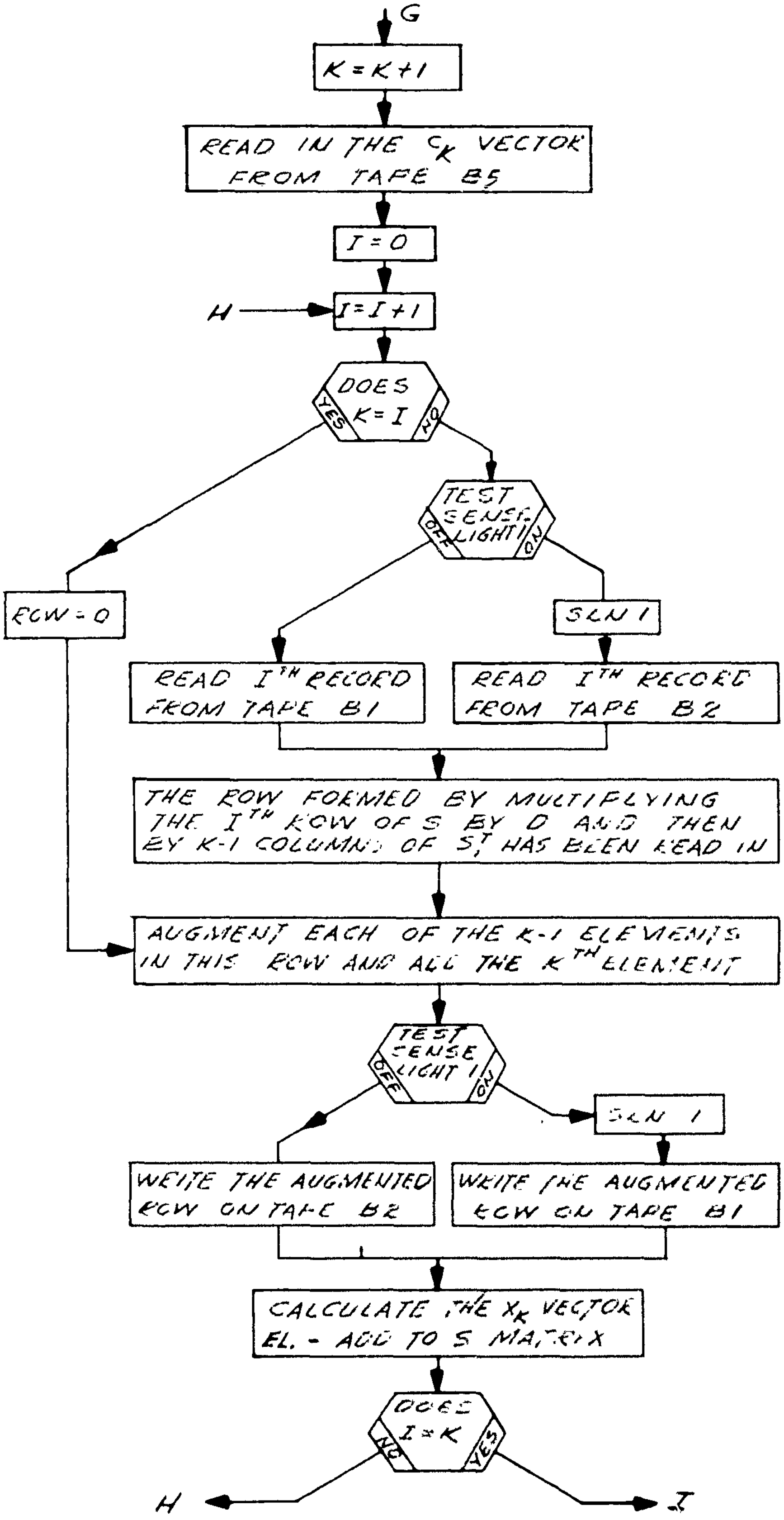
G
K=K+1
READ IN THE C_K VECTOR FROM TAPE B5
I=0
H
I=I+1
DOES K=I
YES
NO
TEST SENSE LIGHT 1
OFF
ON
ROW=0
SLN 1
READ I^{TH} RECORD FROM TAPE B1
READ I^{TH} RECORD FROM TAPE B2
THE ROW FORMED BY MULTIPLYING THE I^{TH} ROW OF S BY D AND THEN BY K-1 COLUMNS OF S^T HAS BEEN READ IN
AUGMENT EACH OF THE K-1 ELEMENTS IN THIS ROW AND ADD THE K^{TH} ELEMENT
TEST SENSE LIGHT 1
OFF
ON
SLN 1
WRITE THE AUGMENTED ROW ON TAPE B2
WRITE THE AUGMENTED ROW ON TAPE B1
CALCULATE THE X_K VECTOR EL. - ADD TO S MATRIX
DOES I=K
NO
YES
H
I

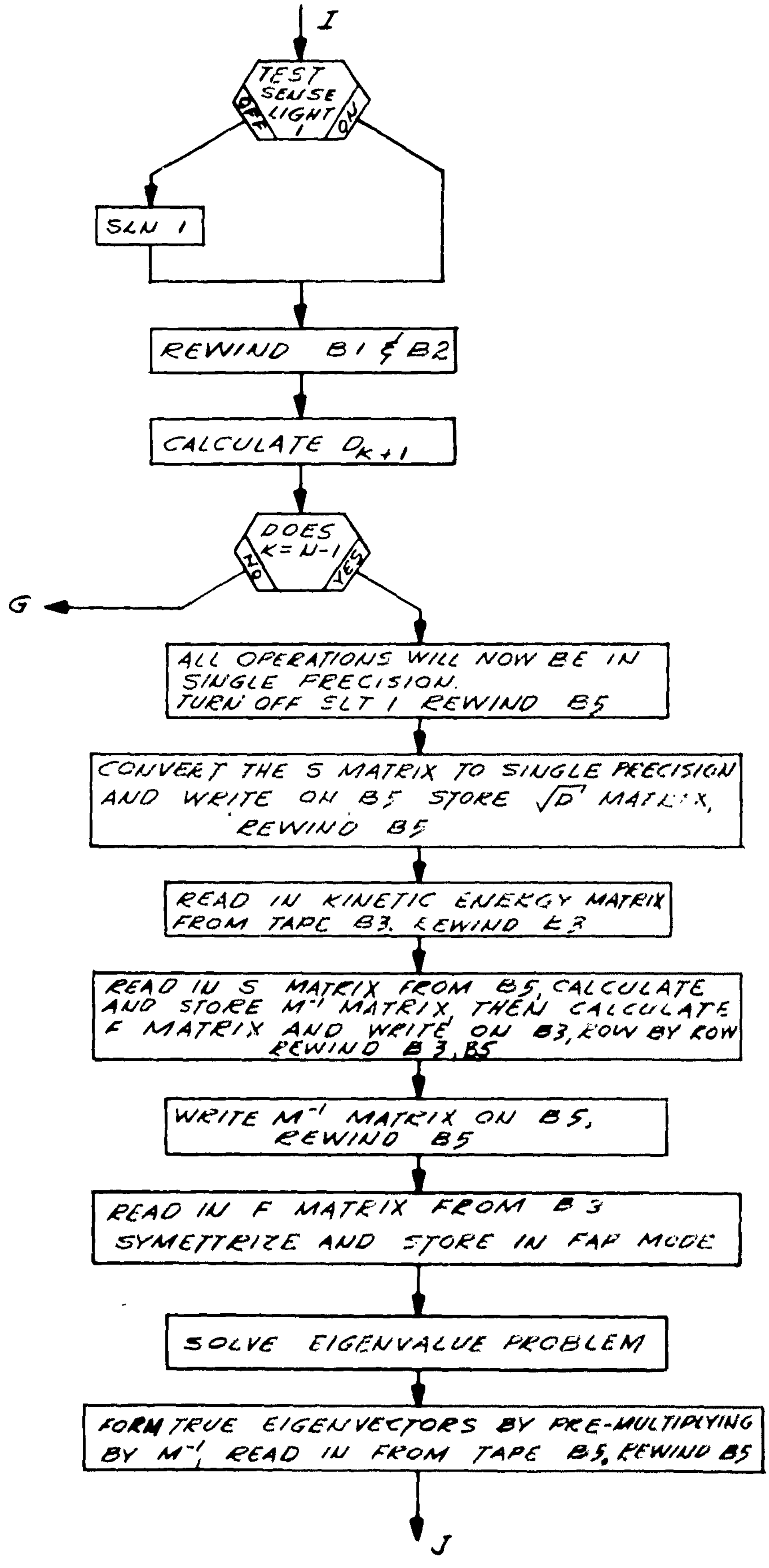
I
TEST SENSE LIGHT 1
OFF
ON
SLN 1
REWIND B1 & B2
CALCULATE D_{K+1}
DOES K = N-1
NO
YES
G
ALL OPERATIONS WILL NOW BE IN SINGLE PRECISION. TURN OFF SLT 1 REWIND B5
CONVERT THE S MATRIX TO SINGLE PRECISION AND WRITE ON B5 STORE $\sqrt{D}$ MATRIX, REWIND B5
READ IN KINETIC ENERGY MATRIX FROM TAPE B3. REWIND B3
READ IN S MATRIX FROM B5, CALCULATE AND STORE M^{-1} MATRIX, THEN CALCULATE F MATRIX AND WRITE ON B3, ROW BY ROW REWIND B3, B5
WRITE M^{-1} MATRIX ON B5, REWIND B5
READ IN F MATRIX FROM B3 SYMETTRIZE AND STORE IN FAP MODE
SOLVE EIGENVALUE PROBLEM
FORM TRUE EIGENVECTORS BY PRE-MULTIPLYING BY M^{-1}, READ IN FROM TAPE B5, REWIND B5
J

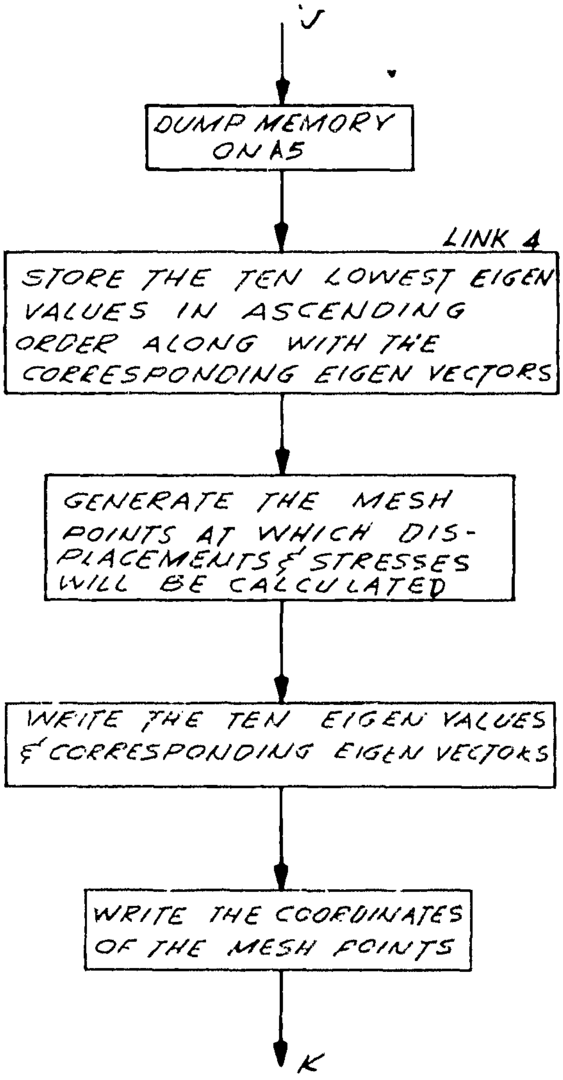
J
DUMP MEMORY ON A5
LINK 4
STORE THE TEN LOWEST EIGEN VALUES IN ASCENDING ORDER ALONG WITH THE CORRESPONDING EIGEN VECTORS
GENERATE THE MESH POINTS AT WHICH DISPLACEMENTS & STRESSES WILL BE CALCULATED
WRITE THE TEN EIGEN VALUES & CORRESPONDING EIGEN VECTORS
WRITE THE COORDINATES OF THE MESH POINTS
K

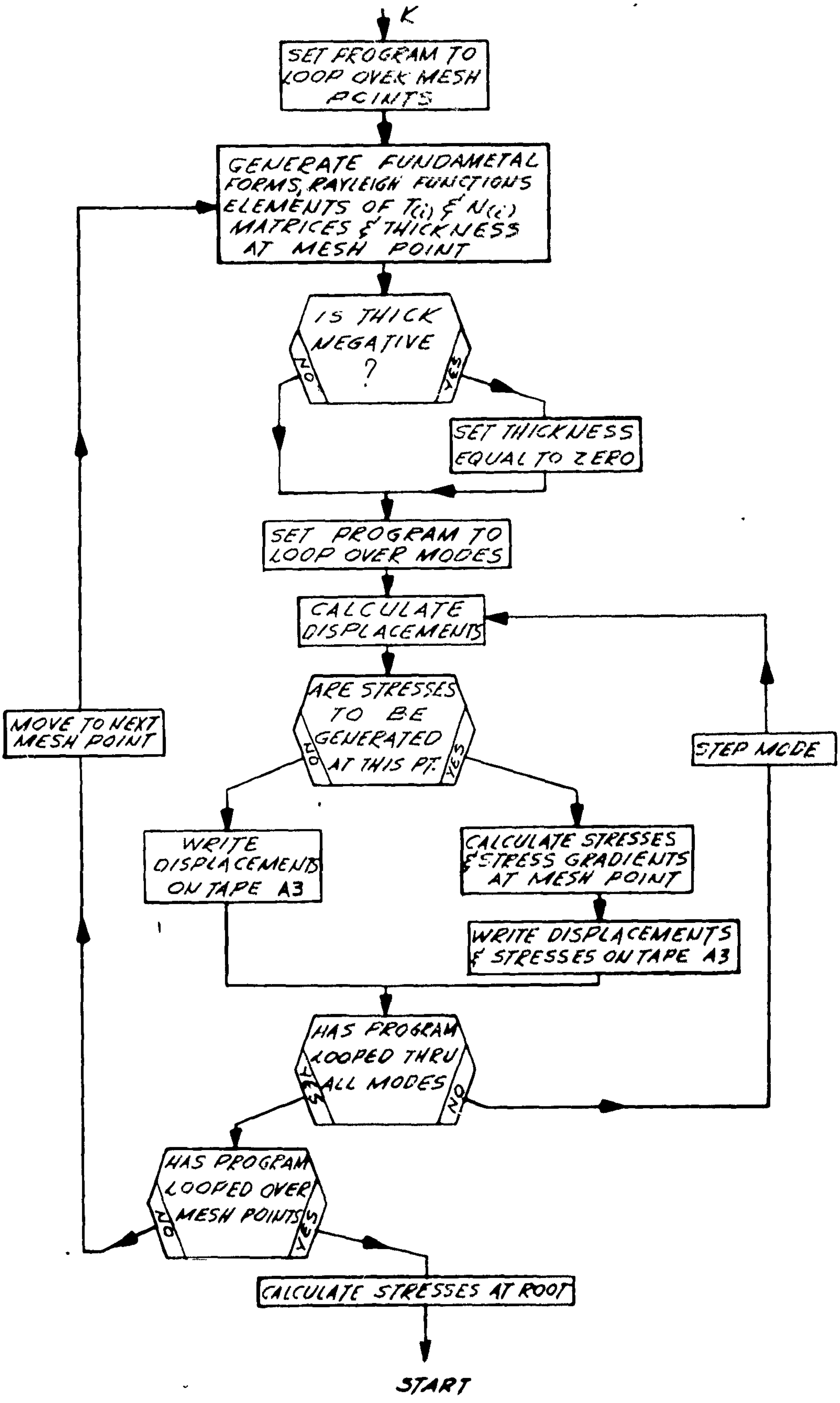
K
SET PROGRAM TO LOOP OVER MESH POINTS
GENERATE FUNDAMETAL FORMS, RAYLEIGH FUNCTIONS ELEMENTS OF T(i) & N(i) MATRICES & THICKNESS AT MESH POINT
IS THICK NEGATIVE ?
NO
YES
SET THICKNESS EQUAL TO ZERO
SET PROGRAM TO LOOP OVER MODES
CALCULATE DISPLACEMENTS
ARE STRESSES TO BE GENERATED AT THIS PT.
NO
YES
STEP MODE
MOVE TO NEXT MESH POINT
WRITE DISPLACEMENTS ON TAPE A3
CALCULATE STRESSES & STRESS GRADIENTS AT MESH POINT
WRITE DISPLACEMENTS & STRESSES ON TAPE A3
HAS PROGRAM LOOPED THRU ALL MODES
YES
NO
HAS PROGRAM LOOPED OVER MESH POINTS
NO
YES
CALCULATE STRESSES AT ROOT
START

BLADE STATIC STRESS ANALYSIS
FLOW DIAGRAM

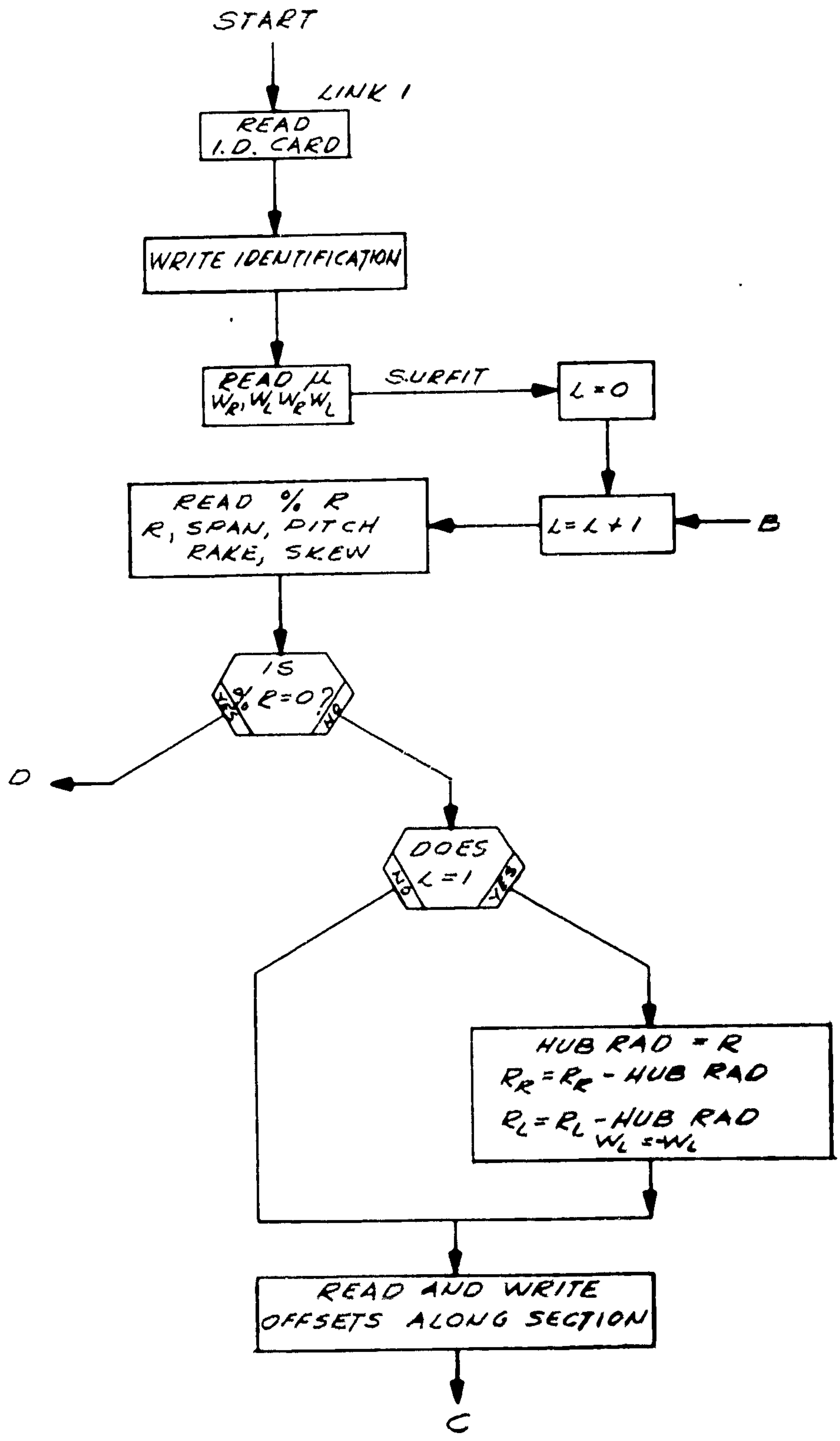
START
LINK 1
READ I.D. CARD
WRITE IDENTIFICATION
READ μ W_R, W_L W_R W_L
SURFIT
$L=0$
$L=L+1$
B
READ % R
R, SPAN, PITCH
RAKE, SKEW
IS %R=0?
YES
NO
D
DOES L=1
NO
YES
HUB RAD = R
$R_R = R_R$ - HUB RAD
$R_L = R_L$ - HUB RAD
$W_L = -W_L$
READ AND WRITE OFFSETS ALONG SECTION
C

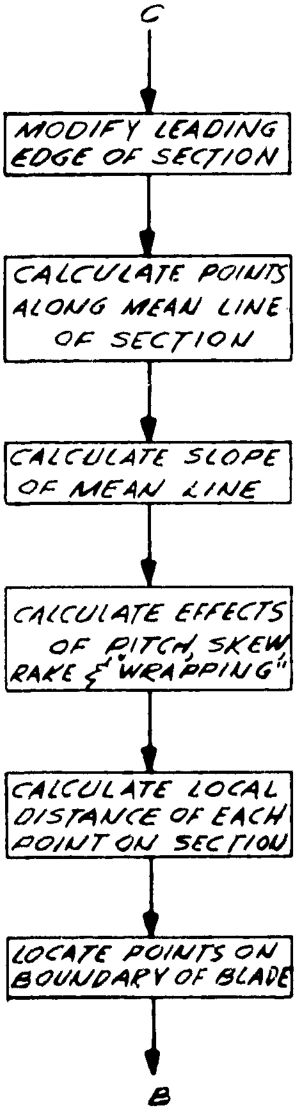
C
MODIFY LEADING EDGE OF SECTION
CALCULATE POINTS ALONG MEAN LINE OF SECTION
CALCULATE SLOPE OF MEAN LINE
CALCULATE EFFECTS OF PITCH, SKEW RAKE & "WRAPPING"
CALCULATE LOCAL DISTANCE OF EACH POINT ON SECTION
LOCATE POINTS ON BOUNDARY OF BLADE
B

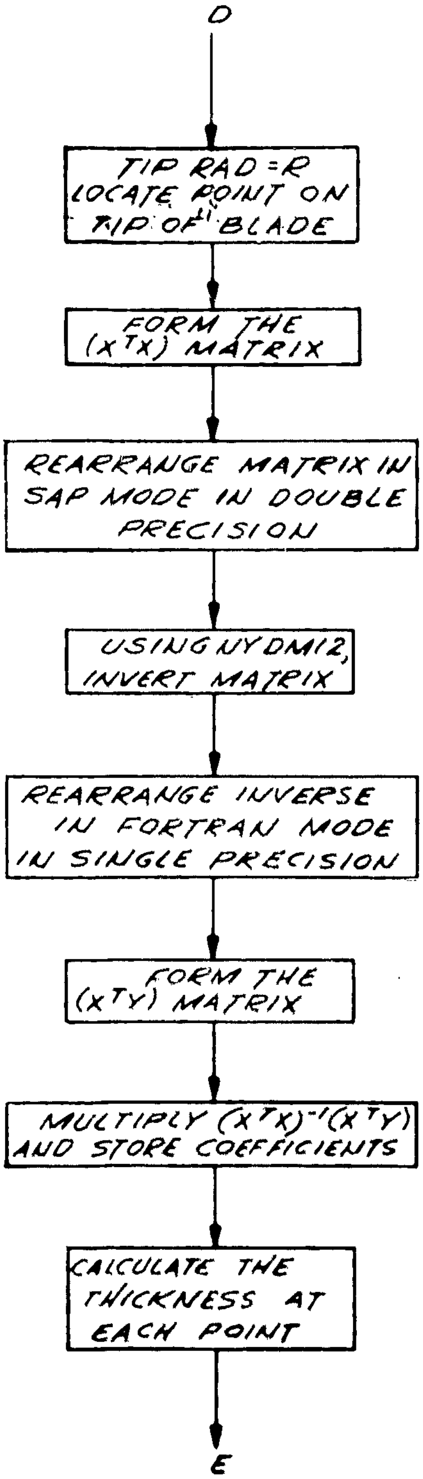
D
TIP RAD = R LOCATE POINT ON TIP OF BLADE
FORM THE (X^TX) MATRIX
REARRANGE MATRIX IN SAP MODE IN DOUBLE PRECISION
USING NYDMI2, INVERT MATRIX
REARRANGE INVERSE IN FORTRAN MODE IN SINGLE PRECISION
FORM THE (X^TY) MATRIX
MULTIPLY $(X^TX)^{-1}(X^TY)$ AND STORE COEFFICIENTS
CALCULATE THE THICKNESS AT EACH POINT
E

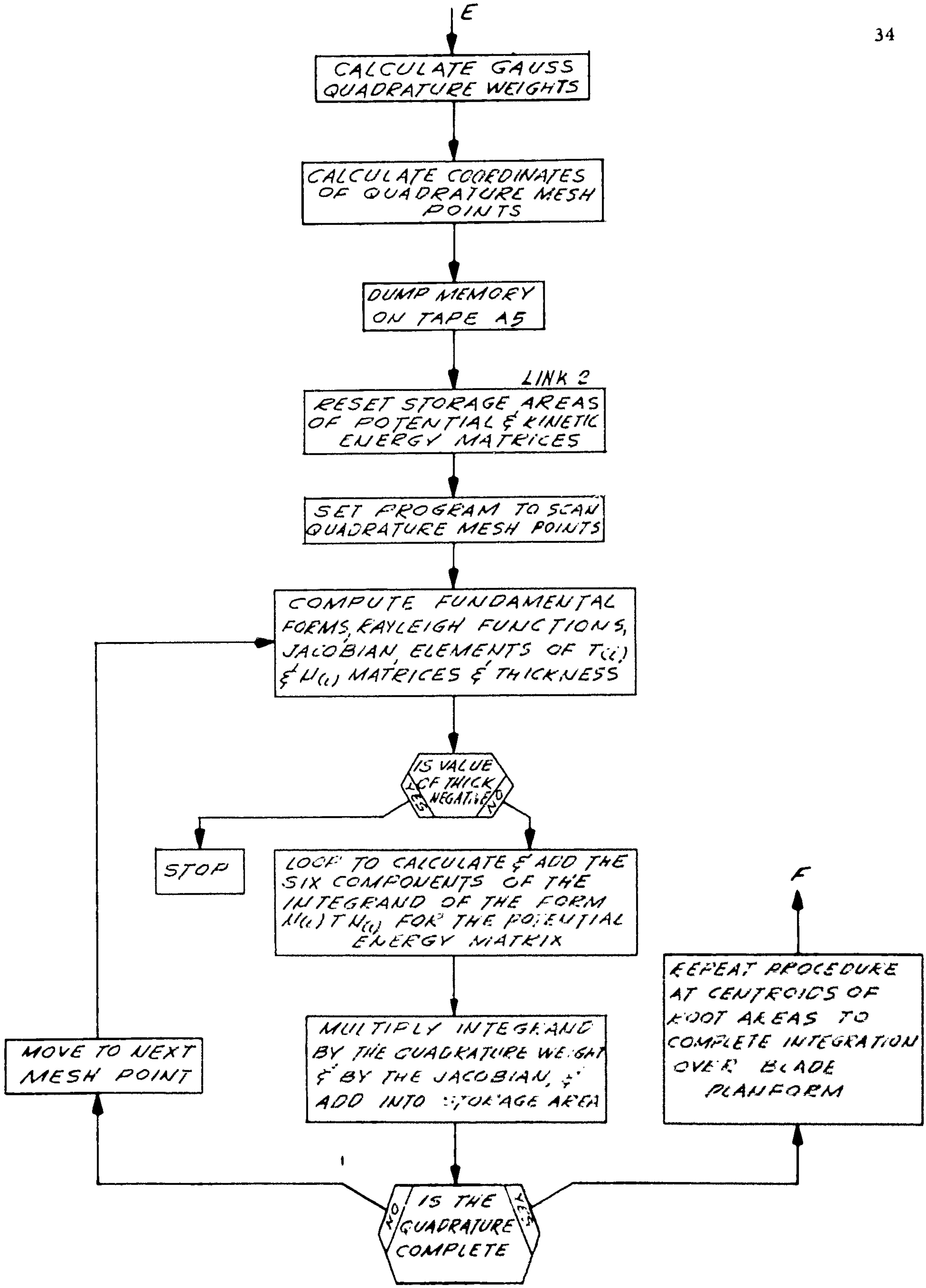
E
CALCULATE GAUSS QUADRATURE WEIGHTS
CALCULATE COORDINATES OF QUADRATURE MESH POINTS
DUMP MEMORY ON TAPE A5
LINK 2
RESET STORAGE AREAS OF POTENTIAL & KINETIC ENERGY MATRICES
SET PROGRAM TO SCAN QUADRATURE MESH POINTS
COMPUTE FUNDAMENTAL FORMS, RAYLEIGH FUNCTIONS, JACOBIAN, ELEMENTS OF T(i) & N(i) MATRICES & THICKNESS
IS VALUE OF THICK NEGATIVE
YES
NO
STOP
LOOP TO CALCULATE & ADD THE SIX COMPONENTS OF THE INTEGRAND OF THE FORM N(i)T N(i) FOR THE POTENTIAL ENERGY MATRIX
MULTIPLY INTEGRAND BY THE QUADRATURE WEIGHT & BY THE JACOBIAN, & ADD INTO STORAGE AREA
MOVE TO NEXT MESH POINT
IS THE QUADRATURE COMPLETE
NO
YES
REPEAT PROCEDURE AT CENTROIDS OF ROOT AREAS TO COMPLETE INTEGRATION OVER BLADE PLANFORM
F

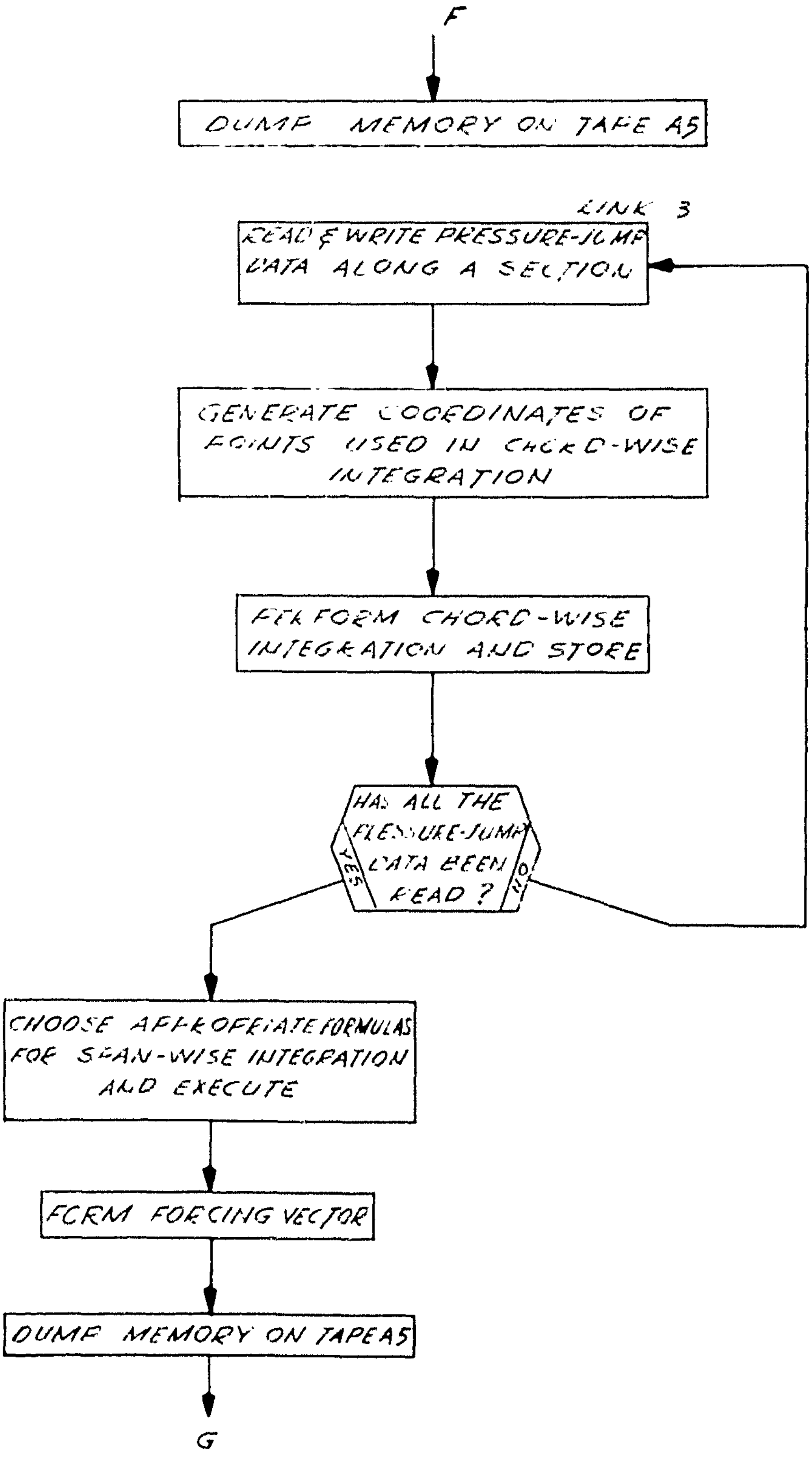
F
DUMP MEMORY ON TAPE A5
LINK 3
READ & WRITE PRESSURE-JUMP DATA ALONG A SECTION
GENERATE COORDINATES OF POINTS USED IN CHORD-WISE INTEGRATION
PERFORM CHORD-WISE INTEGRATION AND STORE
HAS ALL THE PRESSURE-JUMP DATA BEEN READ ?
YES
NO
CHOOSE APPROPRIATE FORMULAS FOR SPAN-WISE INTEGRATION AND EXECUTE
FORM FORCING VECTOR
DUMP MEMORY ON TAPE A5
G

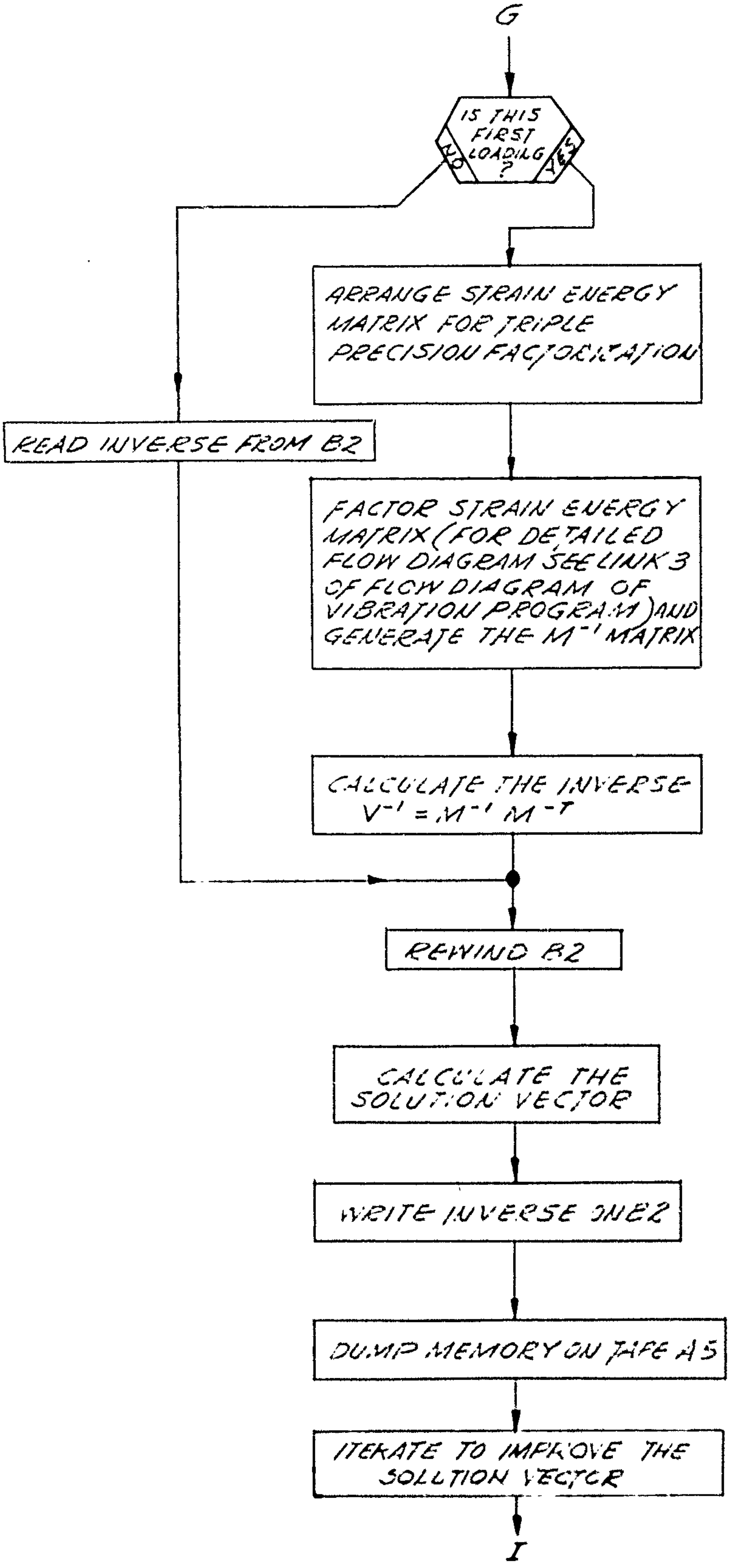
G
IS THIS FIRST LOADING ?
NO
YES
ARRANGE STRAIN ENERGY MATRIX FOR TRIPLE PRECISION FACTORIZATION
READ INVERSE FROM B2
FACTOR STRAIN ENERGY MATRIX (FOR DETAILED FLOW DIAGRAM SEE LINK 3 OF FLOW DIAGRAM OF VIBRATION PROGRAM) AND GENERATE THE M⁻¹ MATRIX
CALCULATE THE INVERSE V⁻¹ = M⁻¹ M⁻ᵀ
REWIND B2
CALCULATE THE SOLUTION VECTOR
WRITE INVERSE ON B2
DUMP MEMORY ON TAPE A5
ITERATE TO IMPROVE THE SOLUTION VECTOR
I

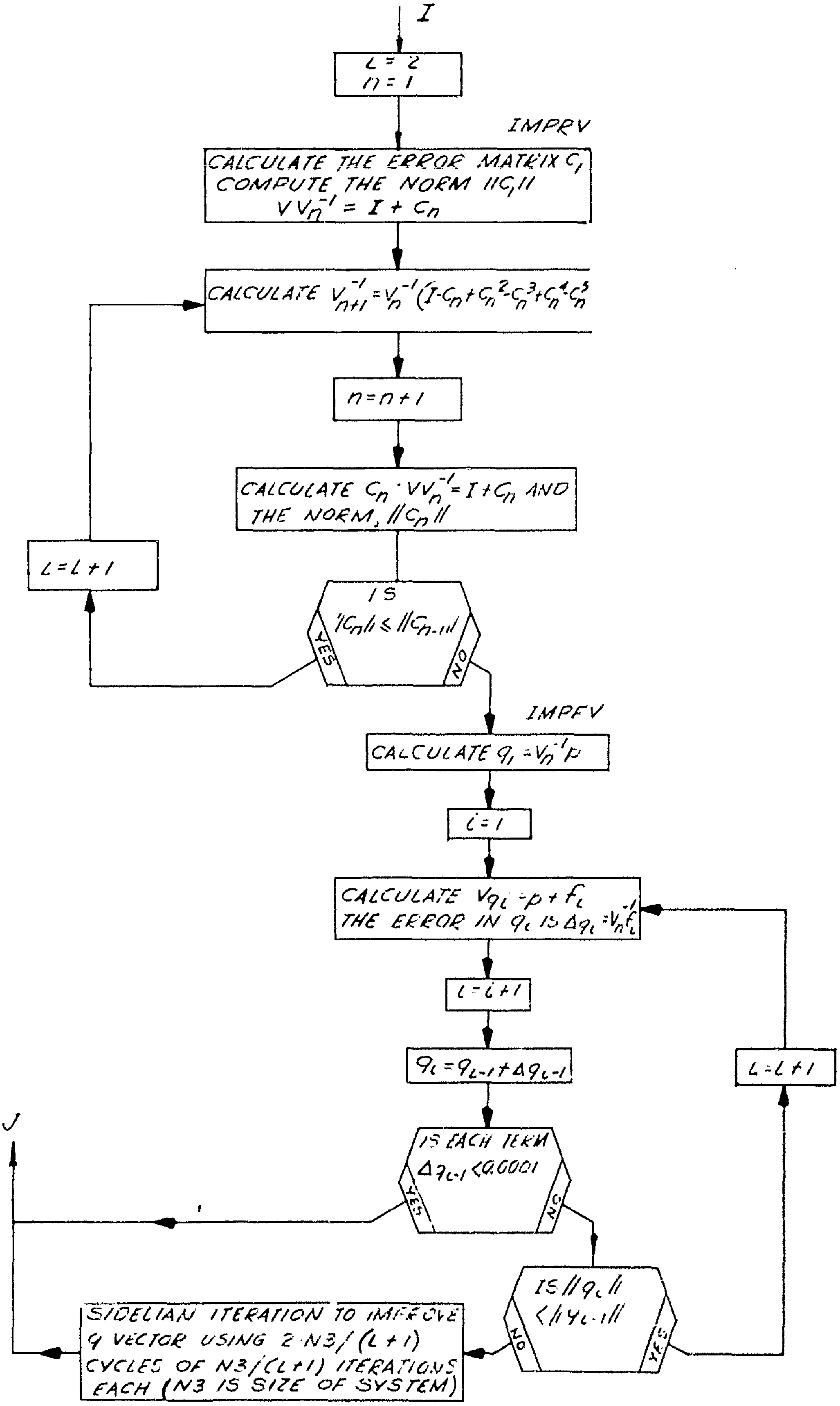
I
L = 2
n = 1
IMPRV
CALCULATE THE ERROR MATRIX C1
COMPUTE THE NORM ‖C1‖
VVn^-1 = I + Cn
CALCULATE Vn+1^-1 = Vn^-1(I-Cn+Cn^2-Cn^3+Cn^4-Cn^5
n=n+1
CALCULATE Cn · VVn^-1 = I+Cn AND
THE NORM, ‖Cn‖
L=L+1
IS ‖Cn‖ ≤ ‖Cn-1‖
YES
NO
IMPEV
CALCULATE q1 = Vn^-1 p
i=1
CALCULATE Vqi = p + fi
THE ERROR IN qi IS Δqi = Vn^-1 fi
i=i+1
qi = qi-1 + Δqi-1
L=L+1
IS EACH TERM
Δqi-1 < 0.0001
YES
NO
J
IS ‖qi‖
< ‖qi-1‖
NO
YES
SIDELIAN ITERATION TO IMPROVE
q VECTOR USING 2·N3/(L+1)
CYCLES OF N3/(L+1) ITERATIONS
EACH (N3 IS SIZE OF SYSTEM)

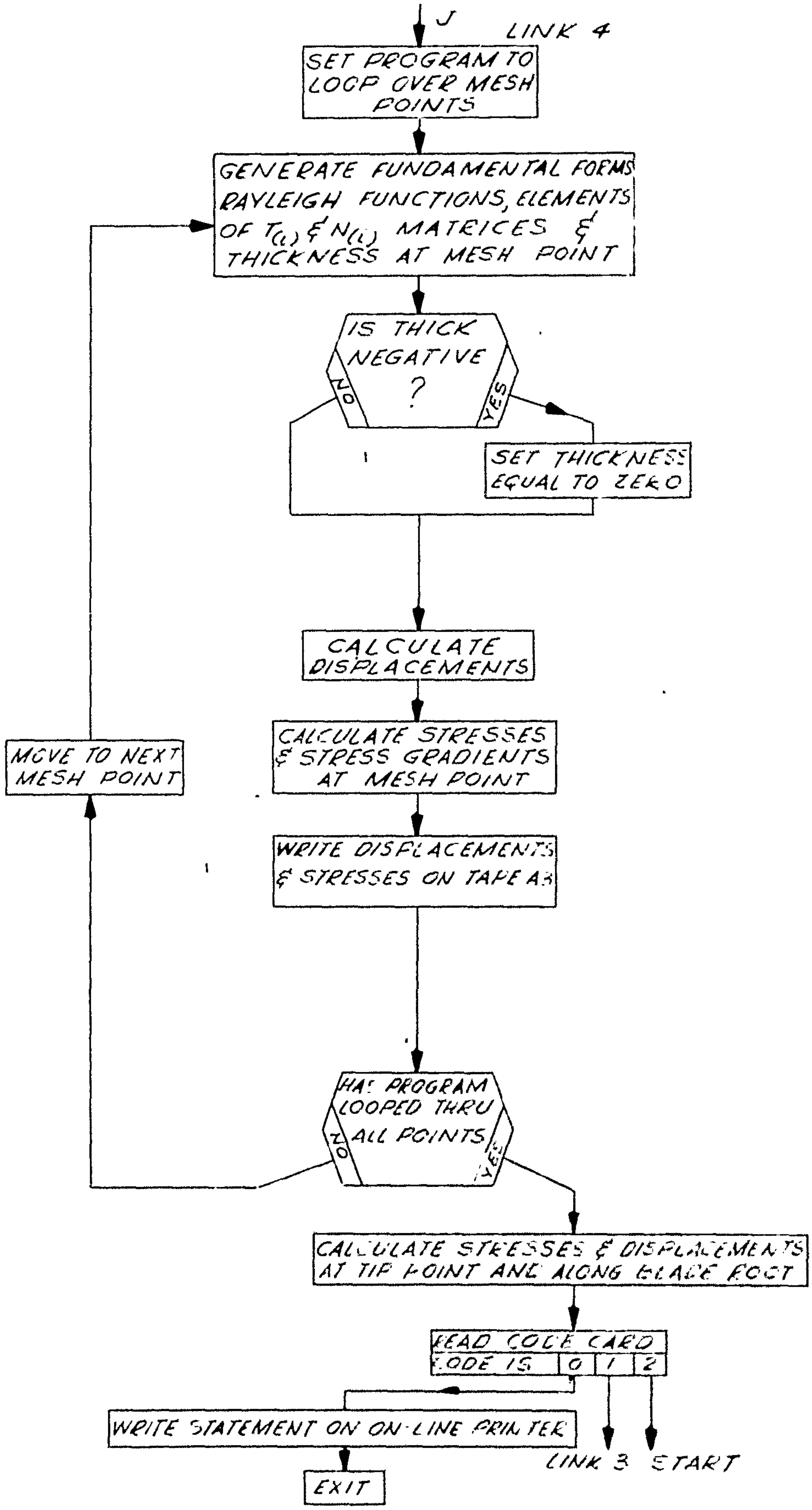
J
LINK 4
SET PROGRAM TO LOOP OVER MESH POINTS
GENERATE FUNDAMENTAL FORMS RAYLEIGH FUNCTIONS, ELEMENTS OF $T_{(i)}$ & $N_{(i)}$ MATRICES & THICKNESS AT MESH POINT
IS THICK NEGATIVE ?
NO
YES
SET THICKNESS EQUAL TO ZERO
CALCULATE DISPLACEMENTS
CALCULATE STRESSES & STRESS GRADIENTS AT MESH POINT
MOVE TO NEXT MESH POINT
WRITE DISPLACEMENTS & STRESSES ON TAPE A3
HAS PROGRAM LOOPED THRU ALL POINTS
NO
YES
CALCULATE STRESSES & DISPLACEMENTS AT TIP POINT AND ALONG BLADE ROOT
READ CODE CARD
CODE IS 0 1 2
WRITE STATEMENT ON ON-LINE PRINTER
EXIT
LINK 3
START

VI. COMPARISON OF RESULTS

Vibration Program:

The table below lists the experimental frequencies obtained from a model of the DD 828 propeller blade (Reference 4), and computed frequencies utilizing 45 degrees of freedom, which was the limit for the previous IBM 704 program, and 90 degrees of freedom. An 8 x 9 quadrature integrating mesh was used for both computer runs. A density of 0.31 lbs./cu. in. and a modulus of elasticity of 15 · 10^6 psi, were assumed. The scale factor between the model and the actual blade is 10.125.

The comparison is made on the basis of similar mode shapes. Note that the mode shape for the third experimental mode corresponds with that obtained by the computer for its second mode, and vise-versa.

MODEL

Mode	Computed		Experimental
	45	90	
1	573	480	446
2	949	800	981 (3)
3	1140	1017	945 (2)
4	1392	1139	1220
5	1496	1392	--
6	2005	1610	1425
7	2441	1845	1640
8	2577	2111	1890
9	2753	2210 (84)	2097
10	3062	2450 (84)	2350

The tables on the following pages indicate the asymptotic behavior of the eigenvalues (and natural frequencies), as the number of degrees of freedom prescribed, is increased. This behavior is graphically illustrated on page 43.

The mode shapes are shown on pages 44 to 53 . The solid lines are drawn from data generated by the program; the broken lines were those detected experimentally. It became increasingly difficult for the experimenter to obtain the mode shapes as the frequency increased; therefore, no comparison is attempted beyond mode number 7.

COMPARISON OF EIGENVALUES

MODE	DEGREES OF FREEDOM					
	30	45	63	75	84	90
1	$0.125\cdot 10^{-4}$	$0.915\cdot 10^{-5}$	$0.776\cdot 10^{-5}$	$0.674\cdot 10^{-5}$	$0.645\cdot 10^{-5}$	$0.641\cdot 10^{-5}$
2	$0.348\cdot 10^{-4}$	$0.251\cdot 10^{-4}$	$0.208\cdot 10^{-4}$	$0.193\cdot 10^{-4}$	$0.182\cdot 10^{-4}$	$0.178\cdot 10^{-4}$
3	$0.455\cdot 10^{-4}$	$0.362\cdot 10^{-4}$	$0.325\cdot 10^{-4}$	$0.306\cdot 10^{-4}$	$0.302\cdot 10^{-4}$	$0.288\cdot 10^{-4}$
4	$0.947\cdot 10^{-4}$	$0.540\cdot 10^{-4}$	$0.413\cdot 10^{-4}$	$0.391\cdot 10^{-4}$	$0.387\cdot 10^{-4}$	$0.361\cdot 10^{-4}$
5	$0.975\cdot 10^{-4}$	$0.623\cdot 10^{-4}$	$0.599\cdot 10^{-4}$	$0.546\cdot 10^{-4}$	$0.545\cdot 10^{-4}$	$0.540\cdot 10^{-4}$
6	$0.175\cdot 10^{-3}$	$0.112\cdot 10^{-3}$	$0.814\cdot 10^{-4}$	$0.788\cdot 10^{-4}$	$0.759\cdot 10^{-4}$	$0.722\cdot 10^{-4}$
7	$0.211\cdot 10^{-3}$	$0.166\cdot 10^{-3}$	$0.118\cdot 10^{-3}$	$0.103\cdot 10^{-3}$	$0.953\cdot 10^{-4}$	$0.948\cdot 10^{-4}$
8	$0.316\cdot 10^{-3}$	$0.185\cdot 10^{-3}$	$0.145\cdot 10^{-3}$	$0.130\cdot 10^{-3}$	$0.130\cdot 10^{-3}$	$0.124\cdot 10^{-3}$
9	$0.434\cdot 10^{-3}$	$0.211\cdot 10^{-3}$	$0.154\cdot 10^{-3}$	$0.138\cdot 10^{-3}$	$0.136\cdot 10^{-3}$	
10	$0.495\cdot 10^{-3}$	$0.261\cdot 10^{-3}$	$0.203\cdot 10^{-3}$	$0.179\cdot 10^{-3}$	$0.167.10^{-3}$	

COMPARISON OF FREQUENCIES FOR VARYING DEGREES OF FREEDOM

MODE	DEGREES OF FREEDOM					
	30	45	63	75	84	90
1	66.1	56.6	52.1	48. 6	47.5	47.4
2	110	93.7	85.3	82.2	79.4	78.9
3	126	113	107	104	103	100
4	182	137	120	117	116	112
5	185	148	145	138	138	137
6	248	198	169	166	163	159
7	272	241	203	190	183	182
8	333	254	225	213	211	208
9	340	272	232	220	218	
10	416	302	267	250	242	

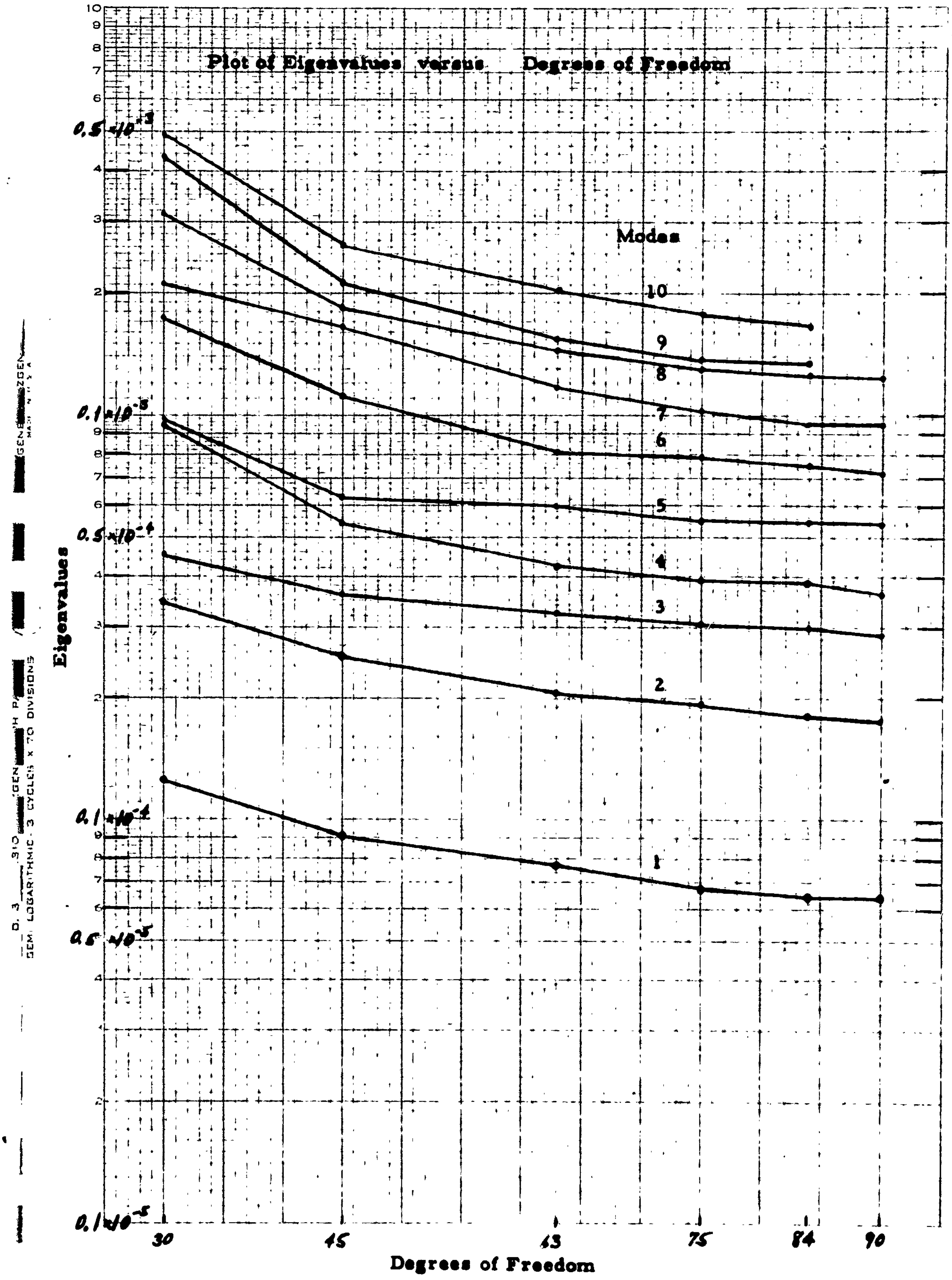
Plot of Eigenvalues versus Degrees of Freedom
Modes
10
9
8
7
6
5
4
3
2
1
Eigenvalues
0.5×10⁻³
0.1×10⁻³
0.5×10⁻⁴
0.1×10⁻⁴
0.5×10⁻⁵
0.1×10⁻⁵
30
45
63
75
84
90
Degrees of Freedom
SEMI LOGARITHMIC 3 CYCLES X 70 DIVISIONS

PROPELLER BLADE

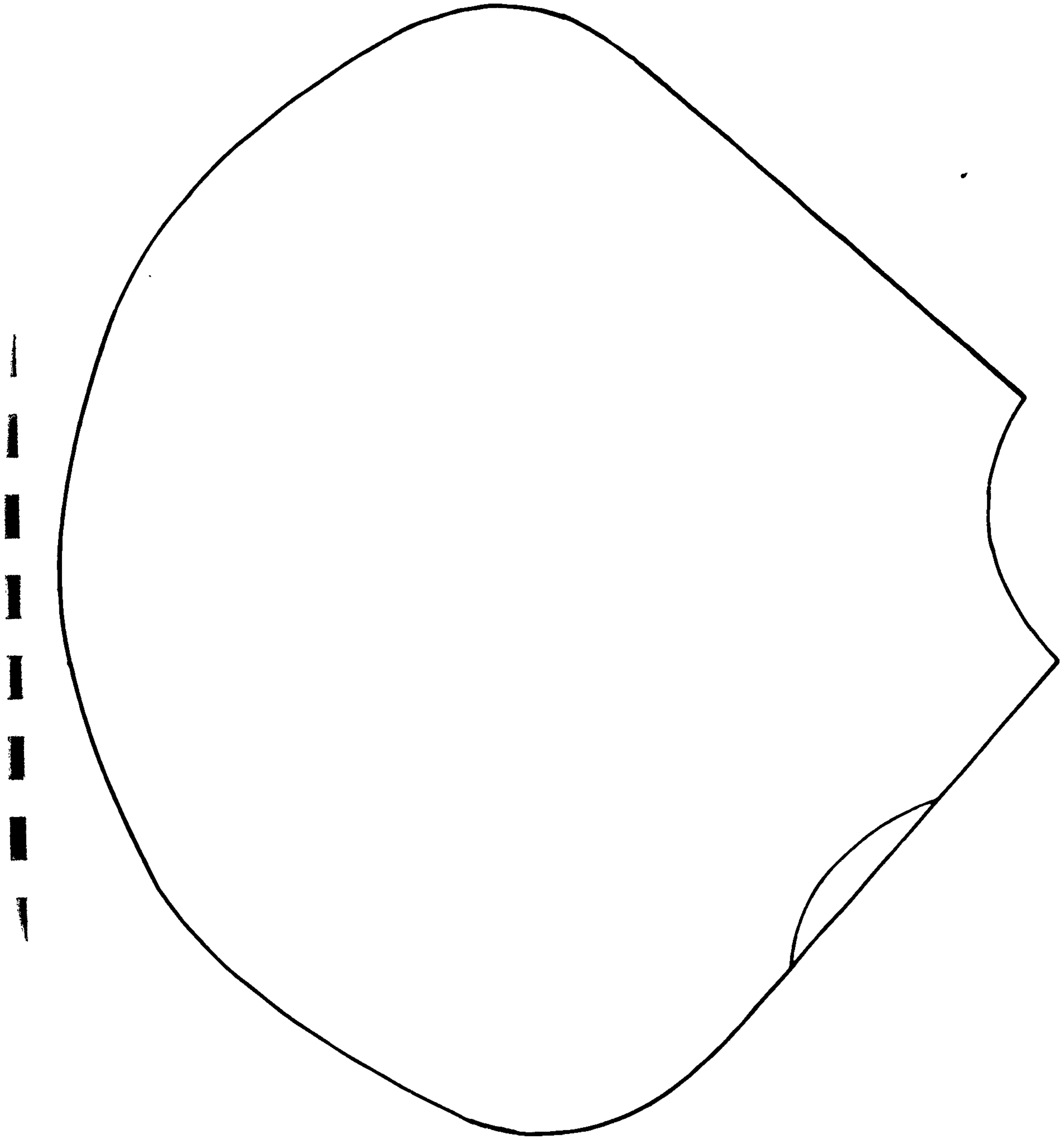

MODE NO. 1

PROPELLER BLADE

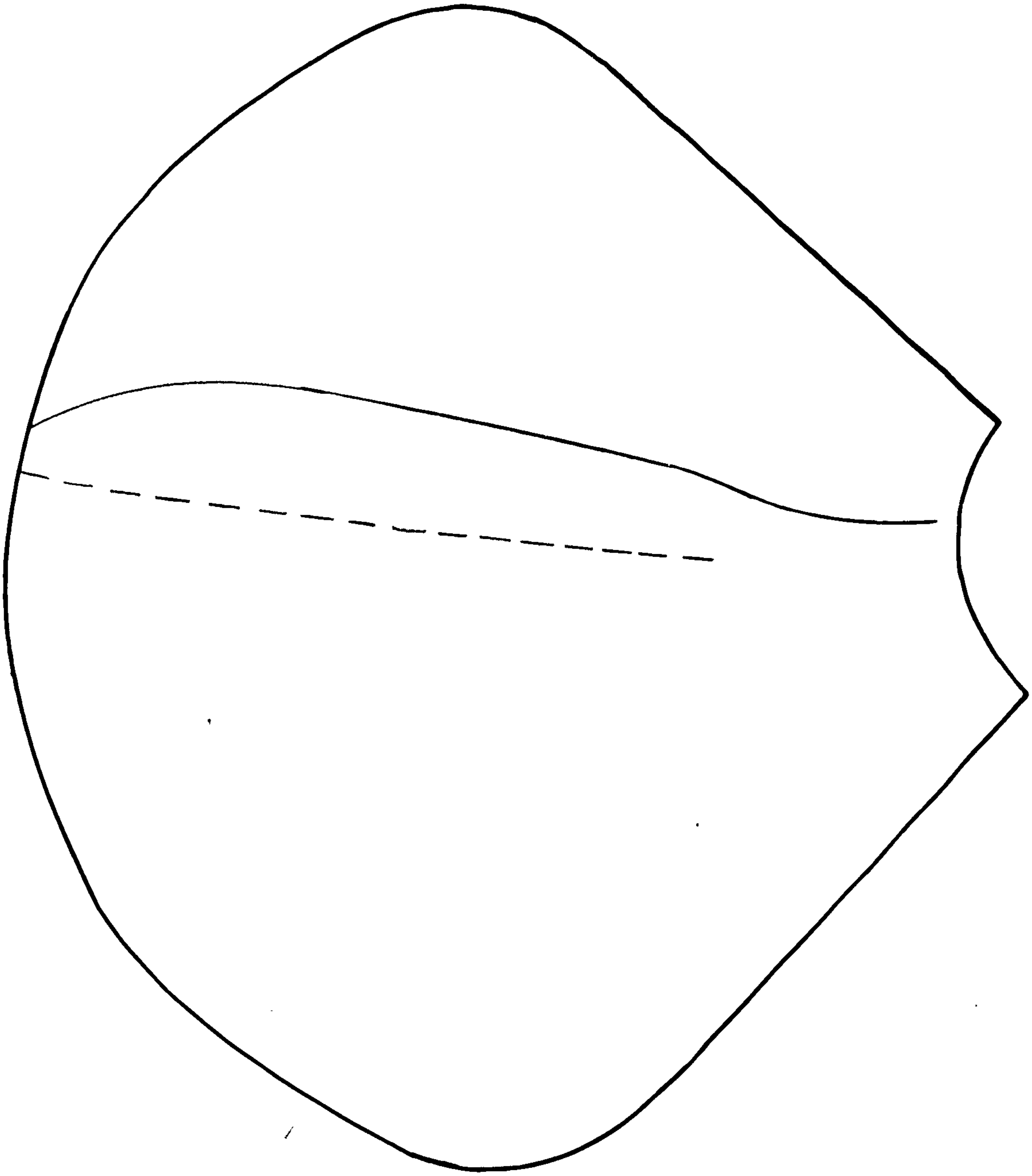

MODE NO. 2

PROPELLER BLADE.

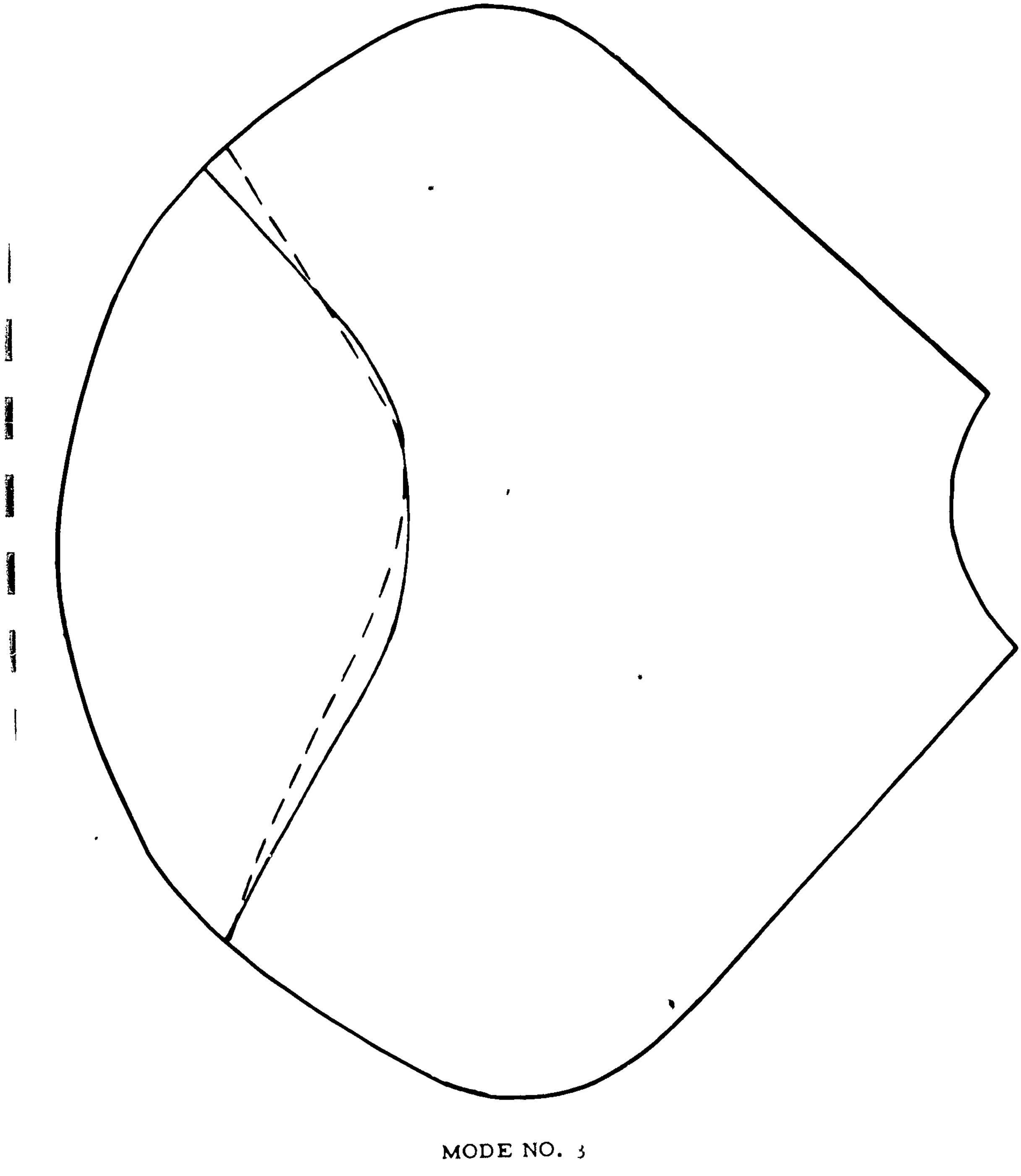

MODE NO. 3

PROPELLER BLADE

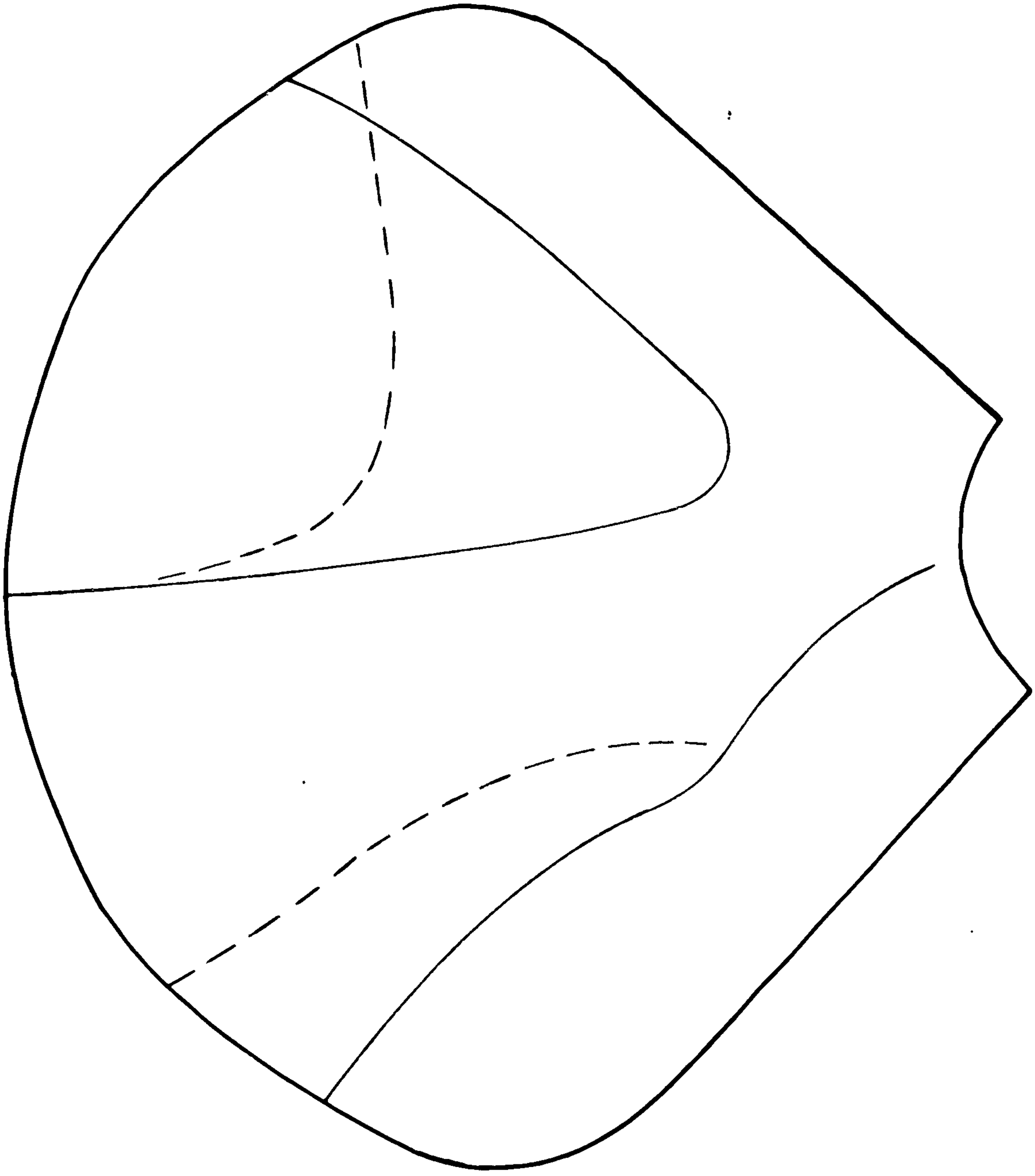

MODE NO. 4

PROPELLER BLADE

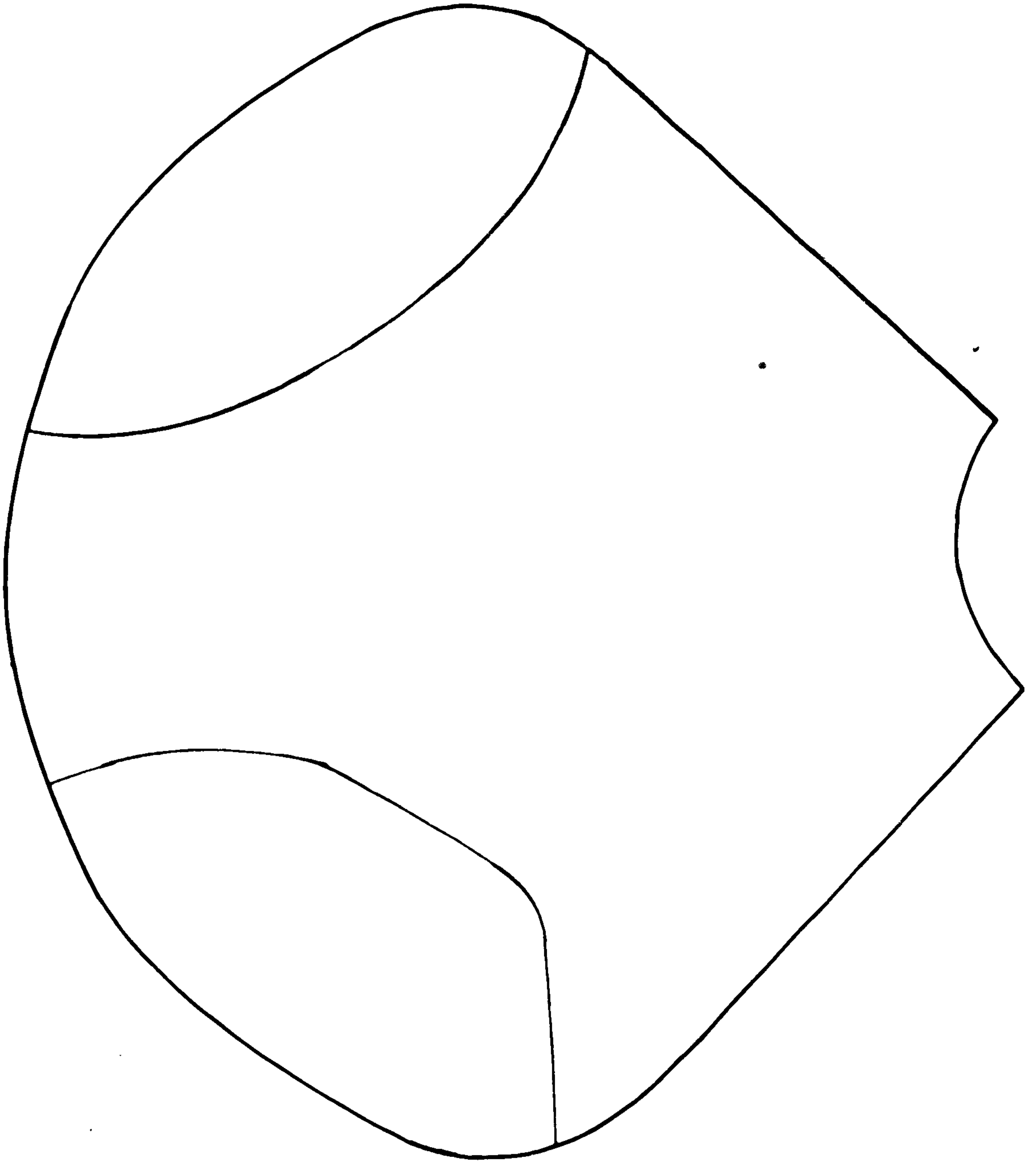

MODE NO. 5

PROPELLER BLADE

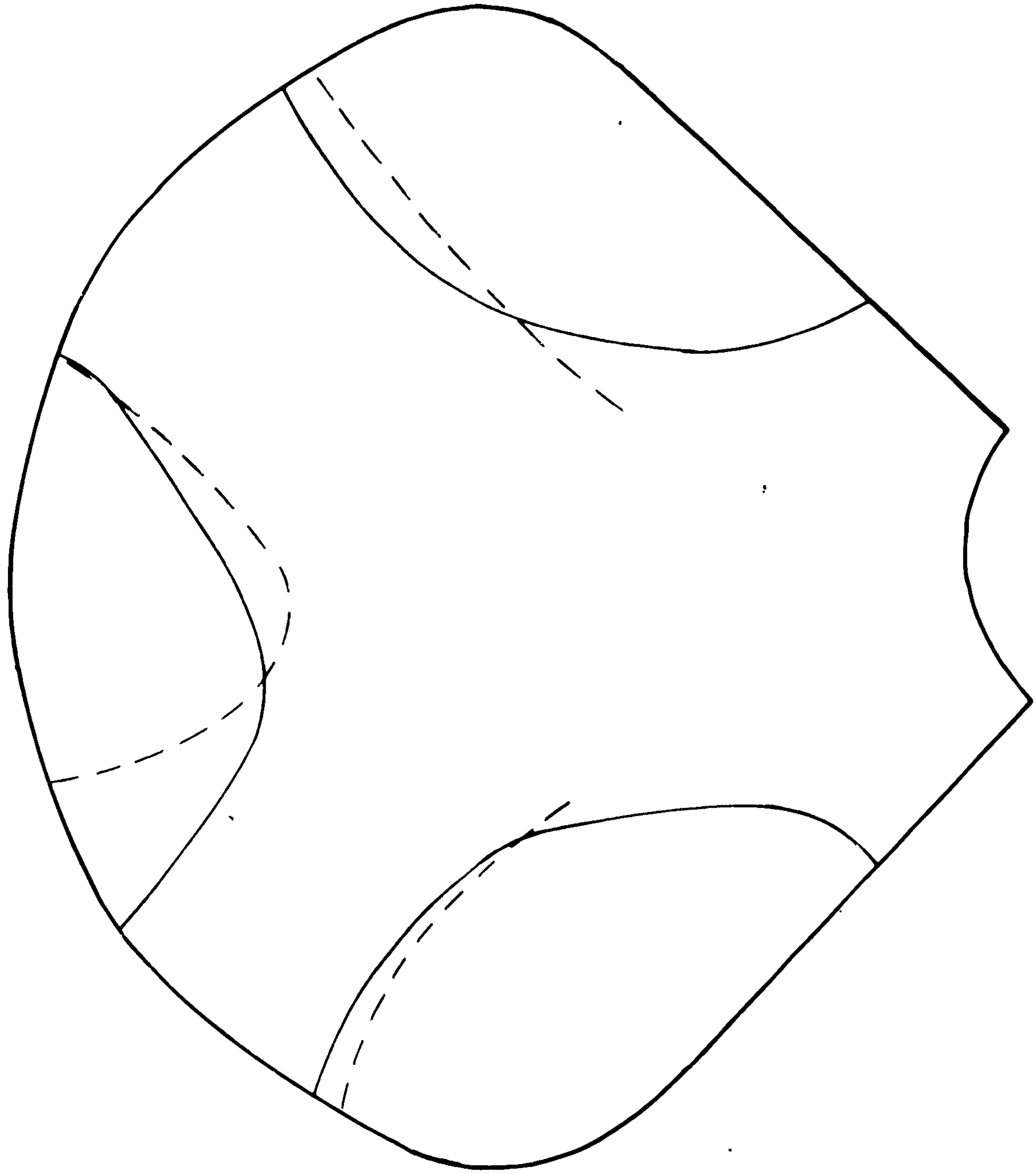

MODE NO. 6

PROPELLER BLADE

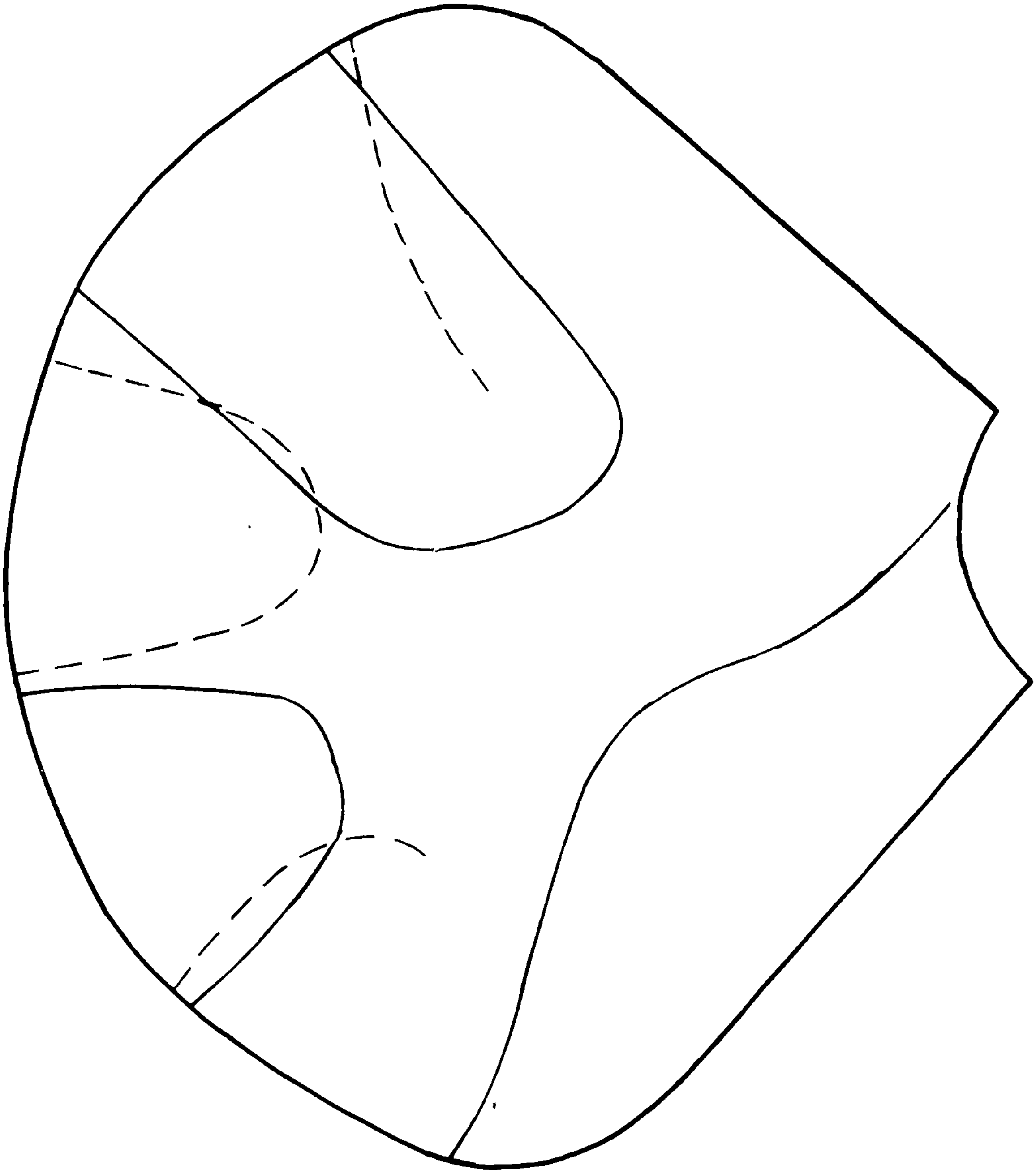

MODE NO. 7

PROPELLER BLADE

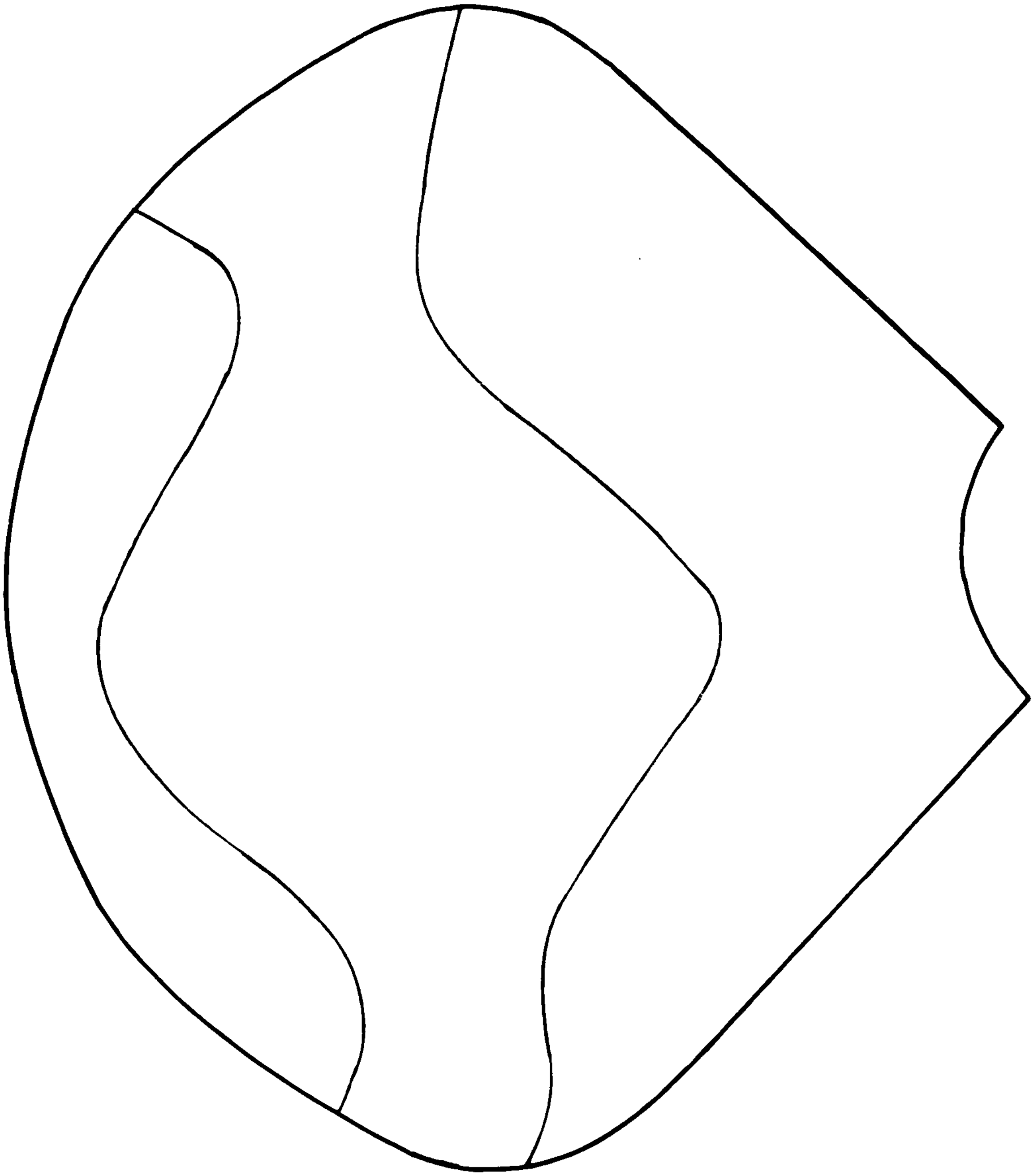

MODE NO. 8

PROPELLER BLADE

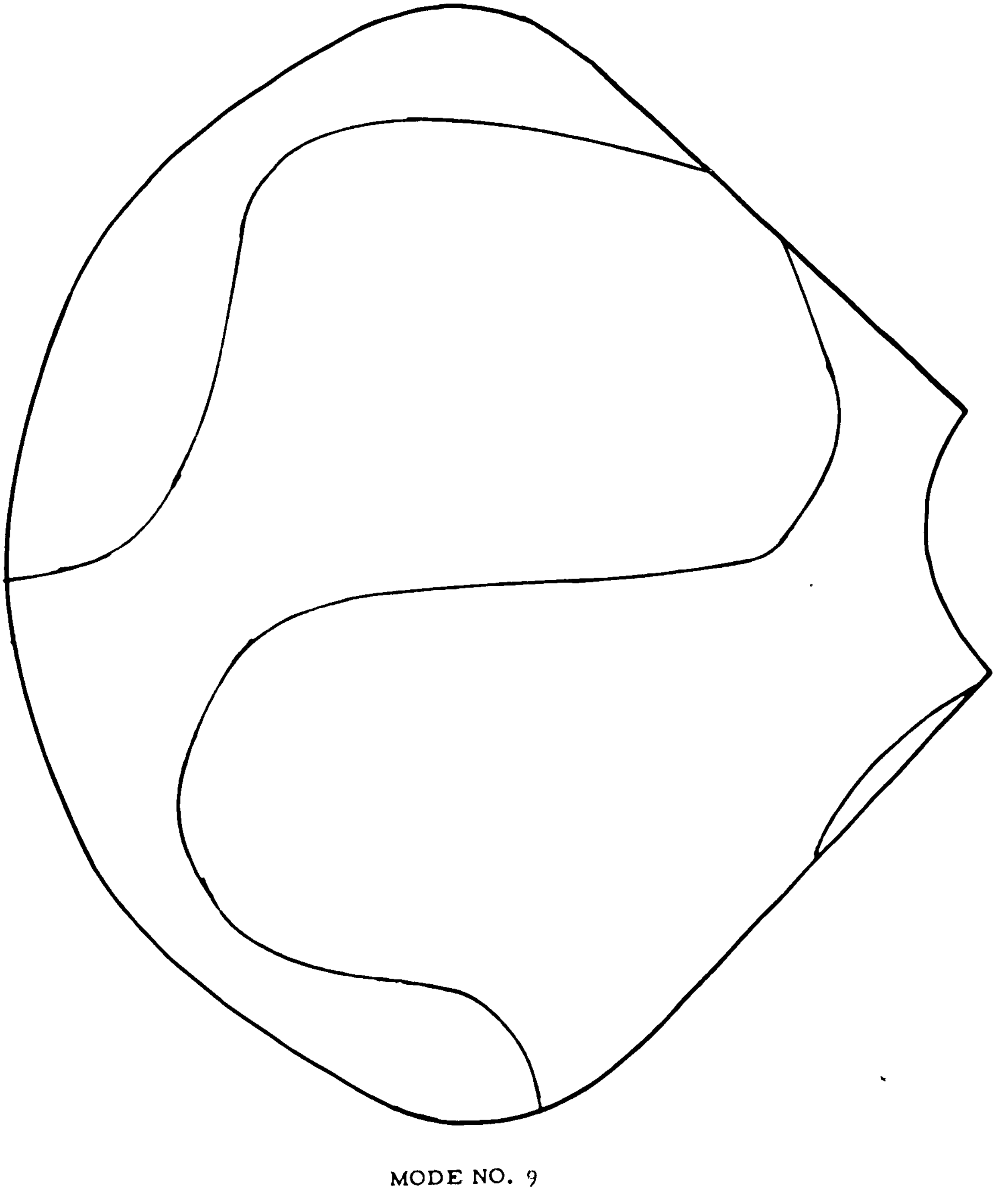

MODE NO. 9

PROPELLER BLADE

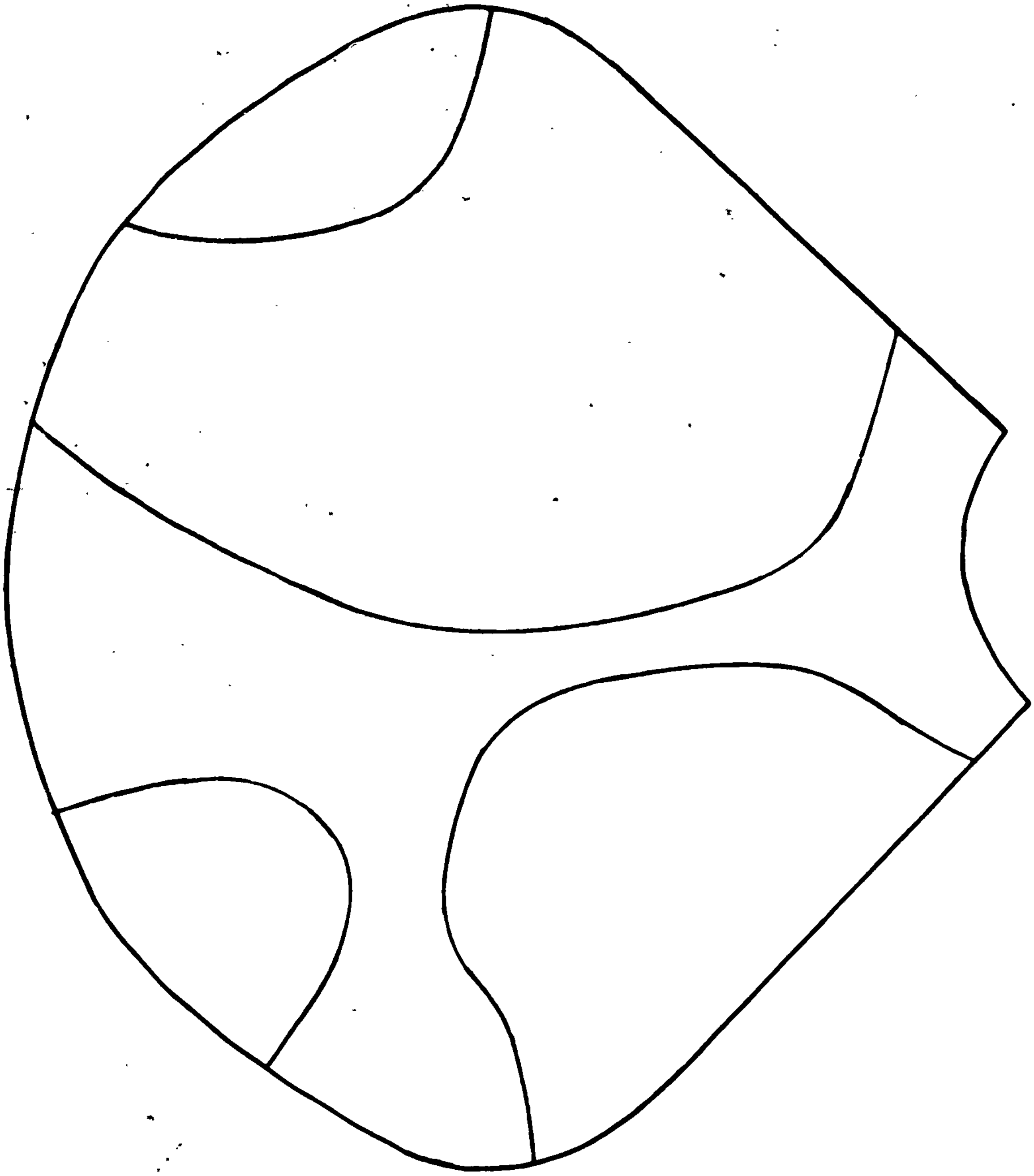

MODE NO. 10

Stress Program

The stress program is subject to the same round-off error problems associated with the vibration program. Indeed, the triple-precision technique used to factor the strain energy matrix, is identical for the two programs. Thus the same restrictions on maximum size of the system that apply for the vibration program, also apply for the stress program.

A parallel series of test runs was conducted on the DD828 propeller blade, using a "peaked" pressure-jump loading. Two runs were conducted at 84 degrees of freedom, one using twice as many iterations to improve the solution vector, as is normally used. The results of the two runs were practically identical, indicating that an adequate number of iterations are being used and that the solution of the system of linear equations, is accurate. Another series of test runs was conducted on a stainless steel propeller, loaded with a uniform pressure distribution.

Discussion

The results of the first series of runs were conducted using 45, 63 and 84 degrees of freedom, and are indicated graphically on the following pages. In addition, detailed displacement and stress distributions are plotted over the blade planform for the run utilizing 84 degrees of freedom.

It is worth noting that as the size of the system grows, the free boundary conditions are satisfied with increasing accuracy. The graph on page 57 clearly indicates this trend, with the span-wise stress (σ^{11}) virtually vanishing at the blade tip for the run utilizing 84 degrees of freedom. In addition, this trend is also true for the chord-wise stress (σ^{22}), indicated on page 56.

The final results obtained by using 84 degrees of freedom for the stainless steel propeller, are graphically shown on pages 58 to 67 .

NO. 340R 20 DIETZGEN GRAPH PAPER
20 X 20 PER INCH

EUGENE DIETZGEN CO.
MADE IN U. S. A.

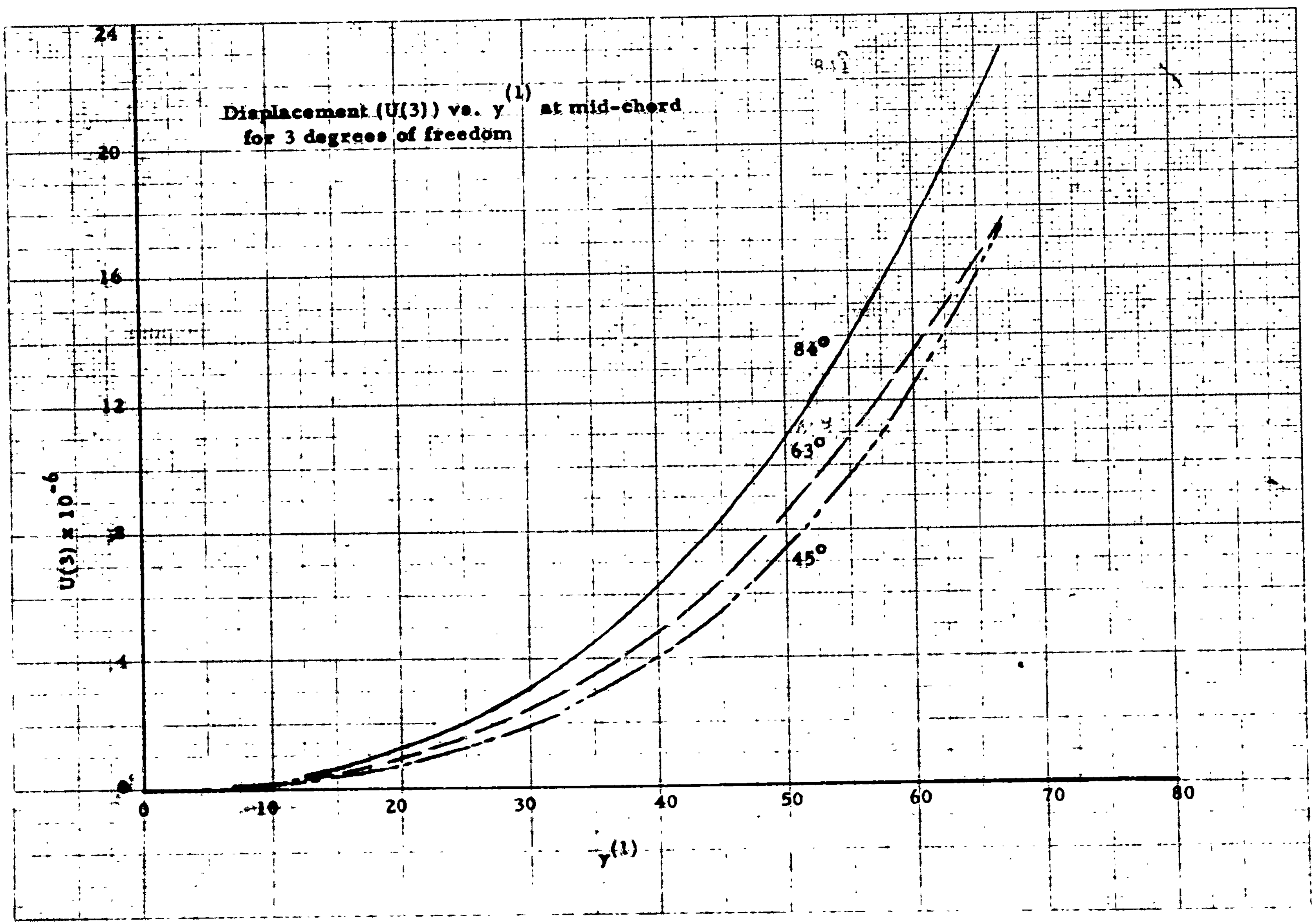

Displacement (U(3)) vs. $y^{(1)}$ at mid-chord for 3 degrees of freedom

NO. 340R-20 DIETZGEN GRAPH PAPER
20 X 20 PER INCH

EUGENE DIETZGEN CO.
MADE IN U. S. A.

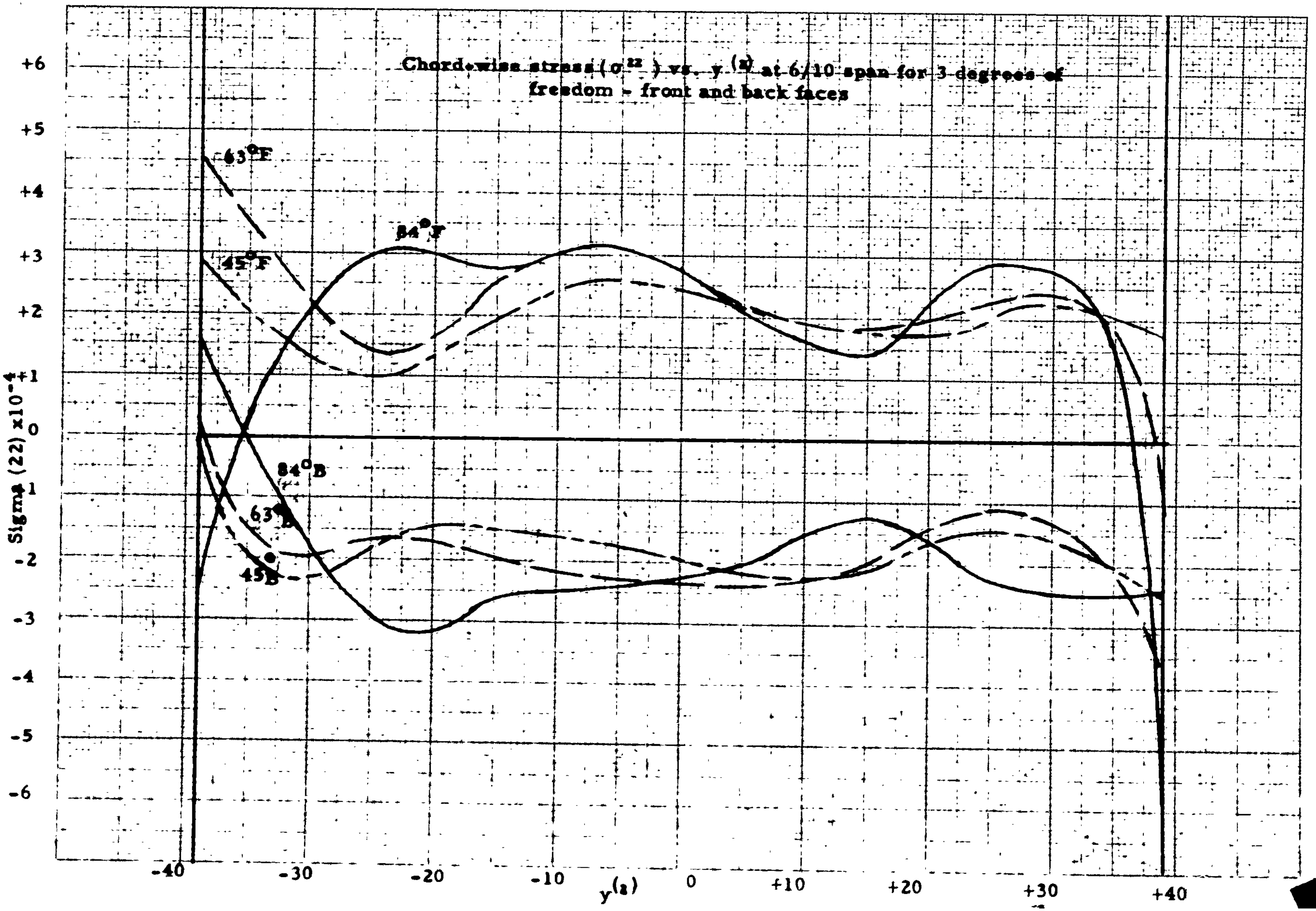

Chordwise stress (σ^{22}) vs. $y^{(2)}$ at 6/10 span for 3 degrees of freedom - front and back faces

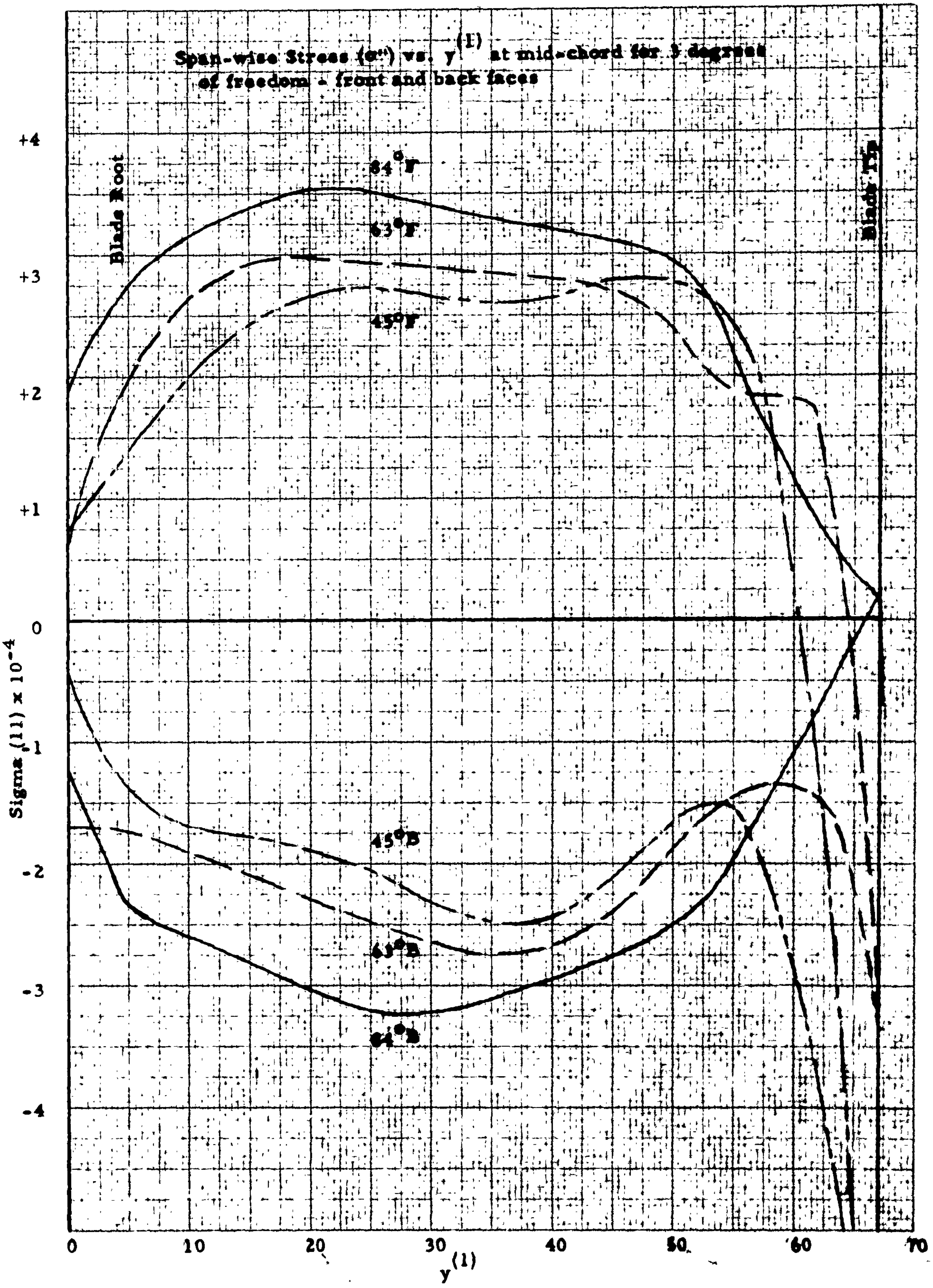

Span-wise Stress (σ'') vs. $y^{(1)}$ at mid-chord for 3 degrees of freedom - front and back faces

EUGENE DIETZGEN CO.
MADE IN U. S. A.

NO. 340R 20 DIETZGEN GRAPH PAPER
20 X 20 PER INCH

PROPELLER BLADE

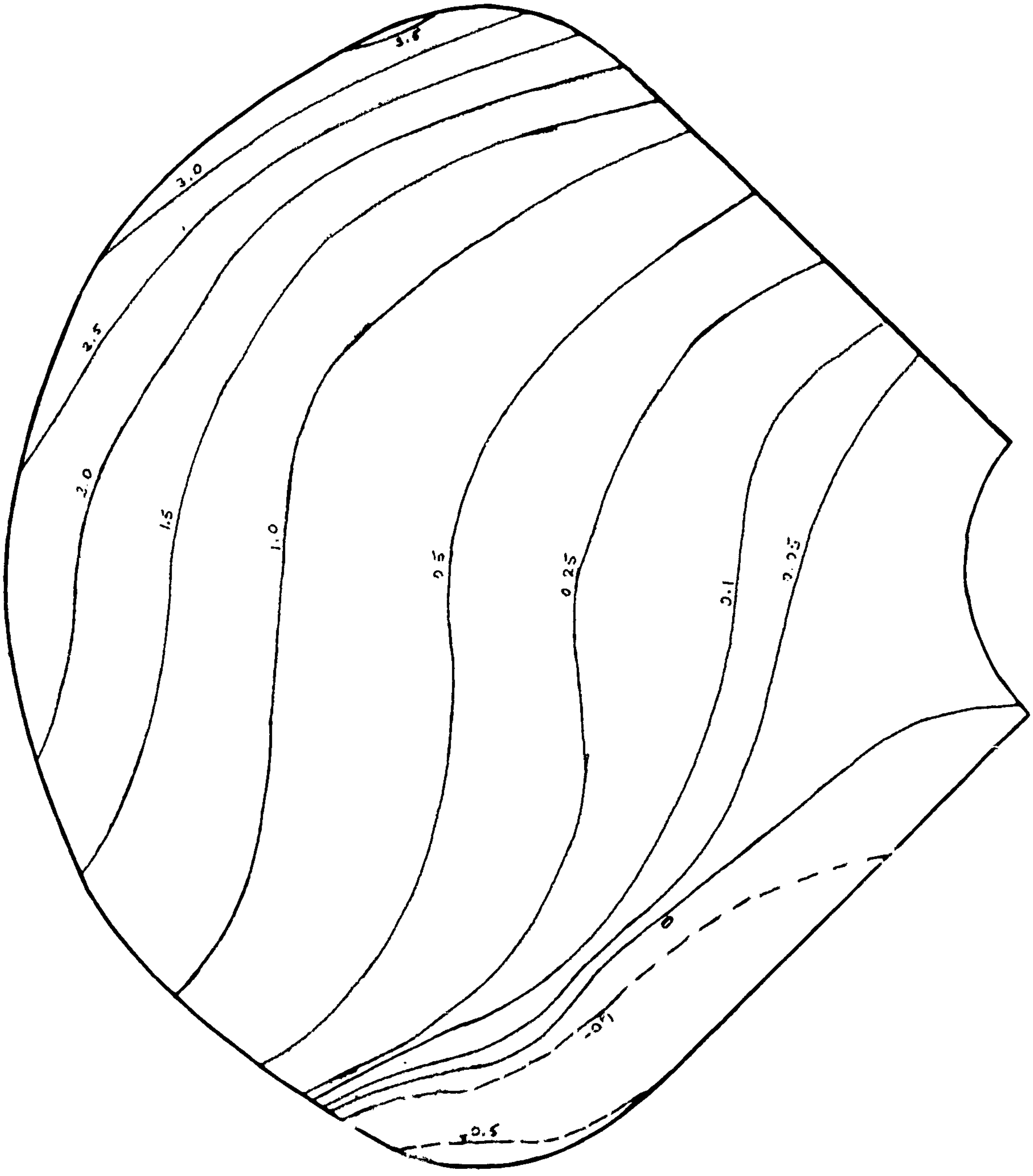

DISPLACEMENT, $U(3) \times 10^{-7}/\epsilon$

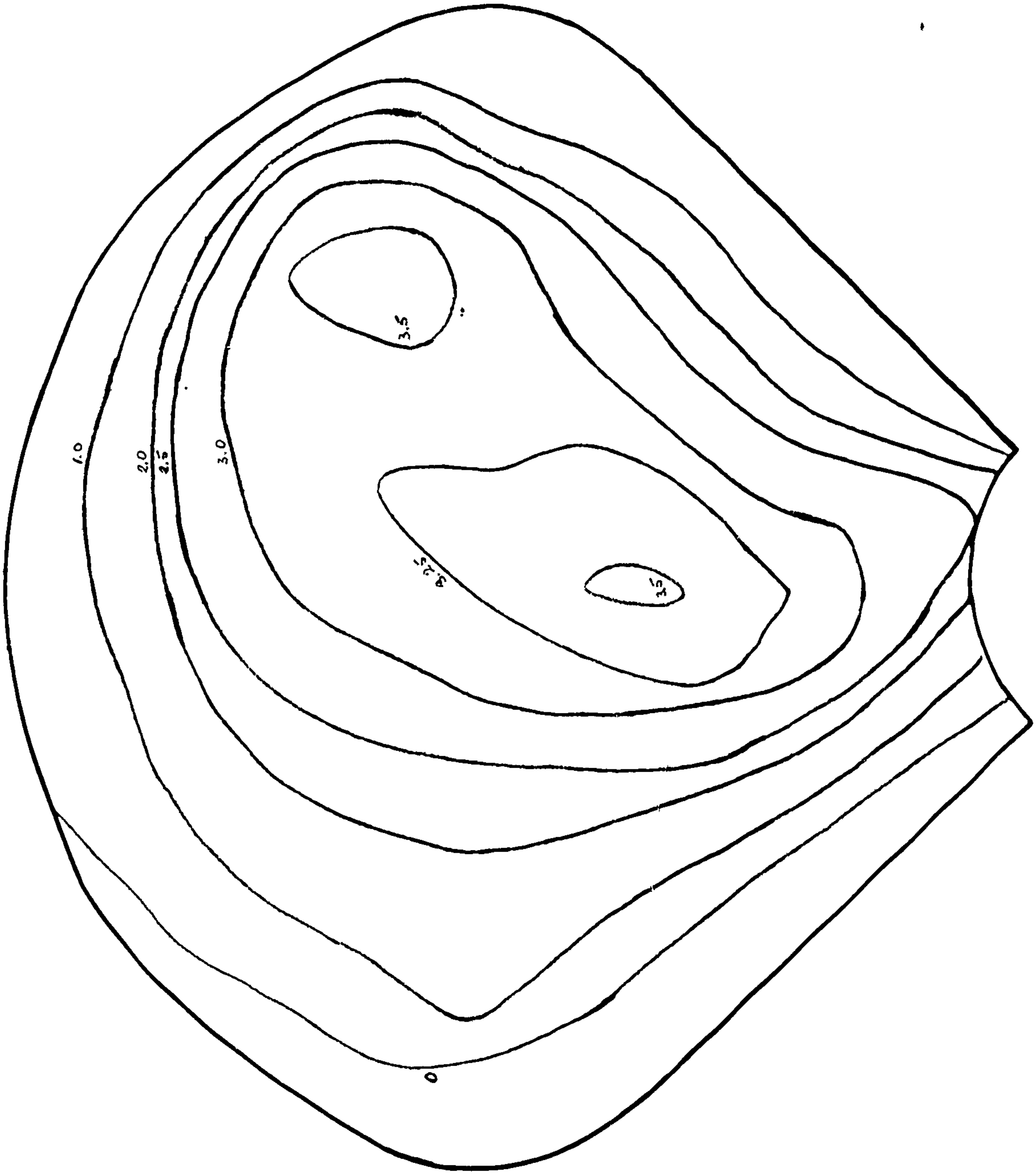

STRESS DISTRIBUTION, $\sigma^{11} \times 10^{-4}$
FRONT FACE

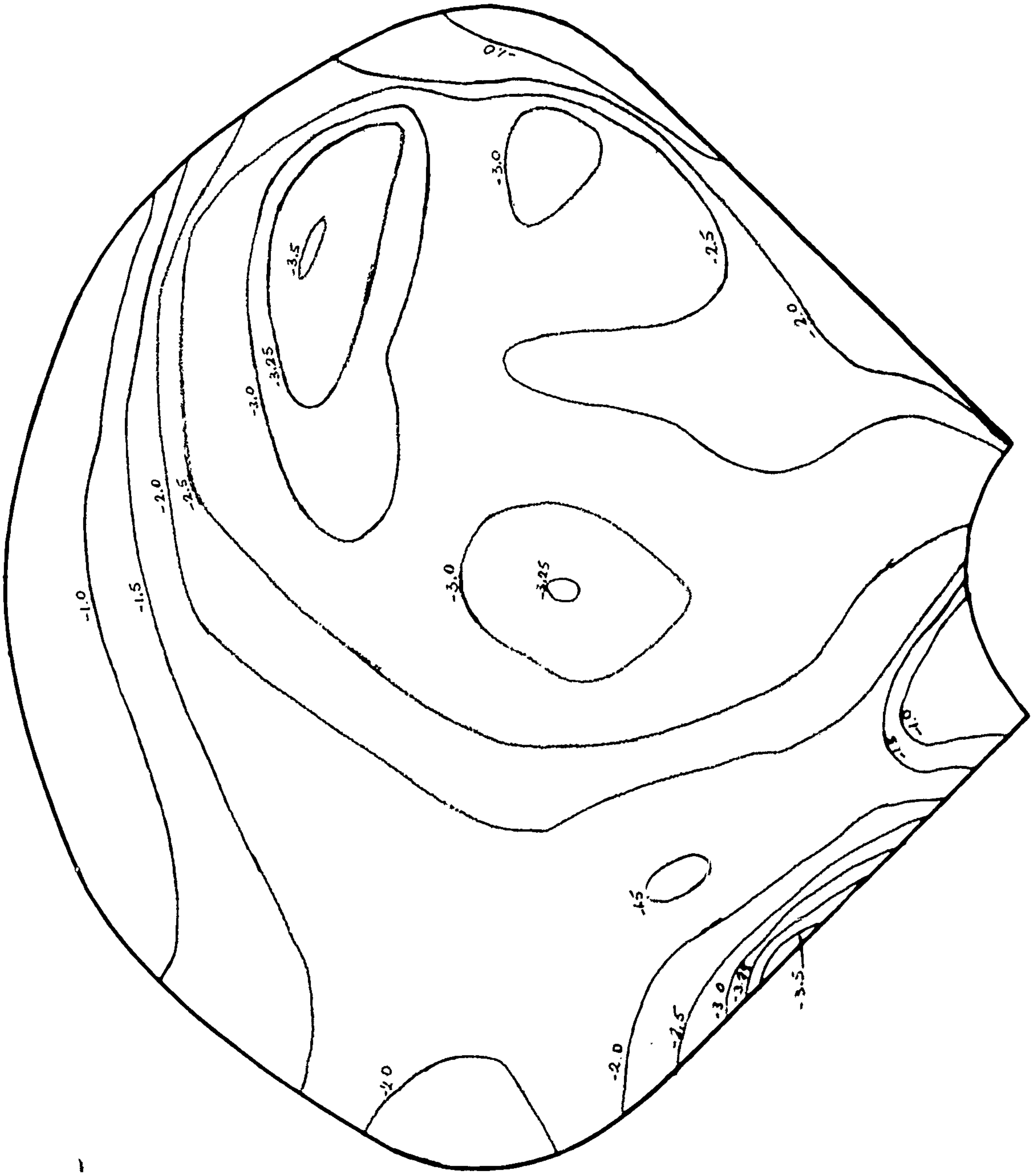

STRESS DISTRIBUTION, $\sigma^{11} \times 10^{-4}$

BACK FACE

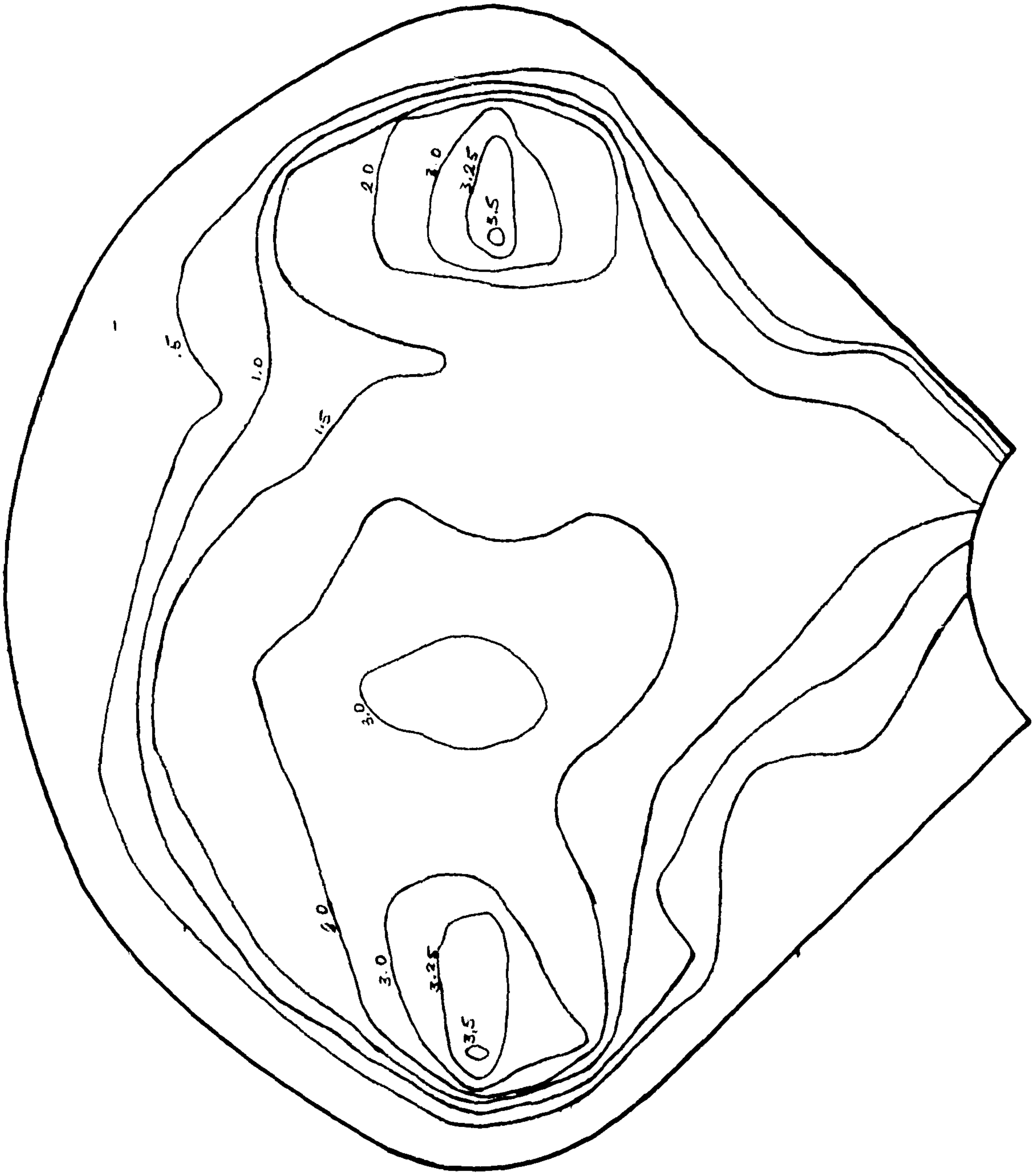

STRESS DISTRIBUTION, $\sigma^{22} \times 10^{-4}$

FRONT FACE

PROPELLER BLADE

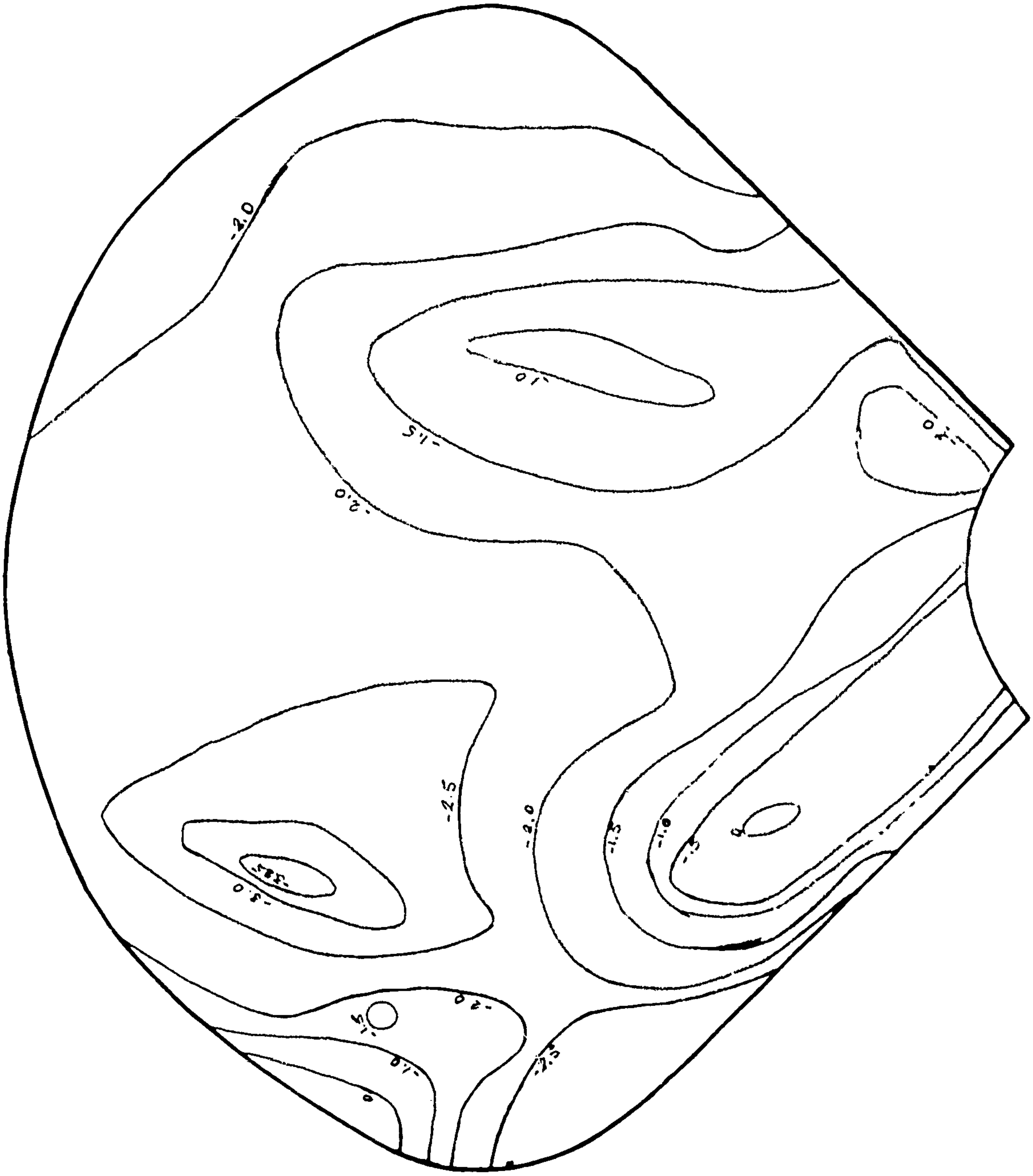

STRESS DISTRIBUTION, $\sigma^{22} \times 10^{-4}$

BACK FACE

S-STEEL PROP 3135

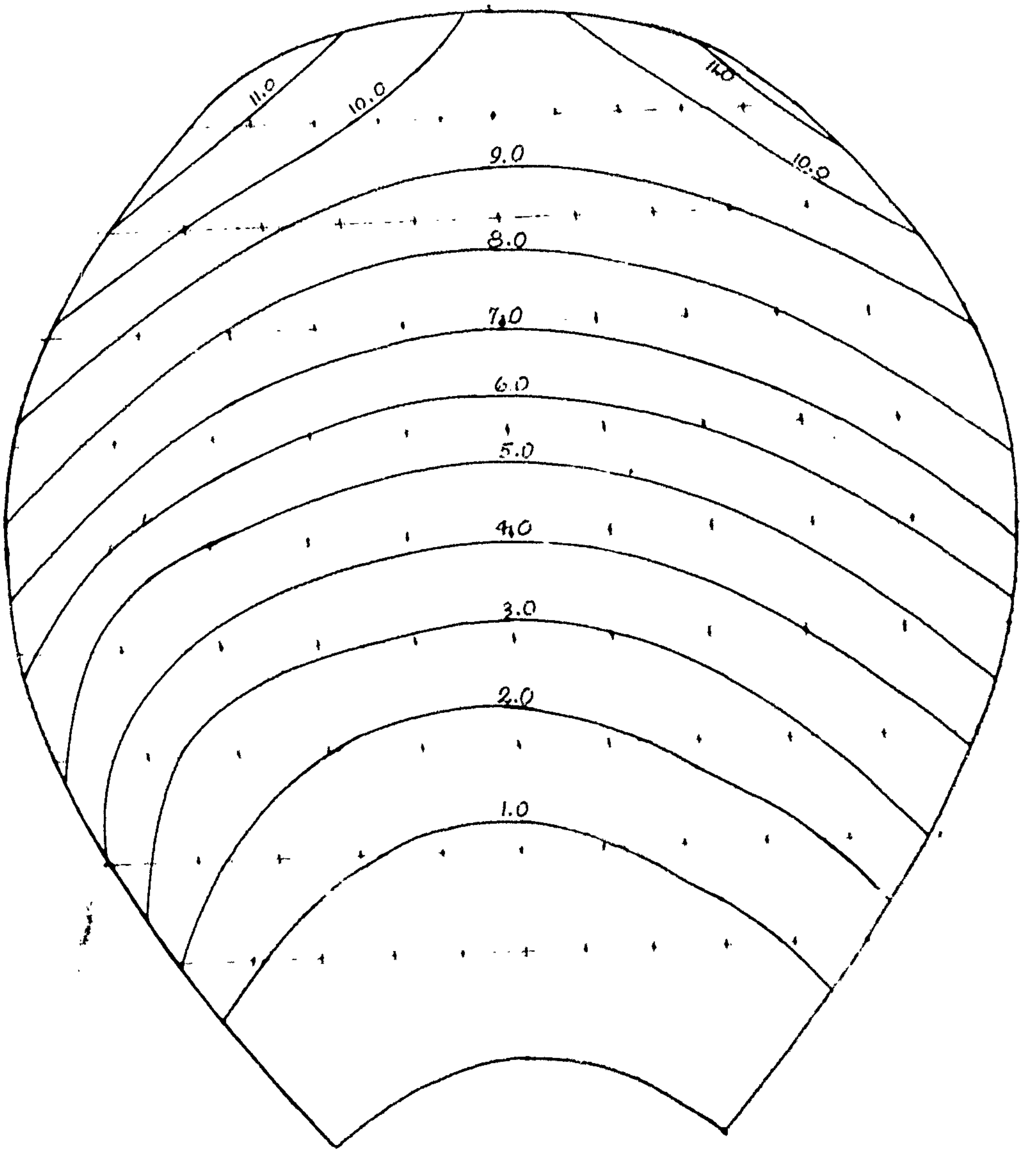

DISPLACEMENT, U(3) x $10^4/\epsilon$

C-STEEL PROP 3133

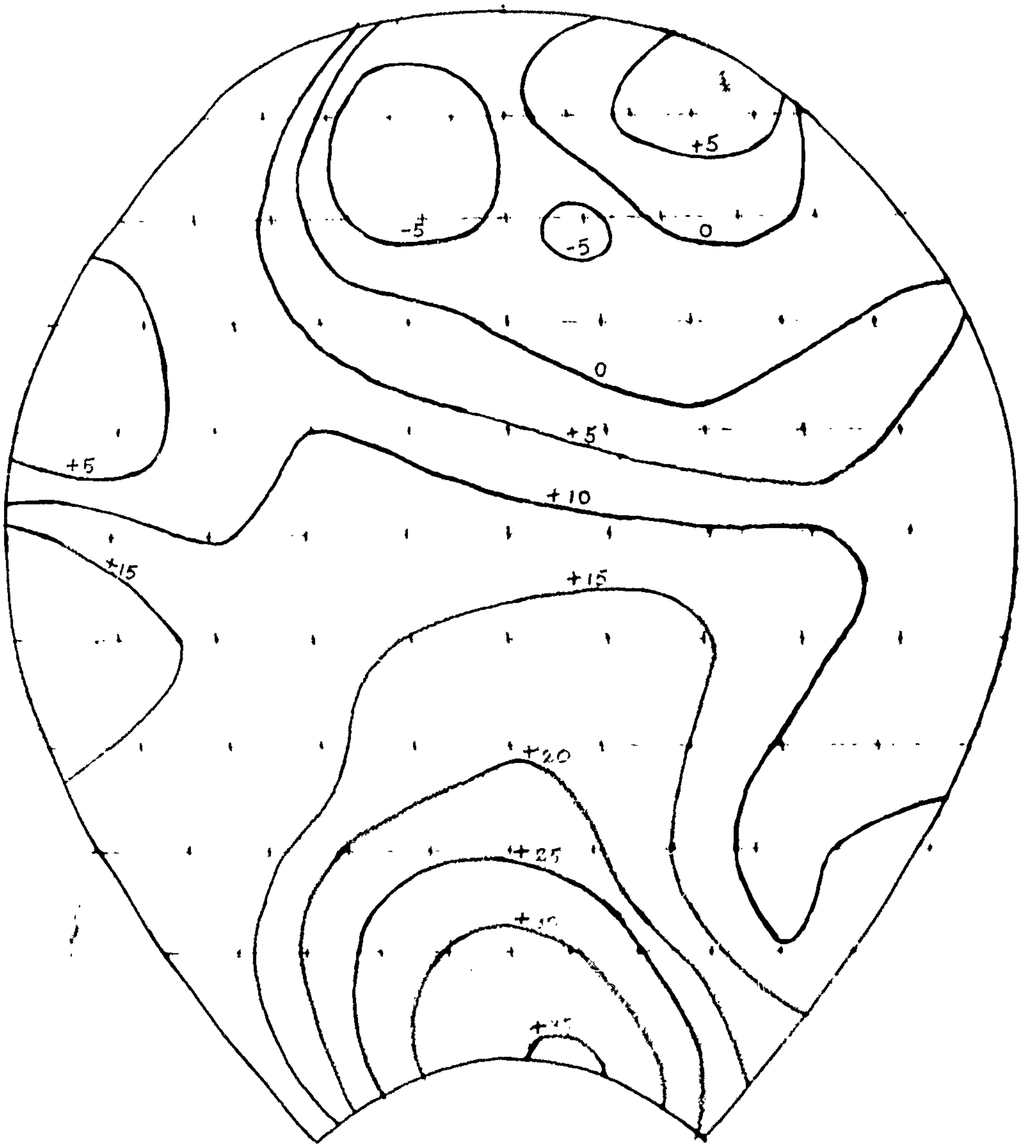

STRESS DISTRIBUTION, $\sigma^{11} \times 10^{-2}$
FRONT FACE

S-STEEL PROP 3133

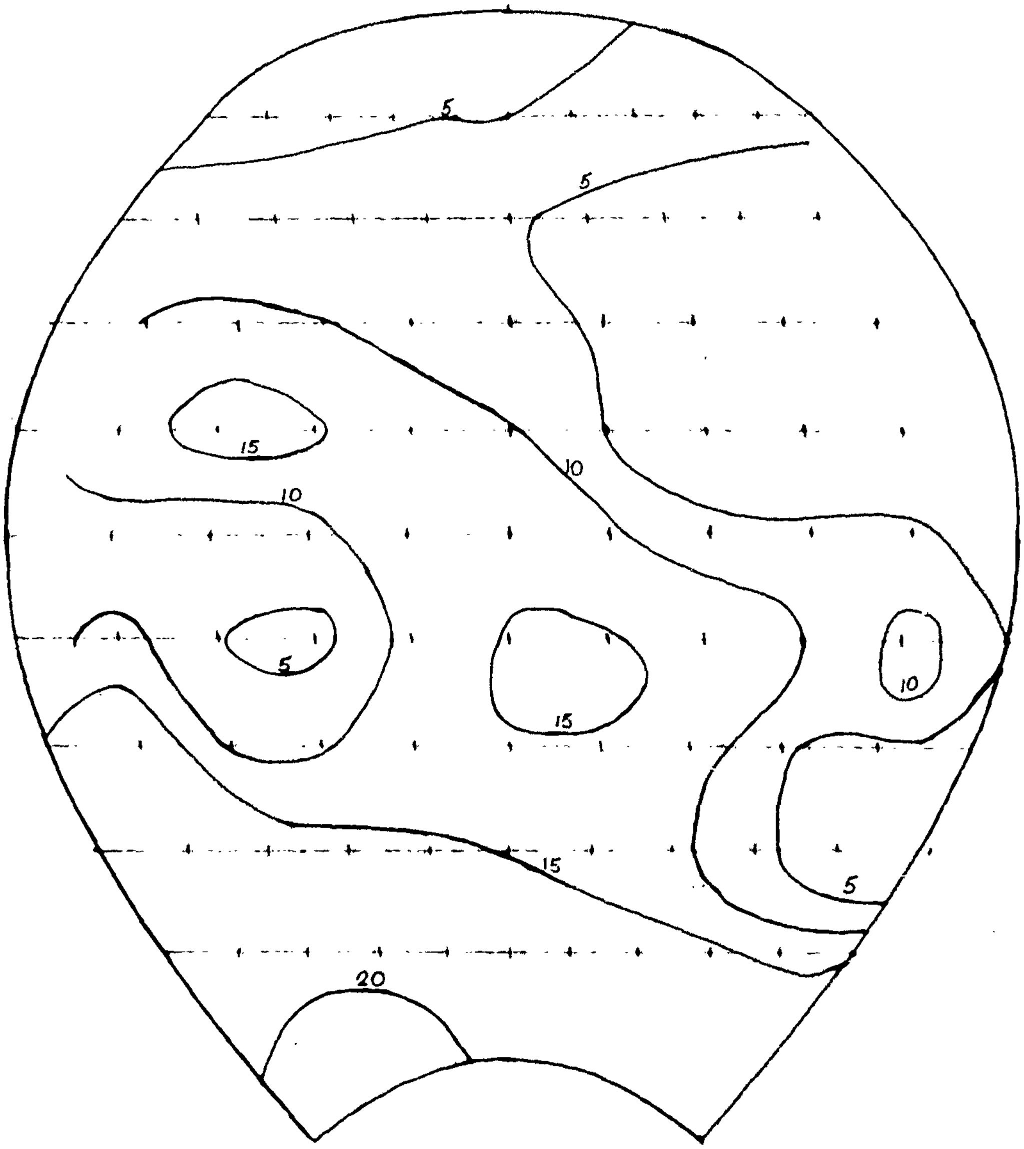

STRESS DISTRIBUTION, $\sigma^{22} \times 10^{-2}$
FRONT FACE

S-STEEL PROP 3135

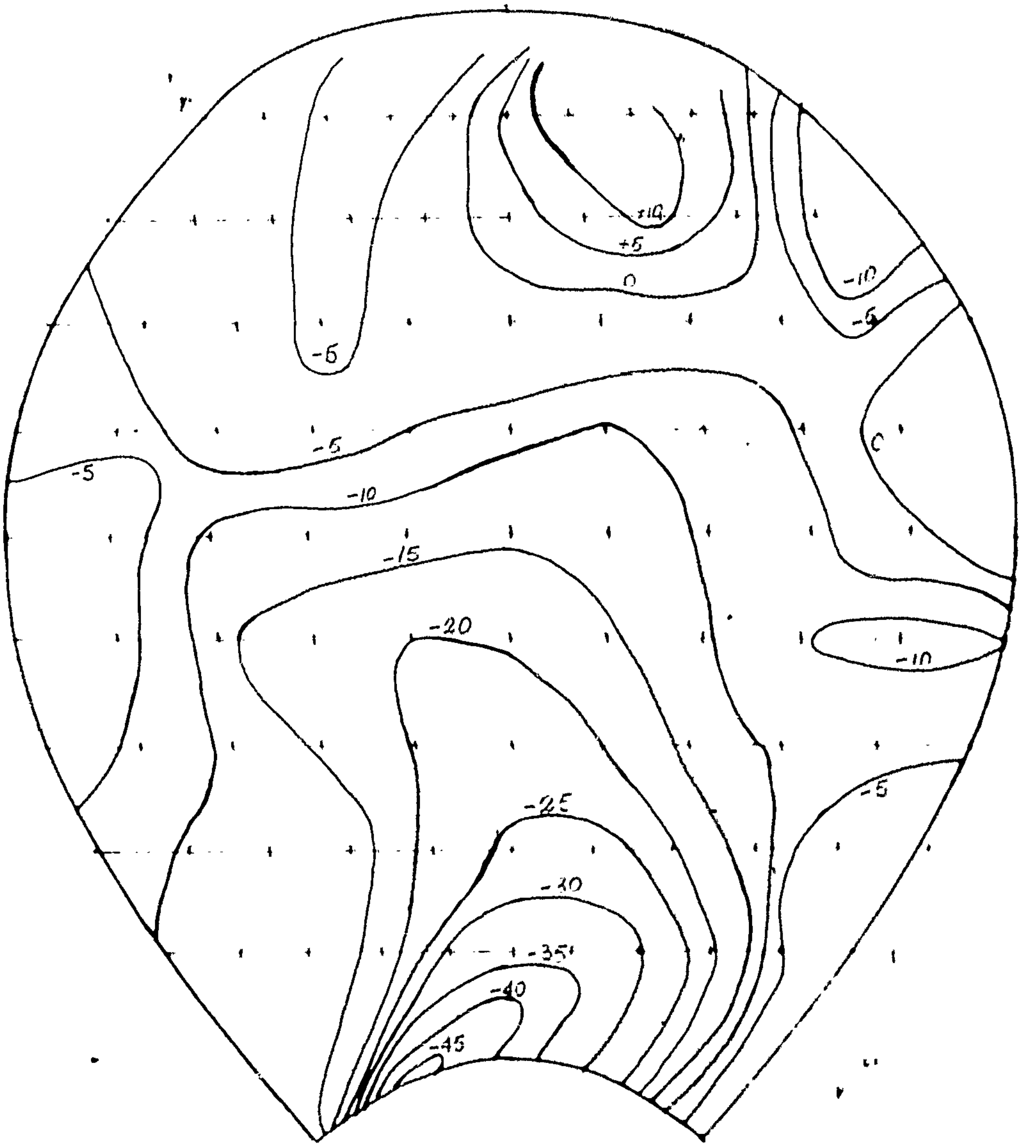

STRESS DISTRIBUTION, $\sigma^1 \times 10^{-2}$
BACK FACE

S-STEEL PROP 3133

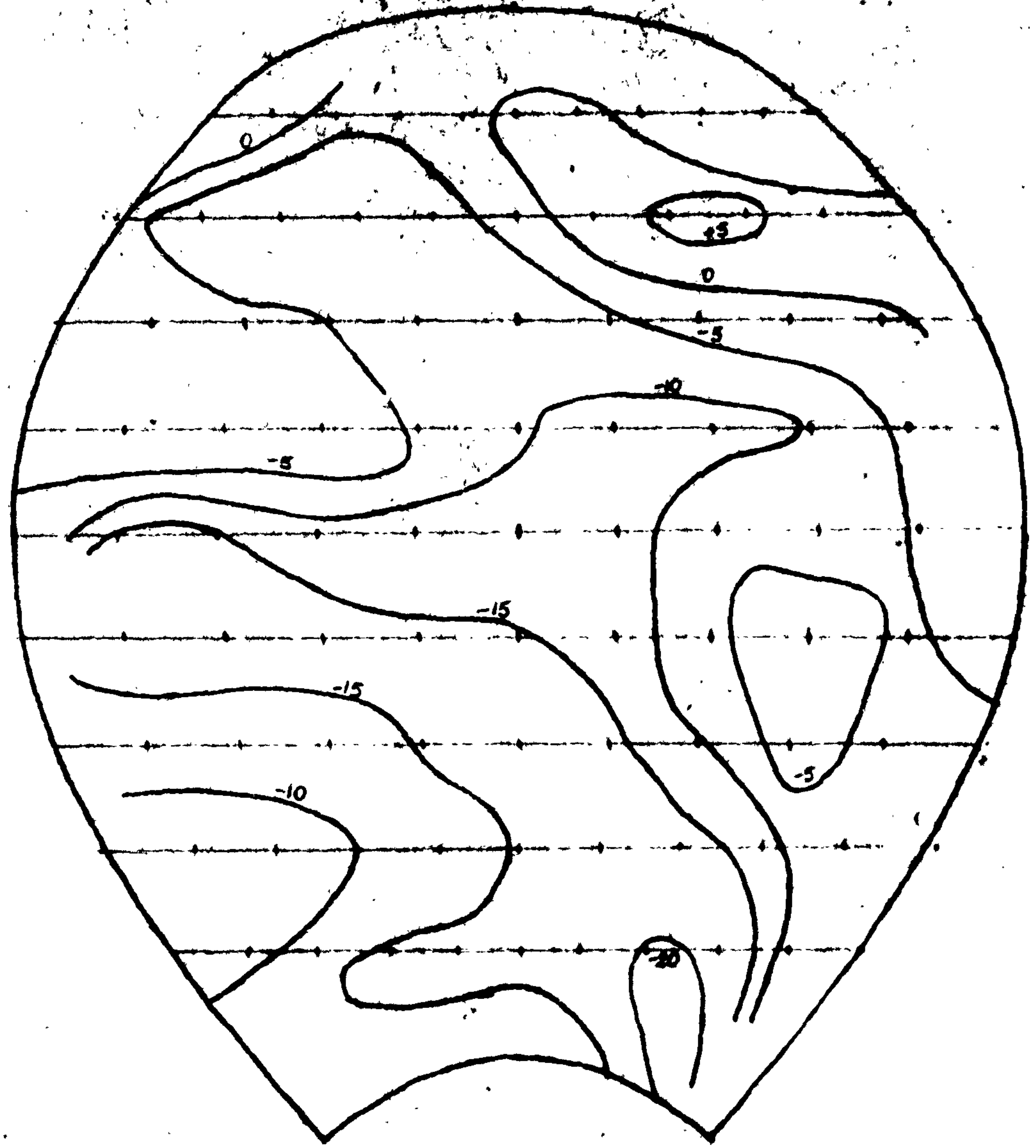

STRESS DISTRIBUTION, $\sigma^{22} \times 10^{-2}$

BACK FACE

VII CONCLUSIONS

An exhaustive series of computer test runs were conducted on a particular propeller blade configuration (DD 828), which was considered to be representative of blades characterized by severe built-in twist, extremely low aspect ratio, and large overhang of thin leading and trailing edges. The results of the runs made by the vibration program indicate conclusively that it is necessary to prescribe a large number of degrees of freedom to obtain satisfactory results, for this type of blade. Unfortunately, the marked growth of accumulated round-off error as the size of the system increases, presents a serious problem. Indeed, this factor defines the upper bound of the allowable number of degrees of freedom which may be prescribed.

This IBM 7090 program was designed to accommodate up to 108 degrees of freedom, which corresponds to a production machine time of approximately 1-1/2 hrs. This limit was imposed by the storage capacity of the computer, as well as by economic considerations with respect to cost of machine time necessary to complete a single run. It was believed that this number would be adequate to cause the natural frequencies to "settle down" and behave asymptotically.

The accumulated round-off error did not permit this series of runs to attain the maximum size for which the program is designed. It was necessary to resort to triple-precision arithmetic in a part of the eigenvalue solution, to curb the round-off error sufficiently to allow a successful run at 90 degrees of freedom. Despite this refinement, the accumulated round-off error caused extraneous negative values for 2 eigenvalues to be printed in the output.

These extraneous values apparently did not effect the remaining 88 eigenvalues as examination of pages to will verify; they did indicate that the accumulated errors were becoming critical, and, as a matter of fact, a subsequent trial run using 96 degrees of freedom failed.

It is believed that the bulk of the accumulated round-off errors is generated in the process of forming and integrating the energy matrices. To alleviate this condition, it would be necessary to utilize double-precision arithmetic in this section of the program. This, however, would be a major programming effort and the increased cost of machine time could triple.

An 8 x 9 integrating quadrature mesh is used. Test runs made with 10 x 10 and 12 x 12 meshes exhibited no significant changes in the eigenvalues; thus, these expensive refinements do not contribute to any increase in accuracy.

For the great majority of blade configurations, it is believed that the present program will generate accurate estimates of the natural frequencies. This series of runs indicates that the natural frequencies have indeed "settled down" at 90 degrees of freedom, and that these figures can be referred to, with confidence. The mode shapes remained essentially unchanged between 75 and 90 degrees of freedom.

The limitation on size due to the accumulation of round-off error, represents a much more severe restriction on stress program than on the vibration program. The natural modes of vibration are an "integrated" property of the entire blade and thus are intrinsically more responsive to "settling down" as the size of the system grows. On the other hand, the stress program mesh furnish quantitatively precise data over the entire domain of the blade planform. To attain the same degree of accuracy for the stress distributions as is now obtained for the vibration frequencies, it is necessary to add more Rayleigh functions, which leads to larger systems of equations.

The method now used to solve the system of linear equations, depends on this system being positive-definite. This condition is negated by the round-off error incurred in forming a large-size strain energy matrix; a technique to solve the system of equations which does not depend upon the property of positive definiteness must be employed in order to accommodate a size larger than say 84 by 84 . A Gaussian elimination process, followed by a Seidelian iteration to improve the solution vector should accomplish this result.

The cost of running the present stress program has been reduced from 1-1/2 hours to approximately 55 minutes. See Appendix II for details. This cost could be further reduced 25-30% by converting the equipment to an IBM 7094 with high-speed, high-density tape units.

REFERENCES

1. Lane, Frank, "A Shell Analysis of Propeller Blade Vibration," Interim Scientific Report No. 1, April 1959.
2. Lieberman, Edward, "Propeller Blade Vibration Analysis," Final Report, GASL Technical Report No. 210, December 1960.
3. Lieberman, Edward, "Propeller Blade Static Stress Analysis," GASL Technical Report No. 225, February 1961.
4. Slutsky, S. and Tamagno, J., "Propeller Blade Vibration Testing," GASL Technical Report No. 213, December 1960.

APPENDIX I

The Rayleigh functions must be chosen to satisfy the displacement boundary conditions at the root, vis. $u_1 = u_2 = 0$ and $\frac{\partial u_3}{\partial y^1} = u_3 = 0$. The geometry of the root is approximated by a parabola of the form, $y^{(2)} = a\,y^{(1)^2} + by^{(1)} + c$. Since the root passes through the origin, the constant term, c, vanishes. The coefficients a, and b, are expressed in terms of the coordinates of the end-points of the root, which are given on input card 2.

The boundary conditions for u_1 and u_2 are satisfied by the functions, φ_1, those for u_3 by the functions ψ_i $(i = 1, 2, \ldots 36)$. These functions are listed below.

$\varphi_1 = (y^{(1)} - ay^{(2)^2} - by^{(2)})$

$\varphi_2 = (y^{(1)} - ay^{(2)^2} - by^{(2)})\,y^{(1)}$

$\varphi_3 = (y^{(1)} - ay^{(2)^2} - by^{(2)})\,y^{(2)}$

$\varphi_4 = (y^{(1)} - ay^{(2)^2} - by^{(2)})\,y^{(1)^2}$

$\varphi_5 = (y^{(1)} - ay^{(2)^2} - by^{(2)})\,y^{(2)^2}$

$\varphi_6 = (y^{(1)} - ay^{(2)^2} - by^{(2)})\,y^{(1)^2}y^{(2)}$

$\varphi_7 = (y^{(1)} - ay^{(2)^2} - by^{(2)})\,y^{(1)^2}\,y^{(2)}$

$\varphi_8 = (y^{(1)} - ay^{(2)^2} - by^{(2)})\,y^{(1)^2}\,y^{(2)^2}$

$\varphi_9 = (y^{(1)} - ay^{(2)^2} - by^{(2)})\,y^{(1)}y^{(2)^2}$

$\varphi_{10} = (y^{(1)} - ay^{(2)^2} - by^{(2)})\,y^{(1)^3}$

$\varphi_{11} = (y^{(1)} - ay^{(2)^2} - by^{(2)})\,y^{(2)^3}$

$\varphi_{12} = (y^{(1)} - ay^{(2)^2} - by^{(2)})\,y^{(2)}$

$\varphi_{13} = (y^{(1)} - ay^{(2)^2} - by^{(2)})\,y^{(1)}\,y^{(2)^3}$

$\varphi_{14} = (y^{(1)} - ay^{(2)^2} - by^{(2)})\,y^{(1)^4}$

$\varphi_{15} = (y^{(1)} - ay^{(2)^2} - by^{(2)})\,y^{(2)^4}$

$\psi_1 = (y^{(1)} - ay^{(2)^2} - by^{(2)})^2$

$\psi_2 = (y^{(1)} - ay^{(2)^2} - by^{(2)})^2\,y^{(1)}$

$\psi_3 = (y^{(1)} - ay^{(2)^2} - by^{(2)})^2\,y^{(2)}$

$\psi_4 = (y^{(1)} - ay^{(2)^2} - by^{(2)})^2\,y^{(1)^2}$

$\psi_5 = (y^{(1)} - ay^{(2)^2} - by^{(2)})\,y^{(2)^2}$

$\psi_6 = (y^{(1)} - ay^{(2)^2} - by^{(2)})^2\,y^{(1)}\,y^{(2)}$

$\psi_7 = (y^{(1)} - ay^{(2)^2} - by^{(2)})^2\,y^{(1)^2}\,y^{(2)}$

$\psi_8 = (y^{(1)} - ay^{(2)^2} - by^{(2)})^2\,y^{(1)^2}\,y^{(2)^2}$

$\psi_9 = (y^{(1)} - ay^{(2)^2} - by^{(2)})^2\,y^{(1)}\,y^{(2)^2}$

$\psi_{10} = (y^{(1)} - ay^{(2)^2} - by^{(2)})^2\,y^{(1)^3}$

$\psi_{11} = (y^{(1)} - ay^{(2)^2} - by^{(2)})^2\,y^{(2)^3}$

$\psi_{12} = (y^{(1)} - ay^{(2)^2} - by^{(2)})^2\,y^{(1)^3}\,y^{(2)}$

$\psi_{13} = (y^{(1)} - ay^{(2)^2} - by^{(2)})^2\,y^{(1)}y^{(2)^3}$

$\psi_{14} = (y^{(1)} - ay^{(2)^2} - by^{(2)})^2\,y^{(1)}\,4$

$\psi_{15} = (y^{(1)} - ay^{(2)^2} - by^{(2)})2\;\;y^{(2)}\,4$

$\varphi_{16} = (y^{(1)} - ay^{(2)2} - by^{(2)})\, y^{(1)5}$

$\varphi_{17} = (y^{(1)} - ay^{(2)2} - by^{(2)})\, y^{(2)5}$

$\varphi_{18} = (y^{(1)} - ay^{(2)2} - by^{(2)})\, y^{(1)4}y^{(2)}$

$\varphi_{19} = (y^{(1)} - ay^{(2)2} - by^{(2)})\, y^{(1)}y^{(2)4}$

$\varphi_{20} = (y^{(1)} - ay^{(2)2} - by^{(2)})\, y^{(1)3}y^{(2)2}$

$\varphi_{21} = (y^{(1)} - ay^{(2)2} - by^{(2)})\, y^{(1)2}y^{(2)3}$

$\varphi_{22} = (y^{(1)} - ay^{(2)2} - by^{(2)})\, y^{(1)6}$

$\varphi_{23} = (y^{(1)} - ay^{(2)2} - by^{(2)})\, y^{(2)6}$

$\varphi_{24} = (y^{(1)} - ay^{(2)2} - by^{(2)})\, y^{(1)5}y^{(2)}$

$\varphi_{25} = (y^{(1)} - ay^{(2)2} - by^{(2)})\, y^{(1)}y^{(2)5}$

$\varphi_{26} = (y^{(1)} - ay^{(2)2} - by^{(2)})\, y^{(1)4}y^{(2)2}$

$\varphi_{27} = (y^{(1)} - ay^{(2)2} - by^{(2)})\, y^{(1)2}y^{(2)4}$

$\varphi_{28} = (y^{(1)} - ay^{(2)2} - by^{(2)})\, y^{(1)3}y^{(2)3}$

$\varphi_{29} = (y^{(1)} - ay^{(2)2} - by^{(2)})\, y^{(1)7}$

$\varphi_{30} = (y^{(1)} - ay^{(2)2} - by^{(2)})\, y^{(2)7}$

$\varphi_{31} = (y^{(1)} - ay^{(2)2} - by^{(2)})\, y^{(1)6}y^{(2)}$

$\varphi_{32} = (y^{(1)} - ay^{(2)2} - by^{(2)})\, y^{(1)}y^{(2)6}$

$\varphi_{33} = (y^{(1)} - ay^{(2)2} - by^{(2)})\, y^{(1)5}y^{(2)2}$

$\varphi_{34} = (y^{(1)} - ay^{(2)2} - by^{(2)})\, y^{(1)2}y^{(2)5}$

$\varphi_{35} = (y^{(1)} - ay^{(2)2} - by^{(2)})\, y^{(1)4}y^{(2)3}$

$\varphi_{36} = (y^{(1)} - ay^{(2)2} - by^{(2)})\, y^{(1)3}y^{(2)4}$

$\psi_{16} = (y^{(1)} - ay^{(2)2} - by^{(2)})^2 y^{(1)5}$

$\psi_{17} = (y^{(1)} - ay^{(2)2} - by^{(2)})^2 y^{(2)5}$

$\psi_{18} = (y^{(1)} - ay^{(2)2} - by^{(2)})^2 y^{(1)4}y^{(2)}$

$\psi_{19} = (y^{(1)} - ay^{(2)2} - by^{(2)})^2 y^{(1)}y^{(2)4}$

$\psi_{20} = (y^{(1)} - ay^{(2)2} - by^{(2)})^2 y^{(1)3}y^{(2)2}$

$\psi_{21} = (y^{(1)} - ay^{(2)2} - by^{(2)})^2 y^{(1)2}y^{(2)3}$

$\psi_{22} = (y^{(1)} - ay^{(2)2} - by^{(2)})^2 y^{(1)6}$

$\psi_{23} = (y^{(1)} - ay^{(2)2} - by^{(2)})^2 y^{(2)6}$

$\psi_{24} = (y^{(1)} - ay^{(2)2} - by^{(2)})^2 y^{(1)5}y^{(2)}$

$\psi_{25} = (y^{(1)} - ay^{(2)2} - by^{(2)})^2 y^{(1)}y^{(2)5}$

$\psi_{26} = (y^{(1)} - ay^{(2)2} - by^{(2)})^2 y^{(1)4}y^{(2)2}$

$\psi_{27} = (y^{(1)} - ay^{(2)2} - by^{(2)})^2 y^{(1)2}y^{(2)4}$

$\psi_{28} = (y^{(1)} - ay^{(2)2} - by^{(2)})^2 y^{(1)3}y^{(2)3}$

$\psi_{29} = (y^{(1)} - ay^{(2)2} - by^{(2)})^2 y^{(1)7}$

$\psi_{30} = (y^{(1)} - ay^{(2)2} - by^{(2)})^2 y^{(2)7}$

$\psi_{31} = (y^{(1)} - ay^{(2)2} - by^{(2)})^2 y^{(1)6}y^{(2)}$

$\psi_{32} = (y^{(1)} - ay^{(2)2} - by^{(2)})^2 y^{(1)}y^{(2)6}$

$\psi_{33} = (y^{(1)} - ay^{(2)2} - by^{(2)})^2 y^{(1)5}y^{(2)2}$

$\psi_{34} = (y^{(1)} - ay^{(2)2} - by^{(2)})^2 y^{(1)2}y^{(2)5}$

$\psi_{35} = (y^{(1)} - ay^{(2)2} - by^{(2)})^2 y^{(1)4}y^{(2)3}$

$\psi_{36} = (y^{(1)} - ay^{(2)2} - by^{(2)})^2 y^{(1)3}y^{(2)4}$

APPENDIX II

A great variety of techniques have been developed and employed to solve large systems of simultaneous equations. The relative usefulness of each technique is intimately related to the size and character of the system in question.. At all times, the programmer must contend with the problem of propagated round-off errors and recognize the economic necessity of minimizing machine time, consistant with the desired accuracy.

In the course of solving the two-matrix eigenvalue problem it was necessary to factor the strain energy matrix using multiple-precision arithmetic which utilized two "words" for the fraction - a total of 71 bits compared with 25 bits used for single precision (plus sign). After attemping several other techniques to solve the system of equations in the stress program all of which proved to be unacceptable for one reason or another, it was decided to utilize the existing coding of the factoring technique to generate an approximate inverse, and then try to improve the solution by various means. Three techniques are used, in series; the improvement effected by one procedure, materially assists the convergence of the following one.

1. Series Expansion to Improve the Inverse

Given a matrix, A, and an approximate inverse $\tilde{A}^{-1} = A^{-1} + E$, then

$$A\tilde{A}^{-1} = A(A^{-1}+E) = I + C \qquad \text{where } C = AE$$

The matrix C may be calculated; E is the error in the approximate inverse. Solving for E, $E = A^{-1}C$

$$E + EC = E(I+C) = A^{-1}C+EC = (A^{-1}+E)C = \tilde{A}^{-1}C$$

$$E(I+C)(I-C) = E(I-C^2) = \tilde{A}^{-1}C(I-C)$$

Multiplying by $(I+C^2)$: $E(I-C^4) = \tilde{A}^{-1}(C-C^2+C^3-C^4)$

In general, $E(I-C^n) = \tilde{A}^{-1}(C+C^2+C^3 - \ldots - C^n)$

Thus the error matrix, E, may be calculated, subject to a truncation error, $-EC^n$. If the matrix C is "sufficiently" small, the series expansion will converge, and the truncation error will be extremely small, compared to E. Then, since $A^{-1} = \tilde{A}^{-1} - E$, we may write

$$A^{-1} = \tilde{A}^{-1} - \tilde{A}^{-1}(C-C^2+C^3 - \ldots - C^n) \text{ or}$$

$$A^{-1} = \tilde{A}^{-1}(I-C+C^2-C^3 \ldots + C^n)$$

For this program, n = 8. If C is "too large", the series will diverge and the entire improvement of the solution will be done by the Seidelian iteration technique. Following this series expansion(if successful) is:

2. Iteration on Forcing Vector

Given the matrix A, a good approximation to its inverse, $\tilde{A}^{-1}$, and the forcing vector, p, in the system $Aq = p$. Then we may write

$q_1 = \tilde{A}^{-1}p$ where q_1 is the first approximation to the solution vector. To improve it, compute p_1; $Aq_1 = p_1$ or $A(q + \Delta q_1) = p + \Delta p_1$. Then we may solve for the error in the solution vector, $\Delta q_1 = \tilde{A}^{-1}\Delta p_1$ and writing $q_2 = q_1 + \Delta q_1$, can repeat the process. For this iteration to converge, the inverse, $\tilde{A}^{-1}$, must be "sufficiently" accurate. Otherwise, we must depend entirely upon the Seidelian iteration.

3. Seidel Iteration on the Solution Vector

Transposing the i^{th} equation of the system, we may solve for the i^{th} element of the solution vector in terms of the best values computed so far, for the other n - 1 elements of the solution vector:

$$q_i = \frac{1}{a_{ii}} \left[p_i - \sum_{\substack{j=1 \\ j \neq i}}^{n} a_{ij}\, q_j \right]$$

The program sweeps through the system many times until either a satisfactory tolerance is achieved or until the upper limit of iterations is attained. Since this iteration technique is unconditionally convergent for positive definite symmetric matrices, the final solution vector will have the necessary accuracy. The upper limit of the number of iterations depends upon the success attained by the previous two techniques. This upper limit is significantly reduced (thus saving machine time) if the prior iterations were successful to some extent.

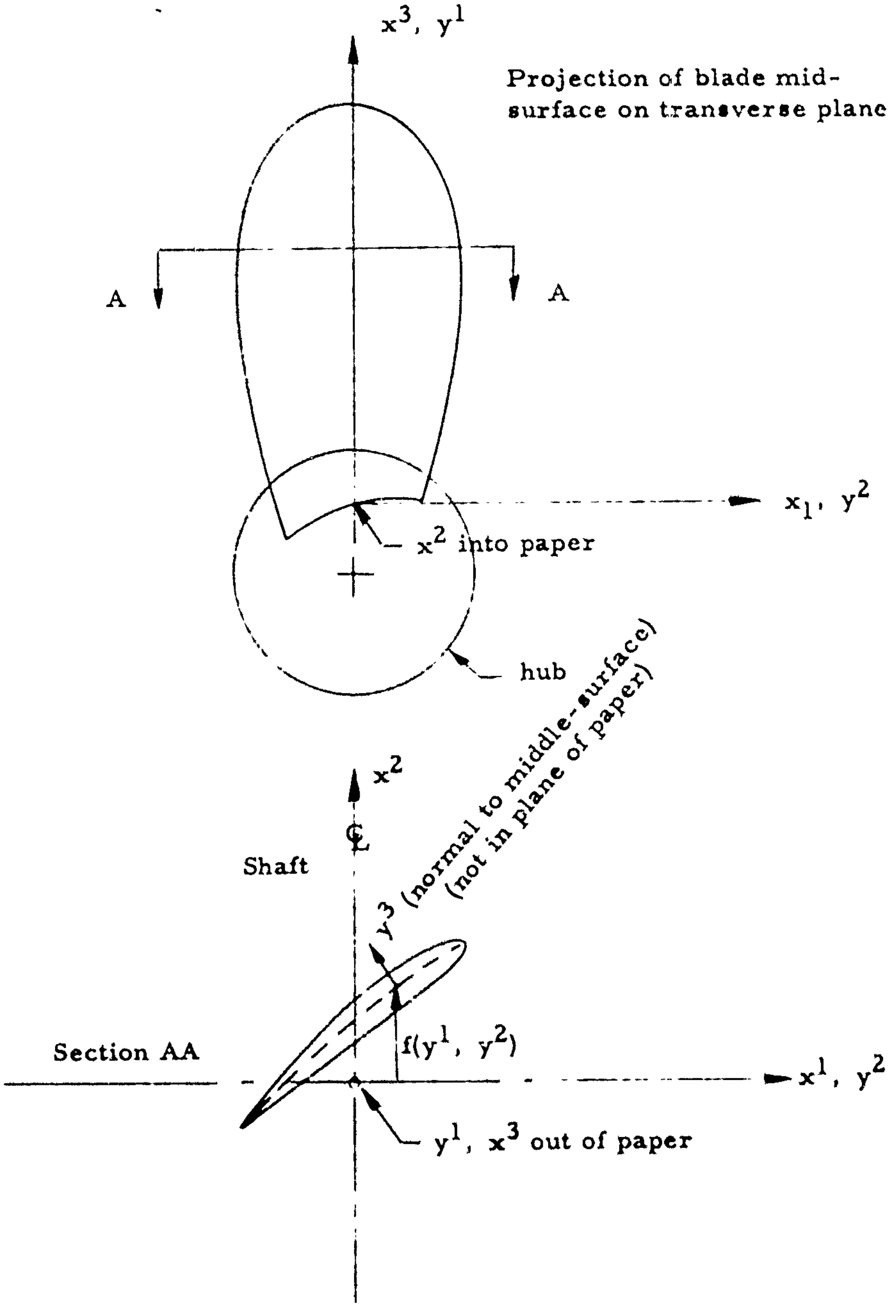
x^3, y^1
Projection of blade mid-surface on transverse plane
A
A
x_1, y^2
x^2 into paper
hub
x^2
℄
Shaft
y^3 (normal to middle-surface) (not in plane of paper)
$f(y^1, y^2)$
Section AA
x^1, y^2
y^1, x^3 out of paper

Fig. 1
Blade Geometry and Coordinate Systems

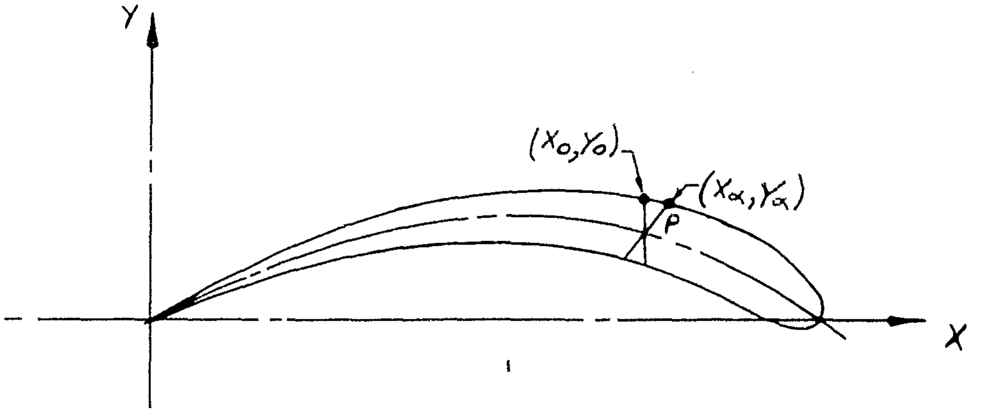
Y
X
(X0,Y0)
(Xα,Yα)
P

Figure 2a

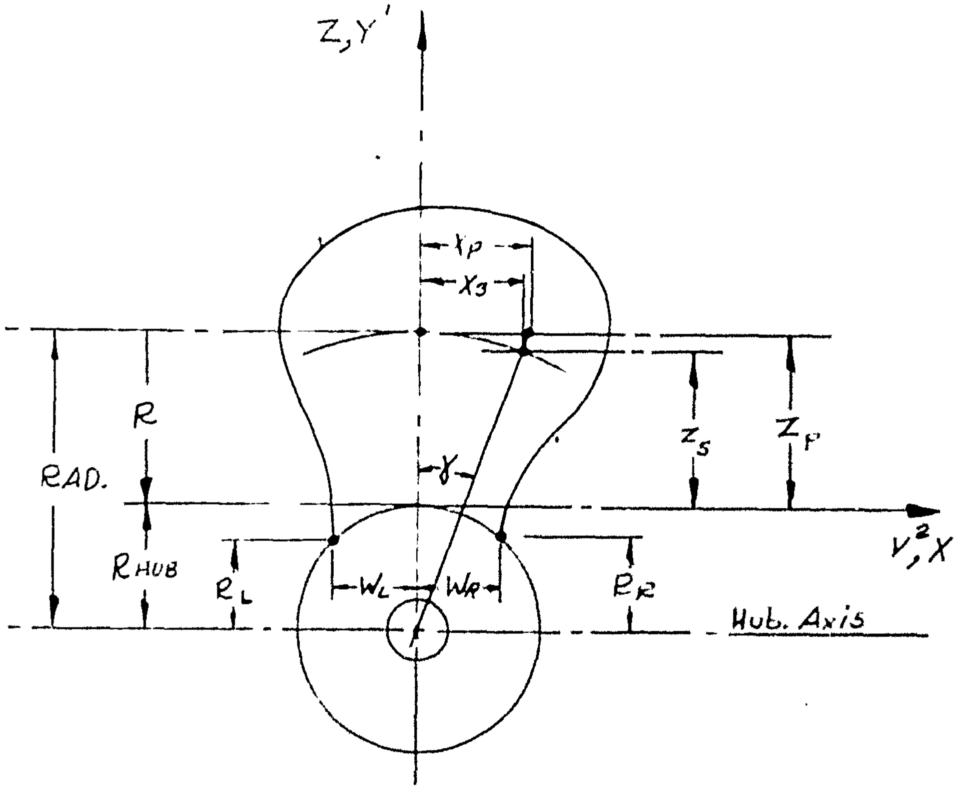
Z, Y'
Xp
X3
R
RAD.
Zs
Zp
γ
Y, X
RHUB
RL
WL
WR
RR
Hub. Axis

Figure 2b

DISTRIBUTION LIST

	Copy No.
Technical Asst to Ch of Bureau (Code 106) Chief, Bureau of Ships Department of the Navy Washington 25, D.C.	1
Information Branch (Code 335) Chief, Bureau of Ships Department of the Navy Washington 25, D.C.	2-4
Preliminary Design (Code 420) Chief, Bureau of Ships Department of the Navy Washington 25, D.C.	5-6
Hull Design (Code 440) Chief, Bureau of Ships Department of the Navy Washington 25, D.C.	7-9
Consultant (Code 108) Commanding Officer & Director David Taylor Model Basin Washington 7, D.C.	10
Library Branch (Code 142) Commanding Officer & Director David Taylor Model Basin Washington 7, D.C.	11-12
Tech Director, Hydromechanics Lab. (Code 500) Commanding Officer & Director David Taylor Model Basin Washington 7, D.C.	13
Contract Res. Admin. (Code 513) Commanding Officer & Director David Taylor Model Basin Washington 7, D.C.	14-15
Ship Powering Divn (Code 520) Commanding Officer & Director David Taylor Model Basin Washington 7, D.C.	16
Res. & Propeller Branch (Code 526) Commanding Officer & Director David Taylor Model Basin Washington 7, D.C.	17
Stability & Control Divn (Code 530) Commanding Officer & Director David Taylor Model Basin Washington 7, D.C.	18
Seaworthiness & Fluid Dyn. Divn (Code 580) Commanding Officer & Director David Taylor Model Basin Washington 7, D.C.	19
Fluid Dynamics Branch (Code 589) Commanding Officer & Director David Taylor Model Basin Washington 7, D.C.	20
Tech. Dir, Structural Mech Lab (Code 700) Commanding Officer & Director David Taylor Model Basin Washington 7, D.C.	21
Chief of Naval Research Fluid Dyn Branch, (Code 438) Department of the Navy Washington 25, D.C.	22-23
Chief, Bureau of Naval Weapons Dyn Section (Code RAAD-222) Attention: Mr. D. Michel Washington 25, D.C.	24
Commander U.S. Naval Ordnance Lab White Oak, Maryland	25
Commander U.S. Naval Ordnance Test Station China Lake, California	26

DISTRIBUTION LIST

	Copy No.
Officer-in-charge Pasadena Annex U.S. Naval Ordnance Test Station Oceanic Research (Code P-508) 3202 E. Foothill Blvd. Pasadena 8, Calif	27-29
Dr. G.B. Schubauer, Chief Fluid Mechanics Section National Bureau of Standards Washington 25, D.C.	30
Dr. J.M. Franklin, Consultant National Bureau of Standards Washington 25, D.C.	31
Mr. I.E. Garrick - Director Langley Research Center Langley Field, Virginia	32
Mr. D.J. Marten - Director Langley Research Center Langley Field, Virginia	33
Natl Research Council of Can. Hydromechanics Lab Ottawa 2, Canada	34
Mr. R.P. Godwin, Acting Ch. Office of Res. & Development Maritime Administration 441 G. Street, N.W. Washington 25, D.C.	35
Commander Armed Svc Tech Inf Agency Attention: TIPDR Arlington Hall Station Arlington 12, Virginia	36-45
Office of Technical Services OTS, Dept of Commerce Washington 25, D.C.	46
Commander Air Res & Development Command Attention: Mechanics Branch AFOSR 14th and Constitution Washington 25, D.C.	47
Commander Wright Air Development Divn Attn: Mr. W.Mykytow, Dyn Branch Wright-Patterson AFB, Ohio	48
Dr. F.H. Todd Superintendent, Ship Divn. National Physical Lab. Teddington, Middlesex, Eng.	49
Head Aerodynamics Division National Physical Lab. Teddington, Middlesex, Eng.	50
Mr. A. Silverleaf National Physical Lab. Teddington, Middlesex, Eng.	51
Head, Aerodynamics Dept. Royal Aircraft Establishment Mr. M.O.W. Wolfe Farnborough, Hants, Eng.	52-53
Boeing Airplane Company Seattle Division Mr. M.J. Turner Seattle, Washington	54
Dr. M.S. Plesset Calif Institute of Technology Pasadena, California	55
Dr. T.Y. Wu Calif. Institute of Technology Pasadena, California	56
Dr. A.J. Acosta Calif. Institute of Technology Pasadena, California	57

DISTRIBUTION LIST

	Copy No.
Mr. A.D. MacLellan Systems Dynamics Group Convair P.O. Box 1950 San Diego 12, California	58
Mr. H.T. Brooke Hydrodynamics Group Convair P.O. Box 1950 San Diego 12, California	59
Mr. W. Targoff Cornell Aeronautical Lab 4455 Genesee Street Buffalo, New York	60
Mr. R. White Cornell Aeronautical Lab 4455 Genesee Street Buffalo, New York	61
Mr. C.J. Henry Director, Davidson Lab Stevens Institute of Technology Hoboken, New Jersey	62-63
Mr. S. Tsakonas Director, Davidson Lab Stevens Institute of Technology Hoboken, New Jersey	64
Electric Boat Division General Dynamics Corp Attn: Mr. Robert McCandliss Groton, Connecticut	65
Gibbs and Cox, Inc. 21 West Street New York, New York	66
Mr. E. Baird Grumman Aircraft Engrg Corp Bethpage, LI, New York	67
Mr. E. Bower Grumman Aircraft Engrg Corp Bethpage, LI, New York	68
Grumman Aircraft Engrg Corp Dyn Developments Division Babylon, New York	69
President, Hydronautics, Inc. 200 Monroe Street Rockville, Maryland	70-71
Lockheed Aircraft Corp Missiles & Space Divn Attn: R.W. Kermeen Palo Alto, California	72
Prof. H. Ashley Mass Institute of Technology Fluid Dyn Research Lab Cambridge 39, Mass	73
Prof. M. Landahl Mass Institute of Technology Fluid Dyn Research Lab Cambridge 39, Mass	74
Prof. J. Dugundji Mass Institute of Technology Fluid Dyn Research Lab Cambridge 39, Mass	75
Midwest Research Institute Attn: Mr. Zeydel 425 Volker Boulevard Kansas City 10, Missouri	76
Ordnance Research Laboratory Pennsylvania State University Dr. M. Sevik University Pk, Pennsylvania	77

DISTRIBUTION LIST

Copy No.

Dr. H.N. Abramson - Director
Dept of Mechanical Sciences
Southwest Research Institute
8500 Celebra Road
San Antonio 6, Texas 78

Mr. G. Ransleben - Director
Dept of Mechanical Sciences
Southwest Research Institute
8500 Celebra Road
San Antonio 6, Texas 79

Editor, Applied Mech Review
Dir - Dept of Mechanical Sci
Southwest Research Institute
8500 Celebra Road
San Antonio 6, Texas 80

Dr. B. Perry
Stanford University
Department of Mathematics
Stanford, California 81

Dr. E.Y. Hsu
Stanford University
Department of Mathematics
Stanford, California 82

State University of Iowa
Iowa Institute of Hydraulic Res
Prof. L. Landweber
Iowa City, Iowa 83

Technical Research Group, Inc
Attn: Dr. P. Kaplan
2 Aerial Way
Syosset, LI, New York 84-85

The Rand Corporation
Attn: Dr. B. Parkin
1700 Main Street
Santa Monica, Calif 86

Copy No.

University of California
Dept of Engrg
Institute of Engrg Res
Attn: Dr. J.V. Wehausen
Berkeley, California 87

Prof H.A. Schade, Head
Dept of Naval Architecture
University of California
Berkeley, California 88

Prof. B. Silberman
St. Anthony Falls Hydraulic Lab
University of Minnesota
Minneapolis, Minn 89

Mr. J.N. Wetzel
St. Anthony Falls Hydraulic Lab
University of Minnesota
Minneapolis, Minn. 90